The magic of magnetic shape memory alloys and crystal structure perspective

L. Straka
FZU – Institute of Physics of the Czech Academy of Sciences, Prague, Czech Republic

&

P. Veřtát, M. Zelený, A. Sozinov, M. Klicpera, H. Seiner, O. Heczko, …

The magic of magnetic shape memory alloys and crystal structure perspective

L. Straka
FZU – Institute of Physics of the Czech Academy of Sciences, Prague, Czech Republic

FZU Institute of Physics of the Czech Academy of Sciences

www.fzu.cz p4f.fzu.cz

Institute of Physics of the Czech Academy of Sciences is a leading research institution in basic and applied physics.

The magic of magnetic shape memory…

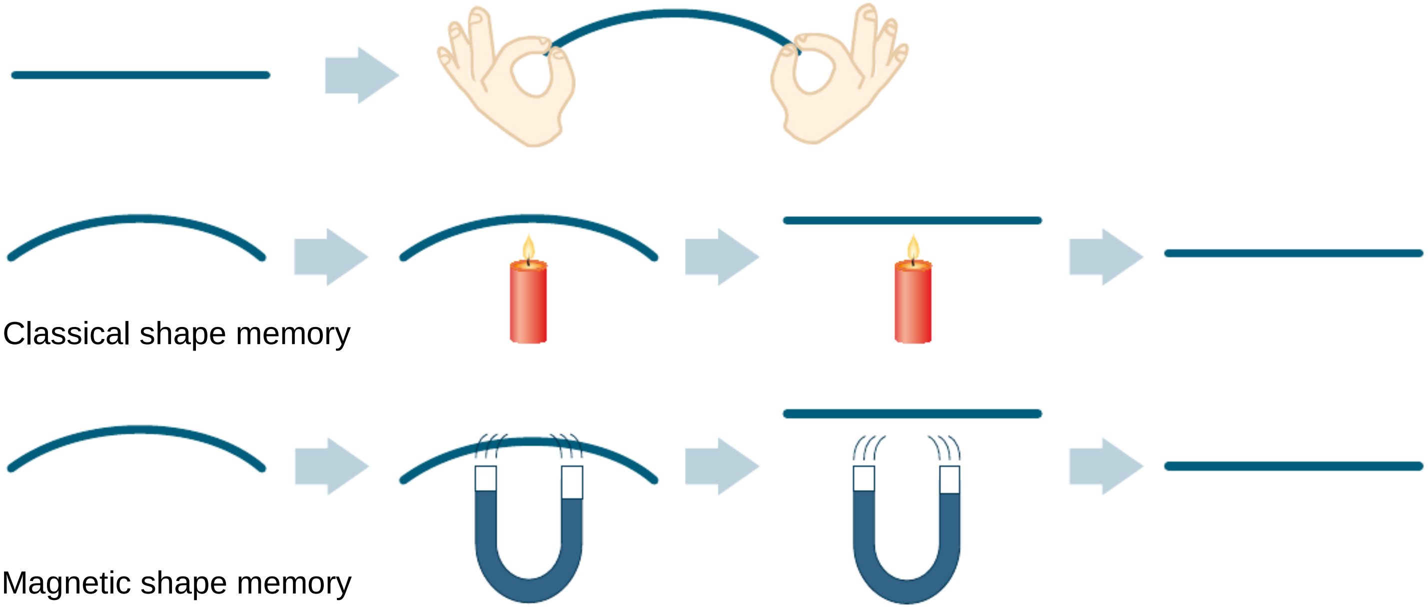

Classical shape memory

Magnetic shape memory

The magic of magnetic shape memory…

- Intro & Macrotwins
- *Movie with examples*
- Microtwins
- Nanotwins
- Summary

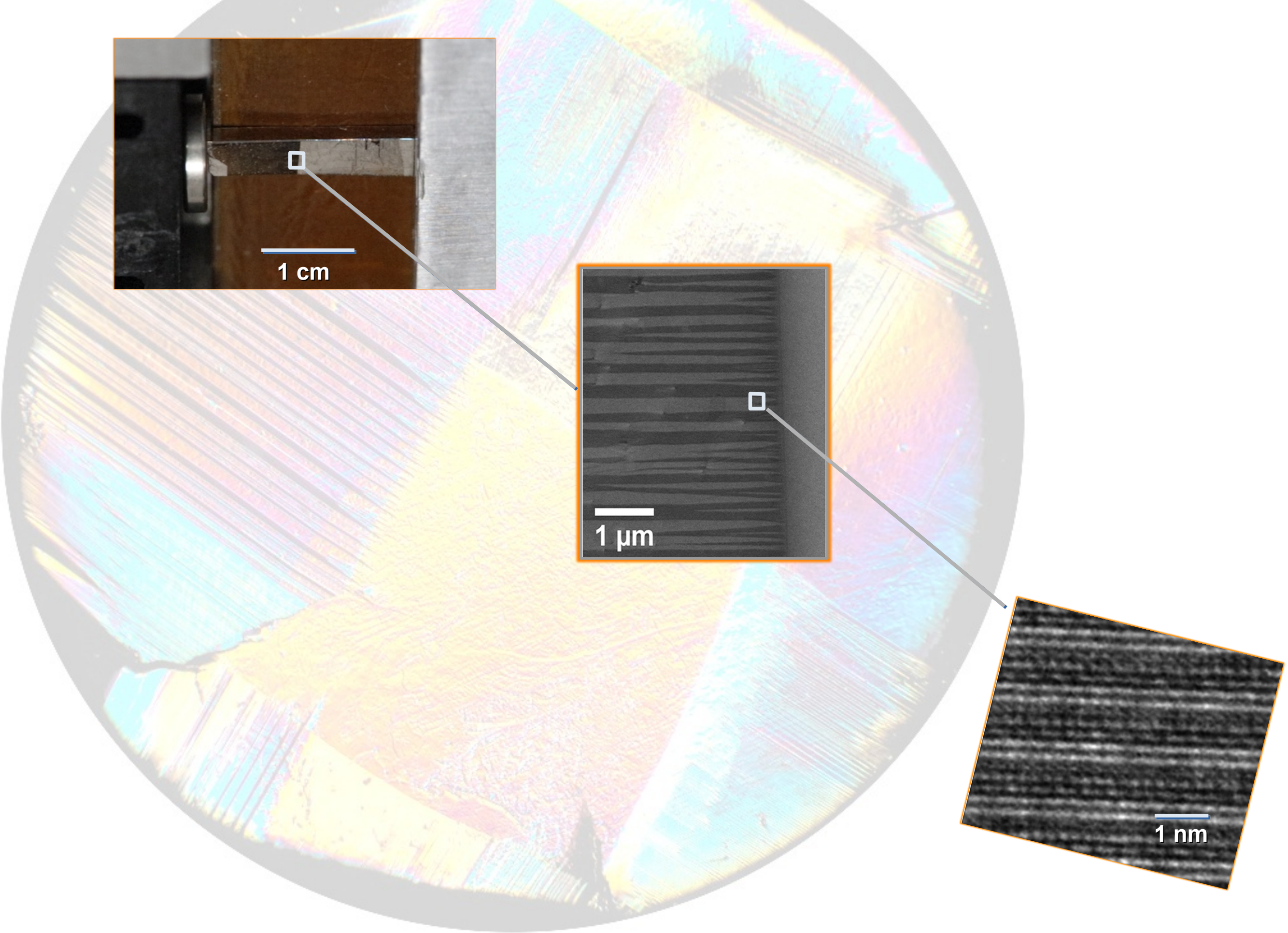

Ni_2MnGa ($Ni_{50}Mn_{25}Ga_{25}$) with the Heusler $L2_1$ structure as the prototype MSM alloy

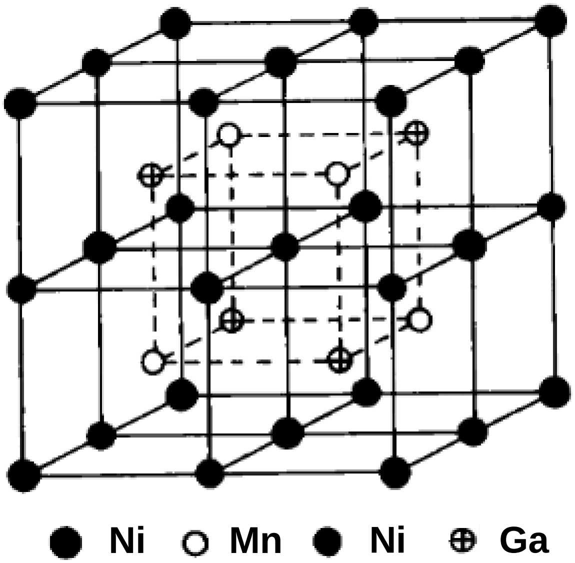

(alternatives: Fe-Pt, Fe-Pd, Nd, $La_{2-x}Sr_xCuO_4$)

Webster, P. J. (1969). Heusler alloys. Contemporary Physics, 10(6), 559–577.

Ni_2MnGa ($Ni_{50}Mn_{25}Ga_{25}$) with the Heusler $L2_1$ structure as the prototype MSM alloy

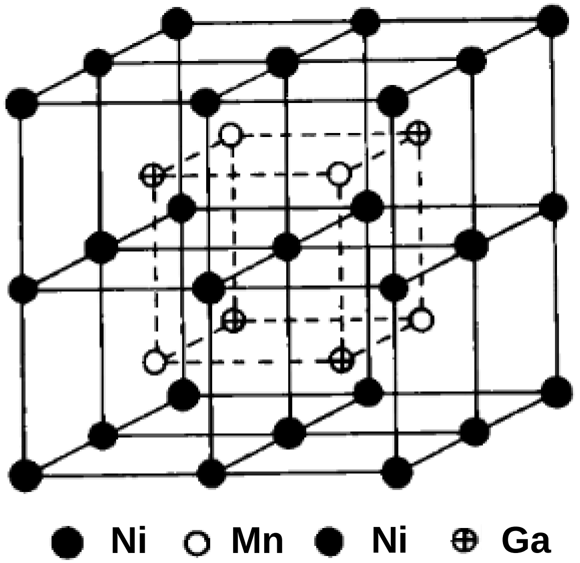

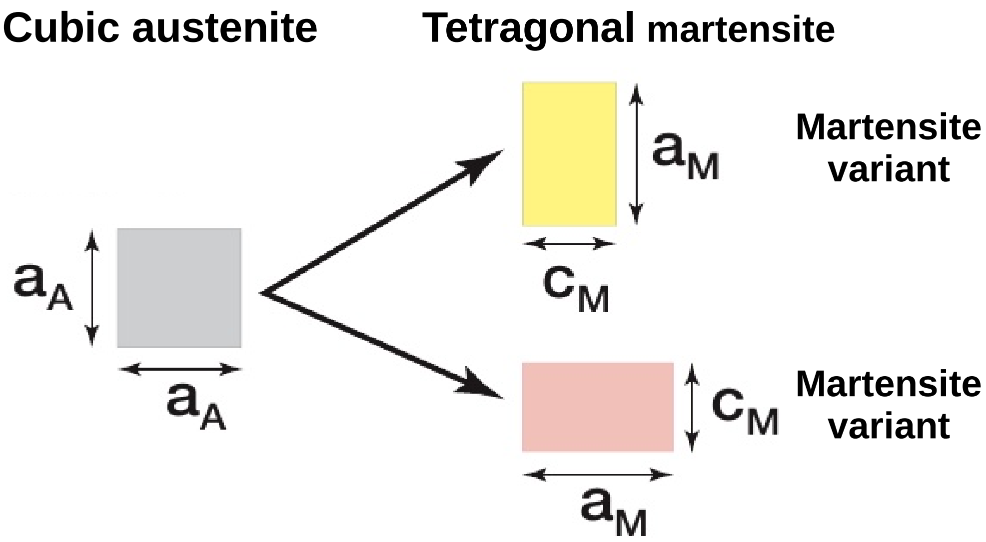

(alternatives: Fe-Pt, Fe-Pd, Nd, $La_{2-x}Sr_xCuO_4$)

Webster, P. J. (1969). Heusler alloys. Contemporary Physics, 10(6), 559–577.

Ni_2MnGa ($Ni_{50}Mn_{25}Ga_{25}$) with the Heusler $L2_1$ structure as the prototype MSM alloy

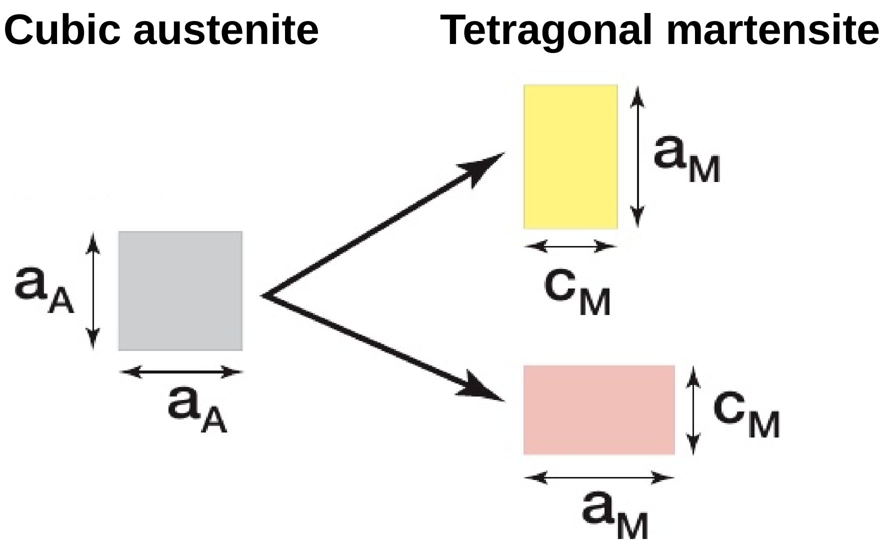

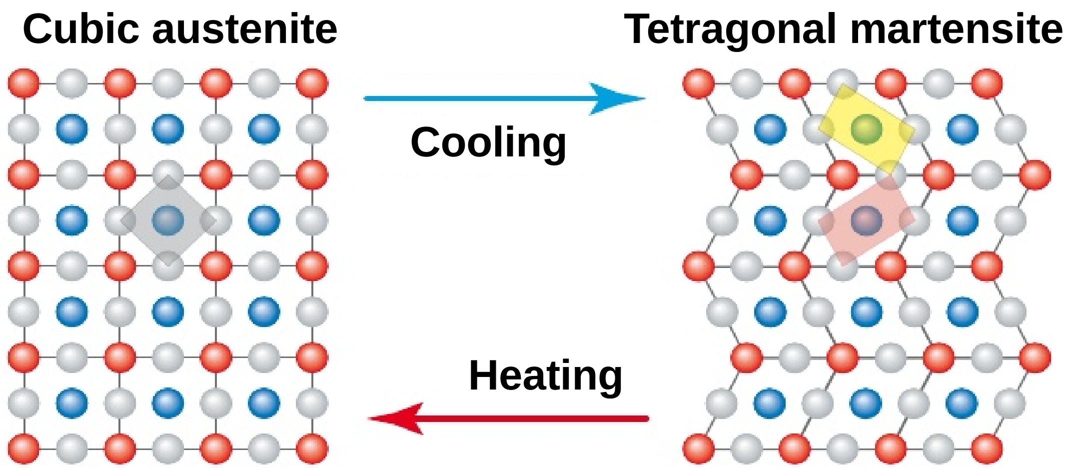

Ni_2MnGa ($Ni_{50}Mn_{25}Ga_{25}$) with the Heusler $L2_1$ structure as the prototype MSM alloy

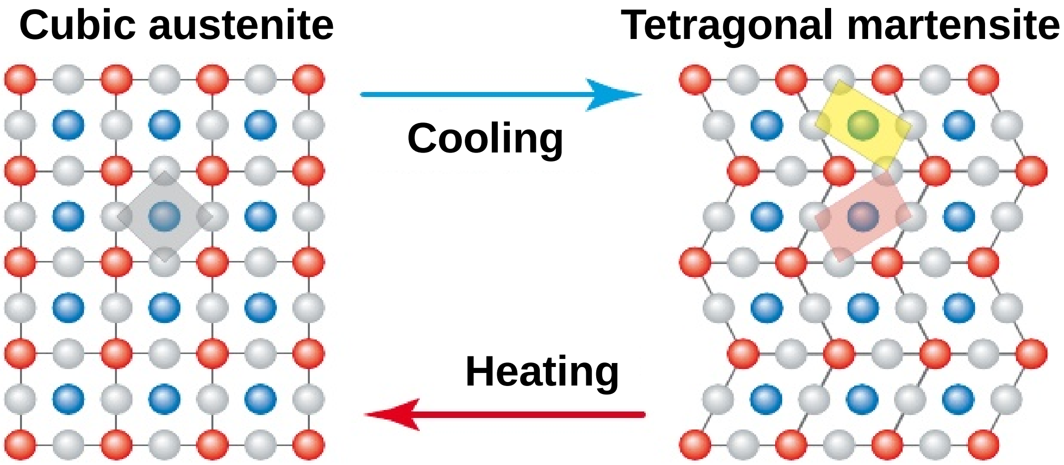

Ni_2MnGa ($Ni_{50}Mn_{25}Ga_{25}$) with the Heusler $L2_1$ structure as the prototype MSM alloy

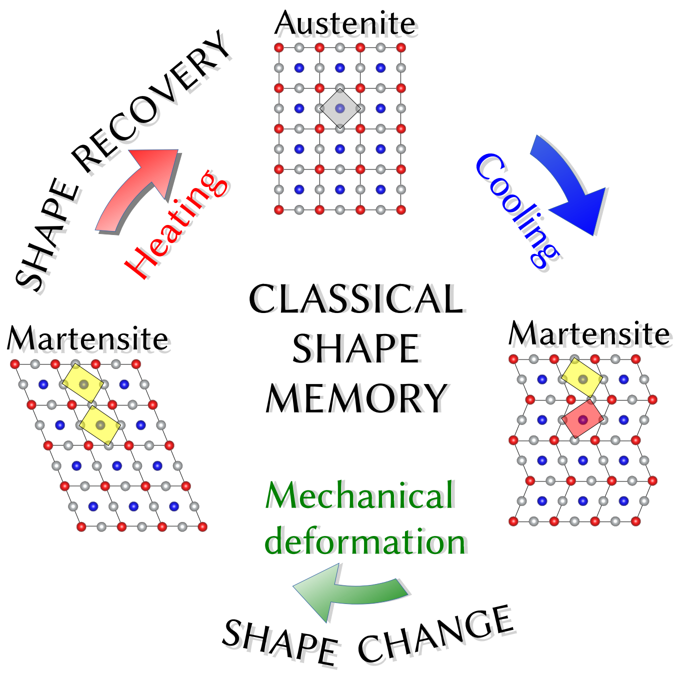

Martensite variant 1 Martensite variant 2 Cubic austenite

Ni_2MnGa ($Ni_{50}Mn_{25}Ga_{25}$) with the Heusler $L2_1$ structure as the prototype MSM alloy

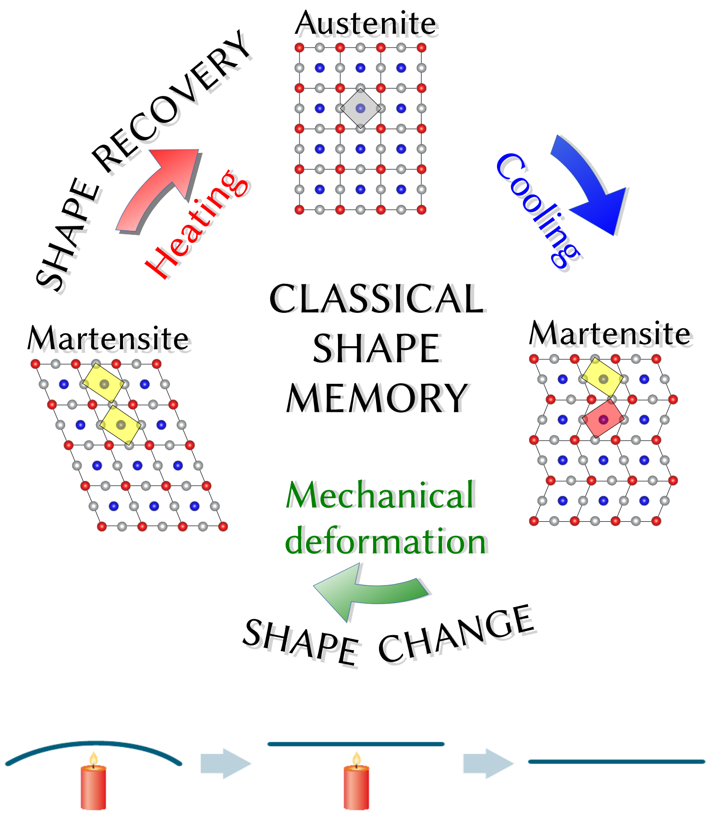

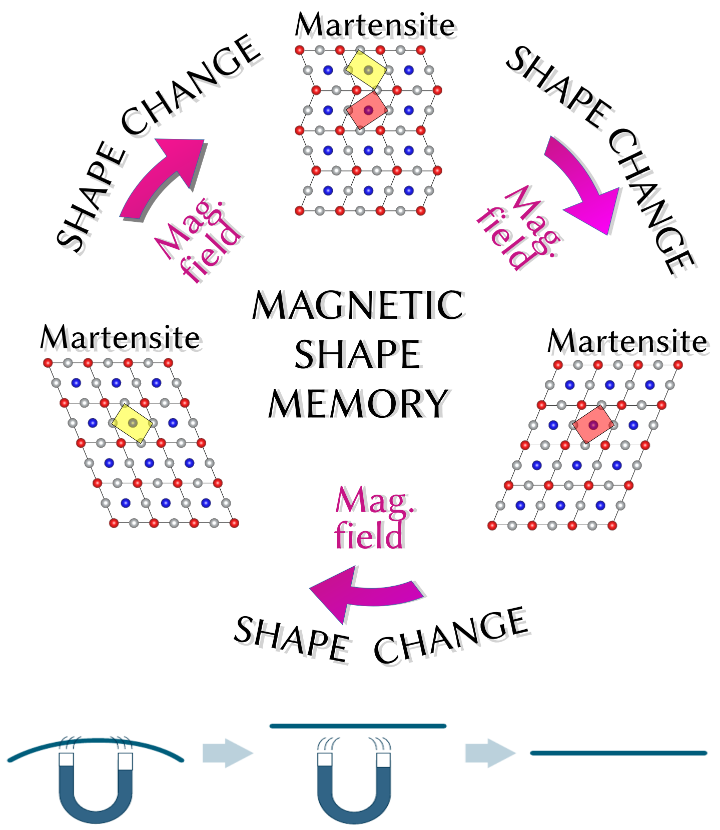

Martensite variant 1 | Martensite variant 2 | Cubic austenite

Ni_2MnGa ($Ni_{50}Mn_{25}Ga_{25}$) with the Heusler $L2_1$ structure as the prototype MSM alloy

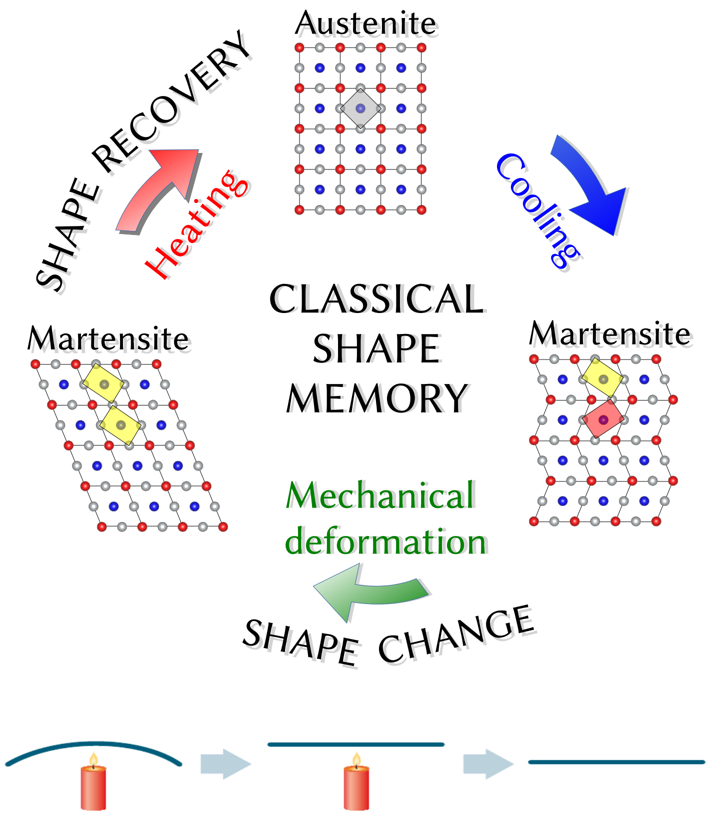

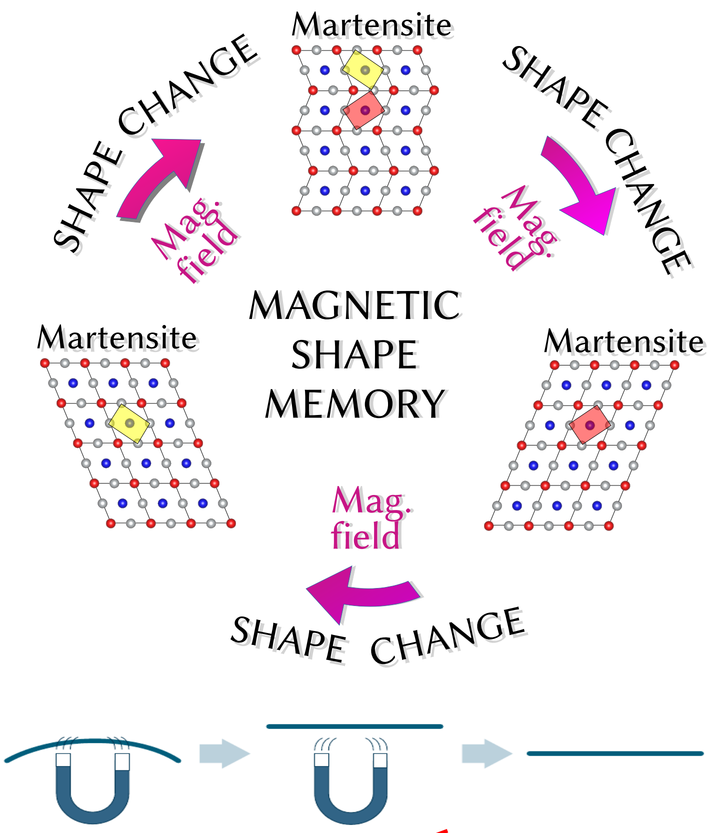

Martensite variant 1

Martensite variant 2

~~Cubic austenite~~

Ni_2MnGa ($Ni_{50}Mn_{25}Ga_{25}$) with the Heusler $L2_1$ structure as the prototype MSM alloy

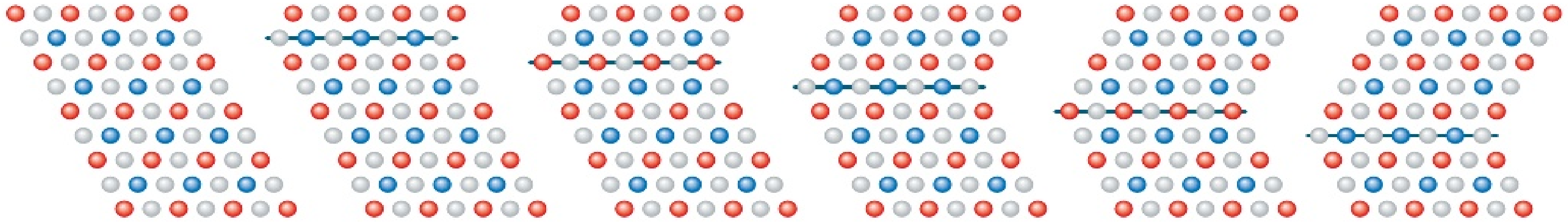

Martensite variant 1

Martensite variant 2

Ni_2MnGa ($Ni_{50}Mn_{25}Ga_{25}$) with the Heusler $L2_1$ structure as the prototype MSM alloy

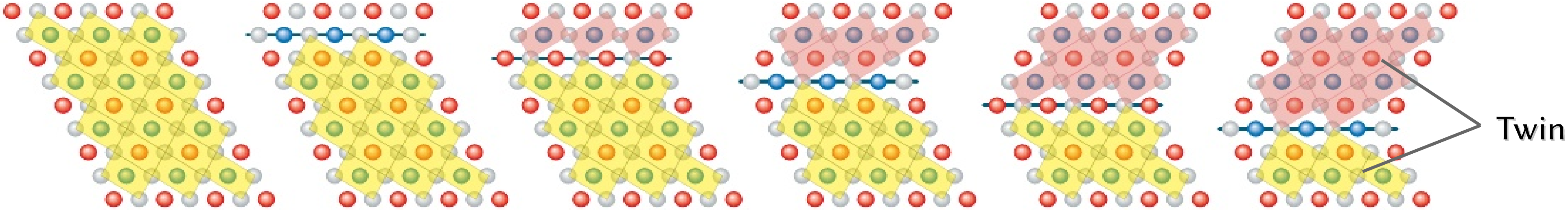

Ni_2MnGa ($Ni_{50}Mn_{25}Ga_{25}$) with the Heusler $L2_1$ structure as the prototype MSM alloy

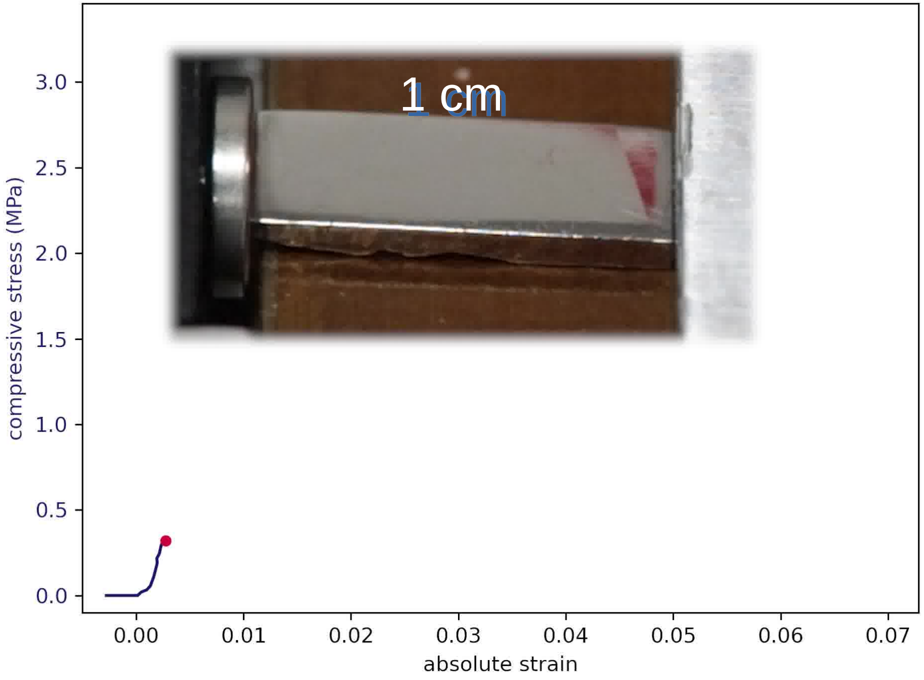

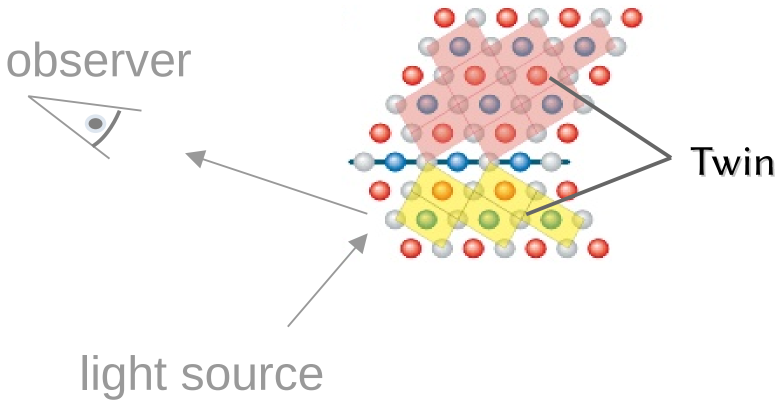

Martensite variant 1

Martensite variant 2

Twin boundary, (101) plane

Musiienko, Denys, et al. J. Materials Research and Technology 14 (2021): 1934-1944.

Ni_2MnGa ($Ni_{50}Mn_{25}Ga_{25}$) with the Heusler $L2_1$ structure as the prototype MSM alloy

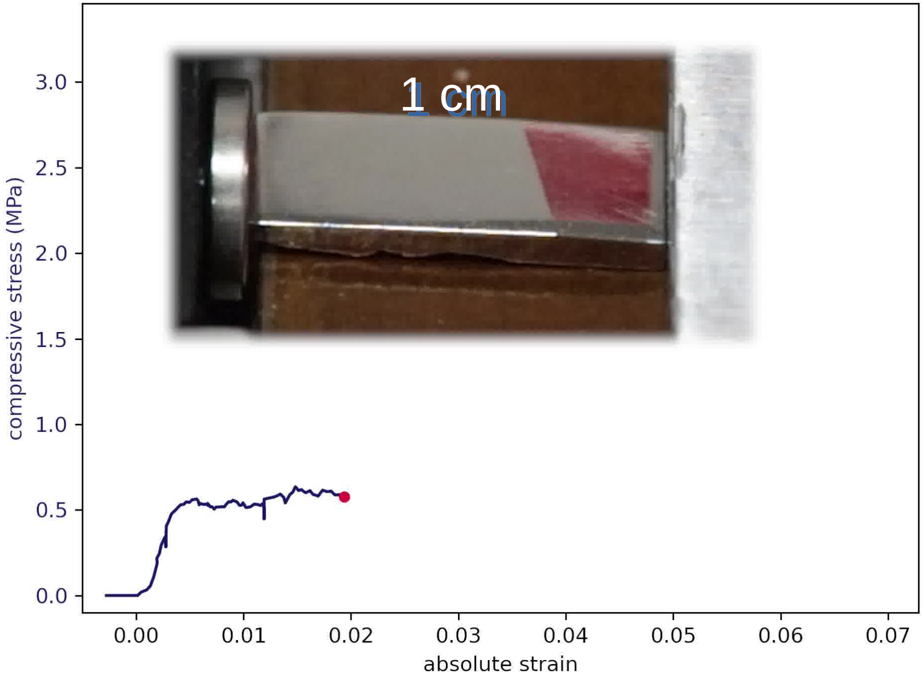

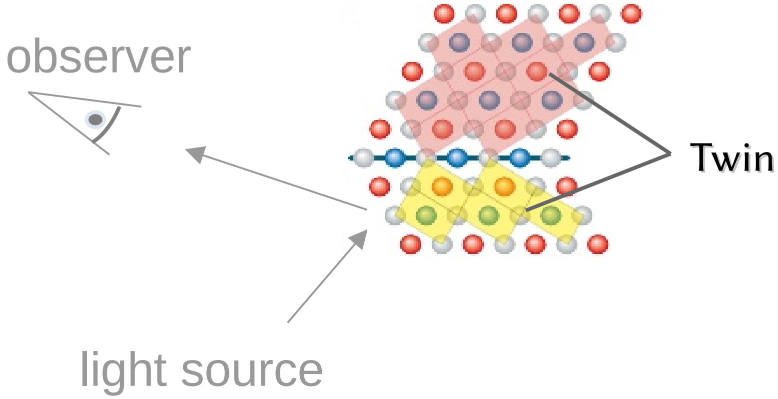

Martensite variant 1 | Martensite variant 2 | Twin boundary, (101) plane

Musiienko, Denys, et al. J. Materials Research and Technology 14 (2021): 1934-1944.

Ni_2MnGa ($Ni_{50}Mn_{25}Ga_{25}$) with the Heusler $L2_1$ structure as the prototype MSM alloy

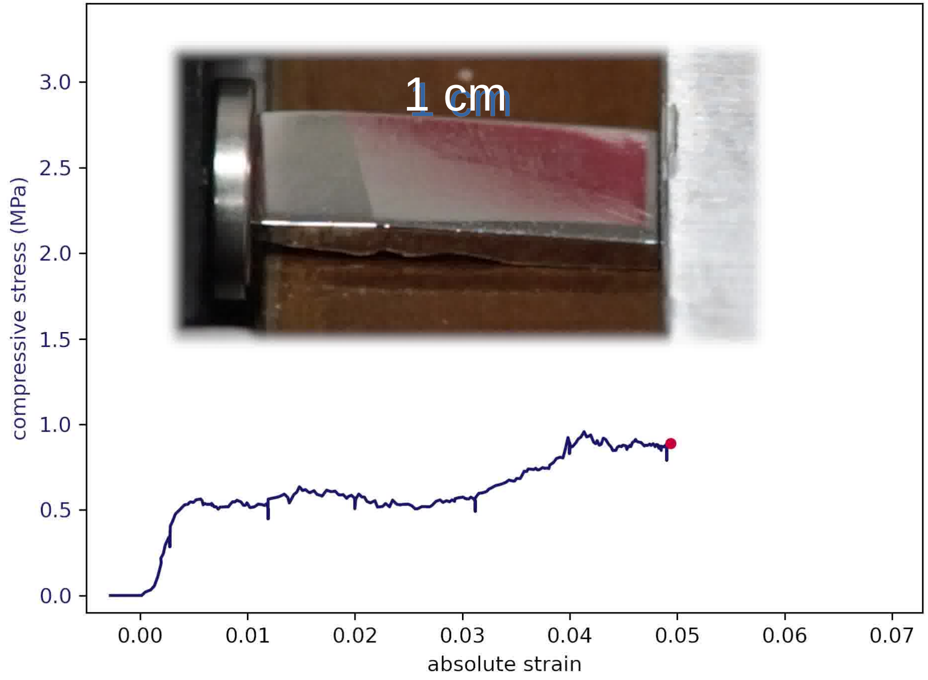

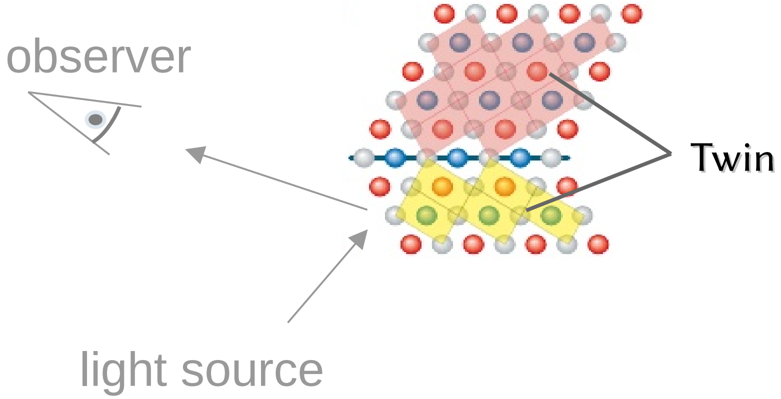

Martensite variant 1 — Martensite variant 2 — Twin boundary, (101) plane

Musiienko, Denys, et al. J. Materials Research and Technology 14 (2021): 1934-1944.

Ni_2MnGa ($Ni_{50}Mn_{25}Ga_{25}$) with the Heusler $L2_1$ structure as the prototype MSM alloy

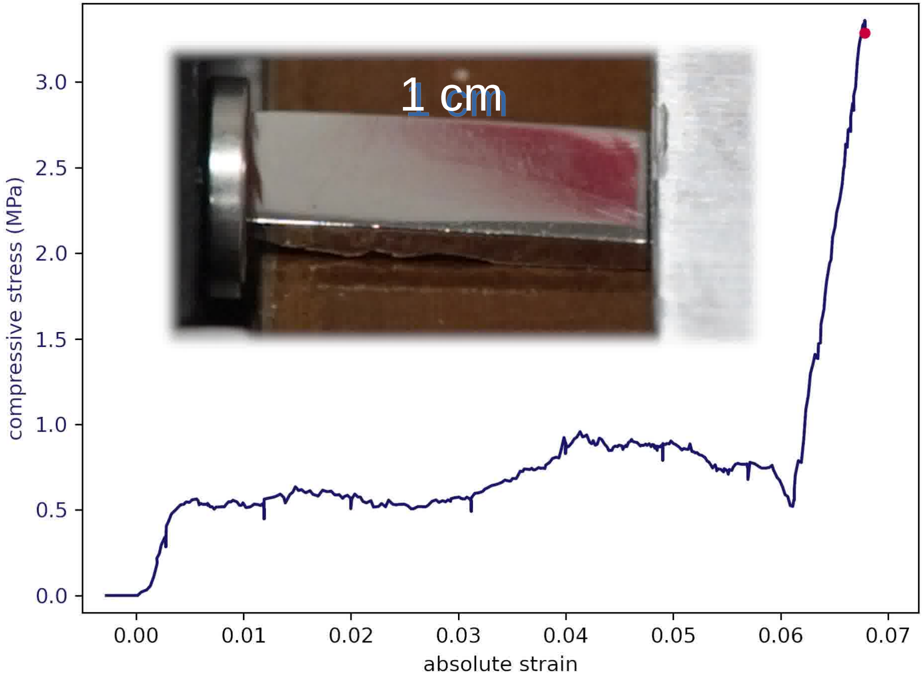

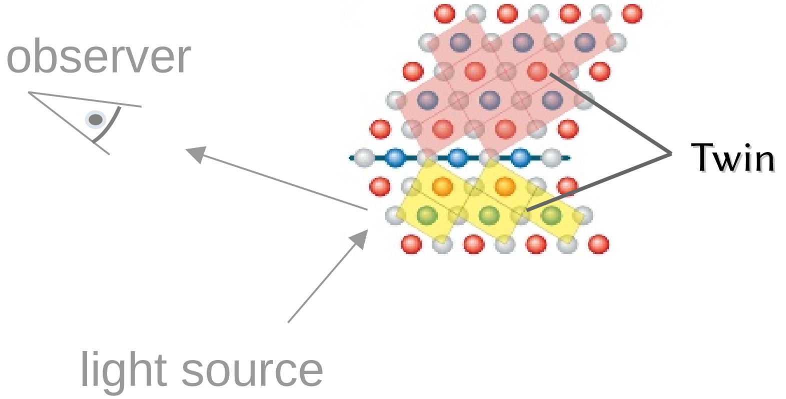

Martensite variant 1

Martensite variant 2

Twin boundary, (101) plane

Musiienko, Denys, et al. J. Materials Research and Technology 14 (2021): 1934-1944.

Ni_2MnGa ($Ni_{50}Mn_{25}Ga_{25}$) with the Heusler $L2_1$ structure as the prototype MSM alloy

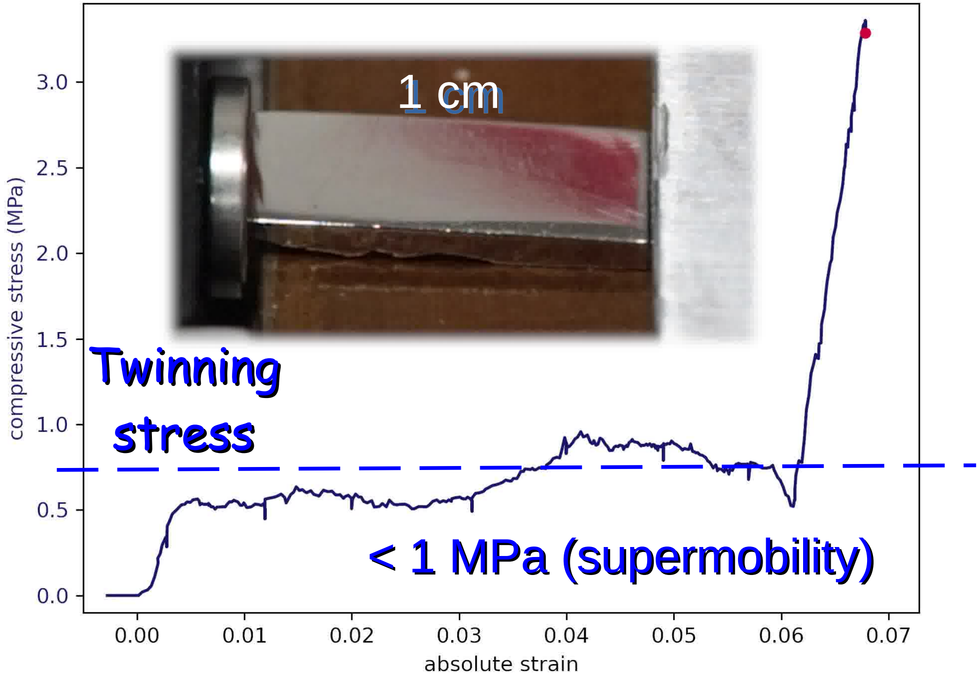

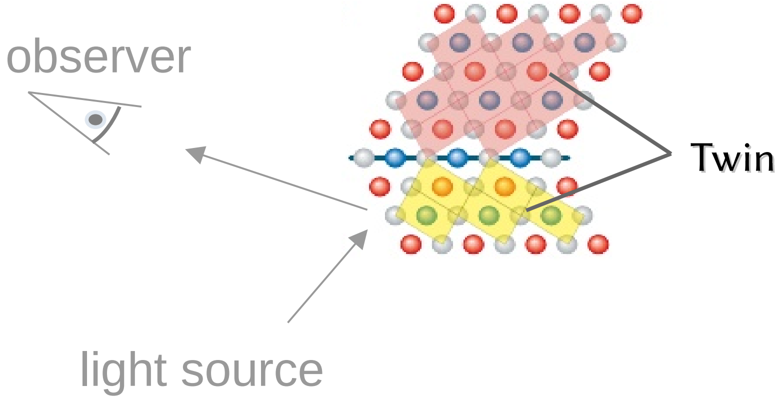

Martensite variant 1 — Martensite variant 2 — Twin boundary, (101) plane

Musiienko, Denys, et al. J. Materials Research and Technology 14 (2021): 1934-1944.

Motivation

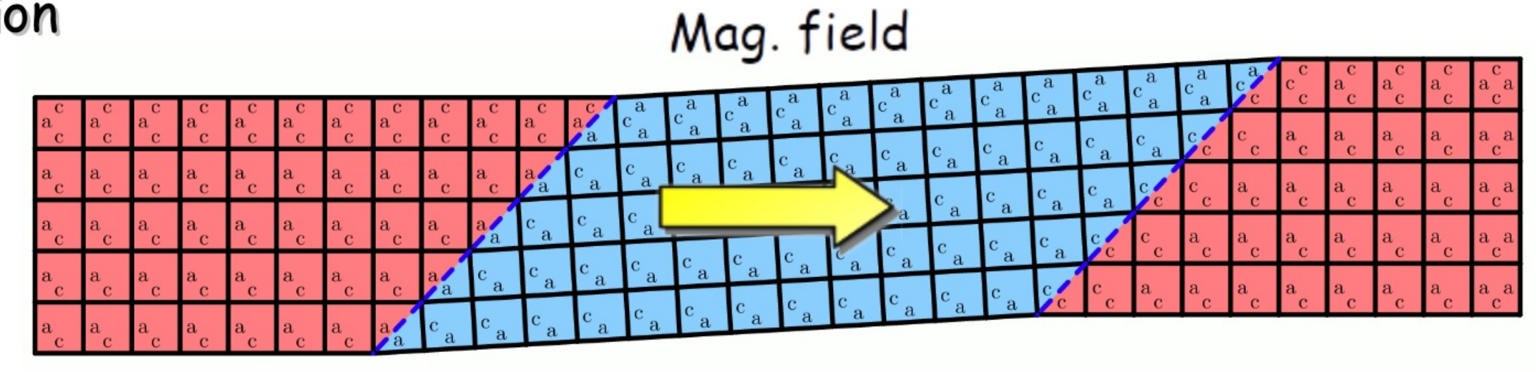

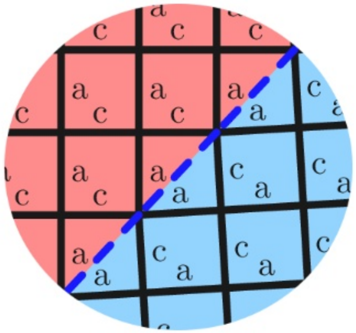

$$W_{MECH} = \sigma_{TW} \cdot \varepsilon_0$$

$$\Delta W_{MAG} = K_U$$

$$\Delta W_{MAG} > W_{MECH}$$

$$\sigma_{TW} < K_U / \varepsilon_0$$

Motivation

Mag. field

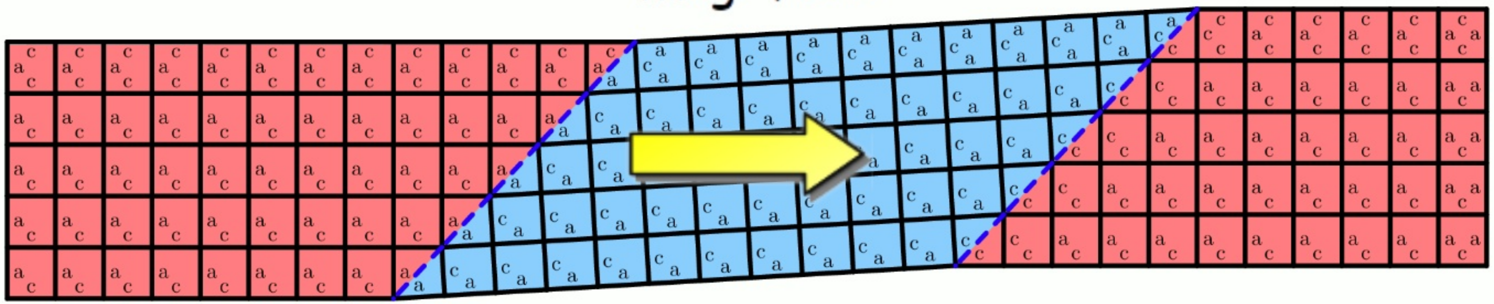

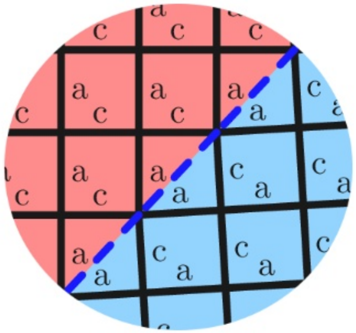

$$W_{MECH} = \sigma_{TW} \cdot \varepsilon_0$$

$$\Delta W_{MAG} = K_U$$

$$\Delta W_{MAG} > W_{MECH}$$

$$\sigma_{TW} < K_U / \varepsilon_0$$

Motivation

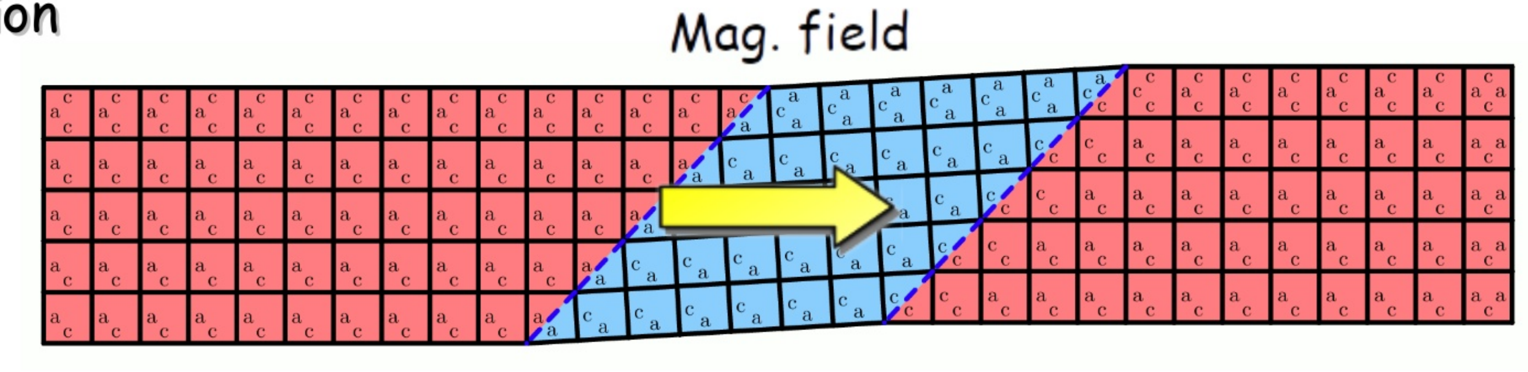

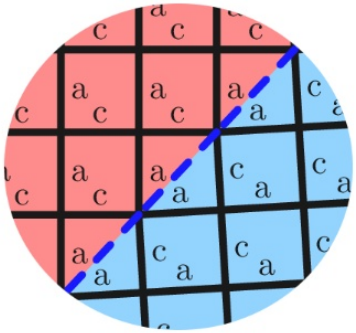

$$W_{MECH} = \sigma_{TW} \cdot \varepsilon_0$$

$$\Delta W_{MAG} = K_U$$

$$\Delta W_{MAG} > W_{MECH}$$

$$\sigma_{TW} < K_U / \varepsilon_0$$

Motivation

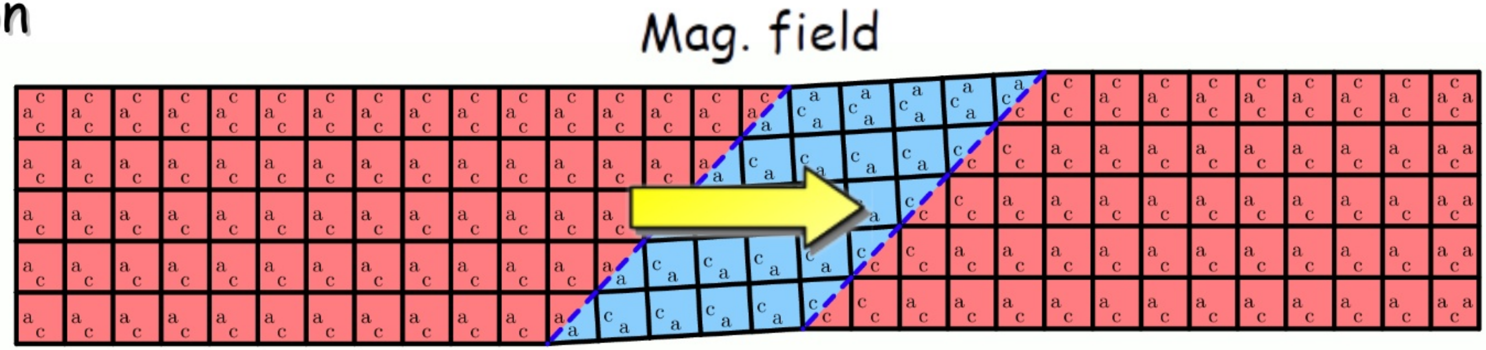

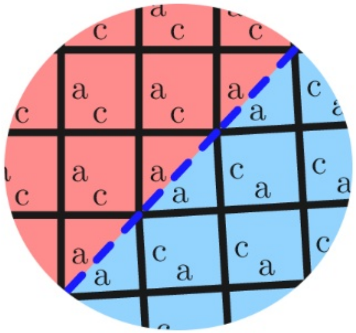

$$W_{MECH} = \sigma_{TW} \cdot \varepsilon_0$$

$$\Delta W_{MAG} = K_U$$

$$\Delta W_{MAG} > W_{MECH}$$

$$\sigma_{TW} < K_U / \varepsilon_0$$

Motivation

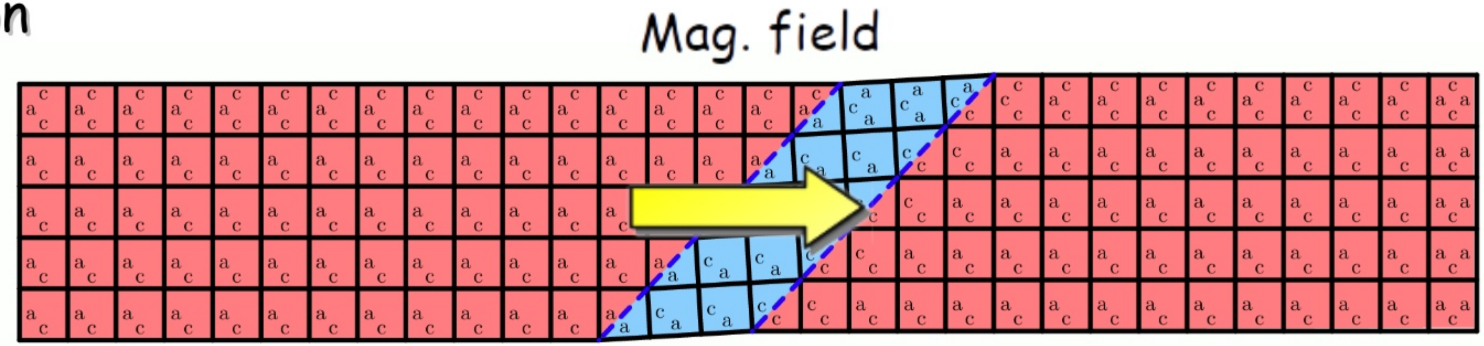

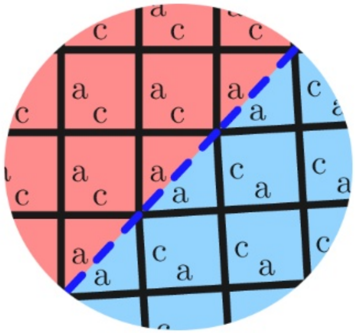

$$W_{MECH} = \sigma_{TW} \cdot \varepsilon_0$$

$$\Delta W_{MAG} = K_U$$

$$\Delta W_{MAG} > W_{MECH}$$

$$\sigma_{TW} < K_U / \varepsilon_0$$

Motivation

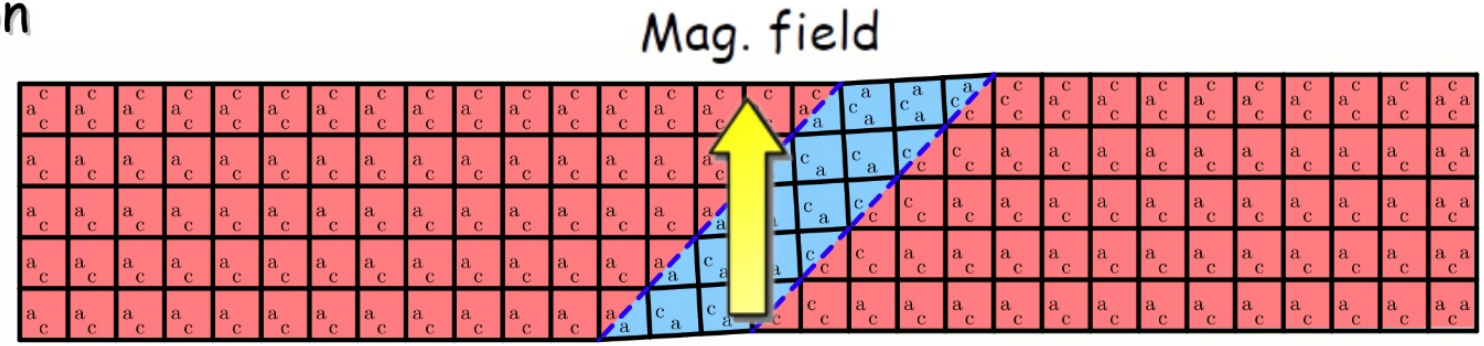

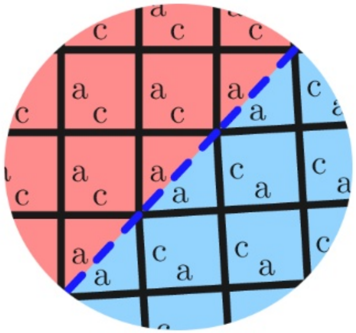

$$W_{MECH} = \sigma_{TW} \cdot \varepsilon_0$$

$$\Delta W_{MAG} = K_U$$

$$\Delta W_{MAG} > W_{MECH}$$

$$\sigma_{TW} < K_U / \varepsilon_0$$

Motivation

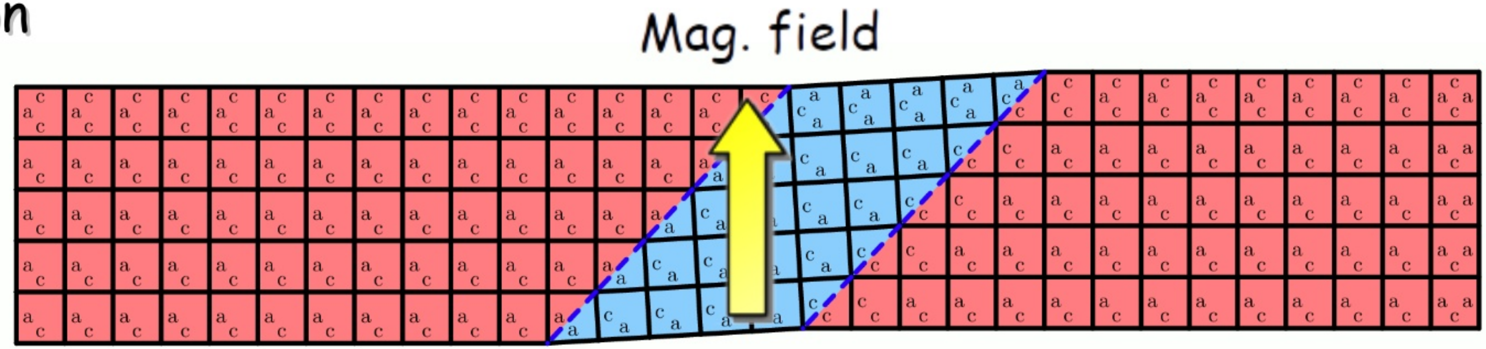

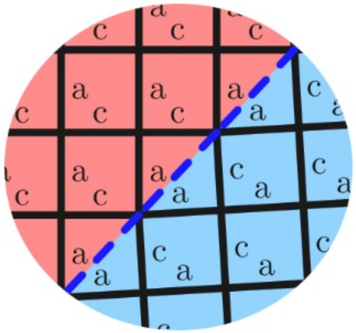

$$W_{MECH} = \sigma_{TW} \cdot \varepsilon_0$$

$$\Delta W_{MAG} = K_U$$

$$\Delta W_{MAG} > W_{MECH}$$

$$\sigma_{TW} < K_U / \varepsilon_0$$

Motivation

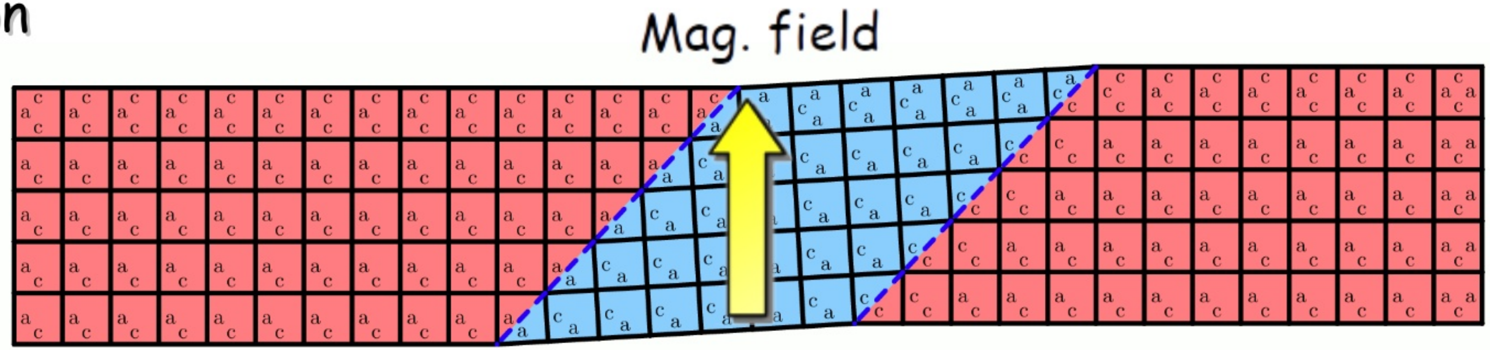

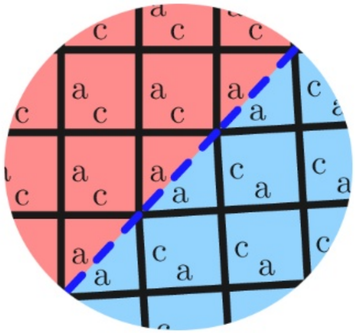

$$W_{MECH} = \sigma_{TW} \cdot \varepsilon_0$$

$$\Delta W_{MAG} = K_U$$

$$\Delta W_{MAG} > W_{MECH}$$

$$\sigma_{TW} < K_U/\varepsilon_0$$

Motivation

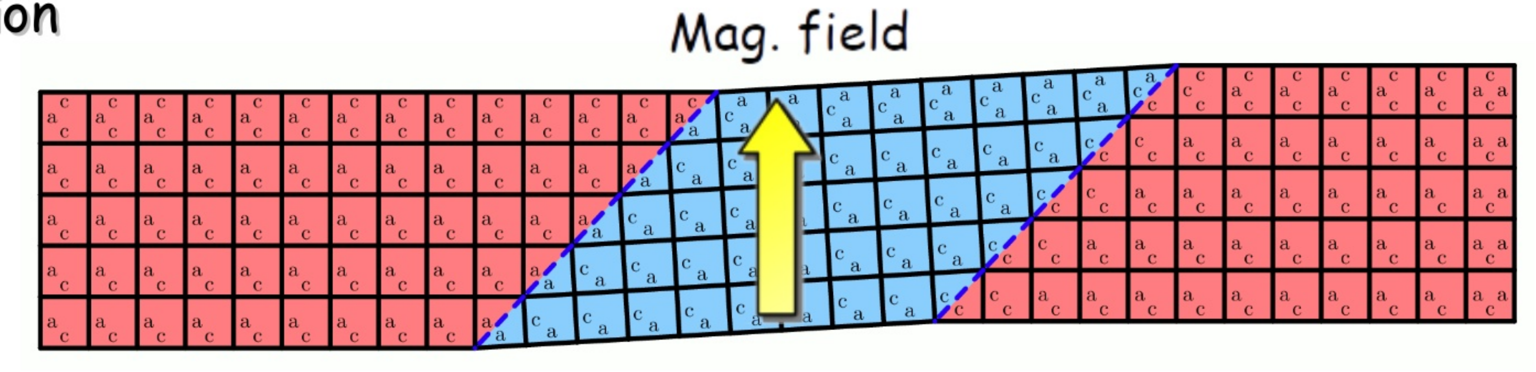

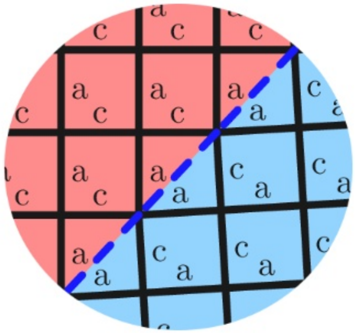

$$W_{MECH} = \sigma_{TW} \cdot \varepsilon_0$$

$$\Delta W_{MAG} = K_U$$

$$\Delta W_{MAG} > W_{MECH}$$

$$\sigma_{TW} < K_U / \varepsilon_0$$

Motivation

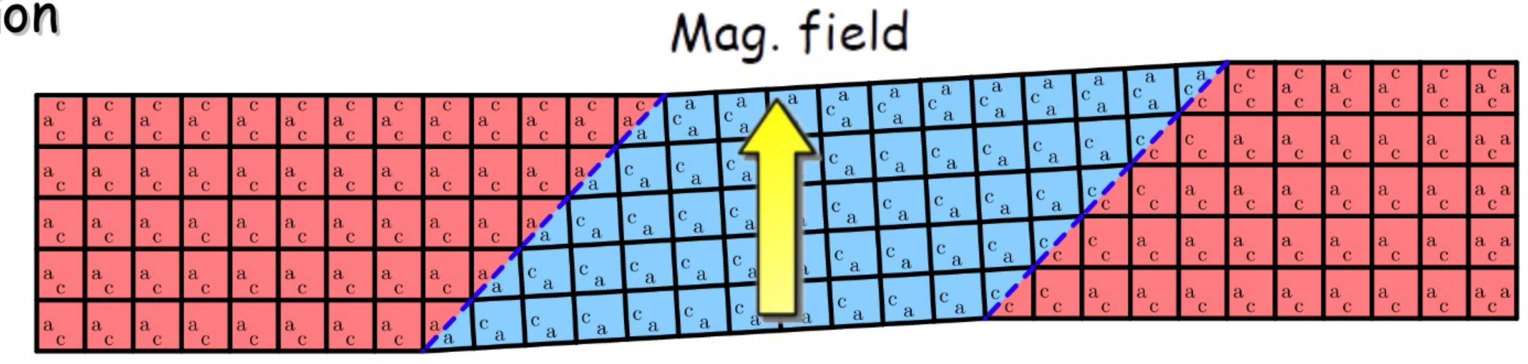

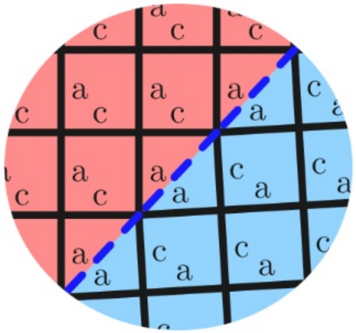

$$W_{MECH} = \sigma_{TW} \cdot \varepsilon_0$$

$$\Delta W_{MAG} = K_U$$

$$\Delta W_{MAG} > W_{MECH}$$

$$\sigma_{TW} < K_U / \varepsilon_0$$

Motivation

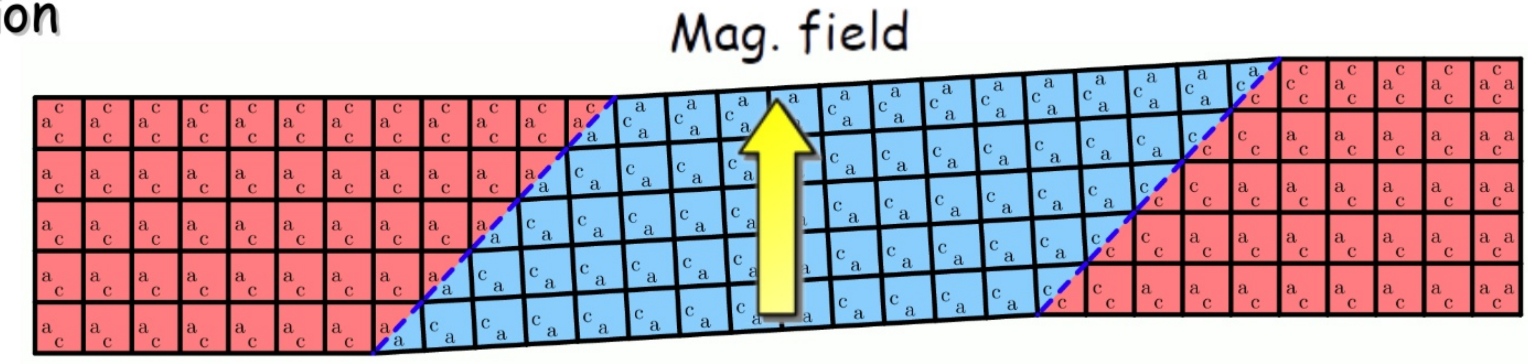

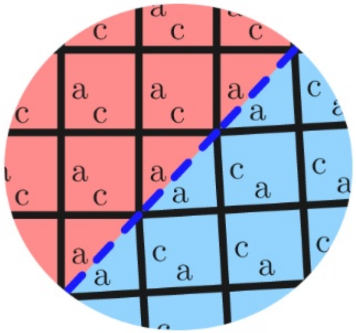

$$W_{MECH} = \sigma_{TW} \cdot \varepsilon_0$$

$$\Delta W_{MAG} = K_U$$

$$\Delta W_{MAG} > W_{MECH}$$

$$\sigma_{TW} < K_U/\varepsilon_0$$

Ni_2MnGa ($Ni_{50}Mn_{25}Ga_{25}$) with the Heusler $L2_1$ structure as the prototype MSM alloy

Magnetic Shape Memory Effect

Mart. reorientation
MIR, ~ 0.01 -1 T

Mart. transformation
MIM, ~ 1-100 T

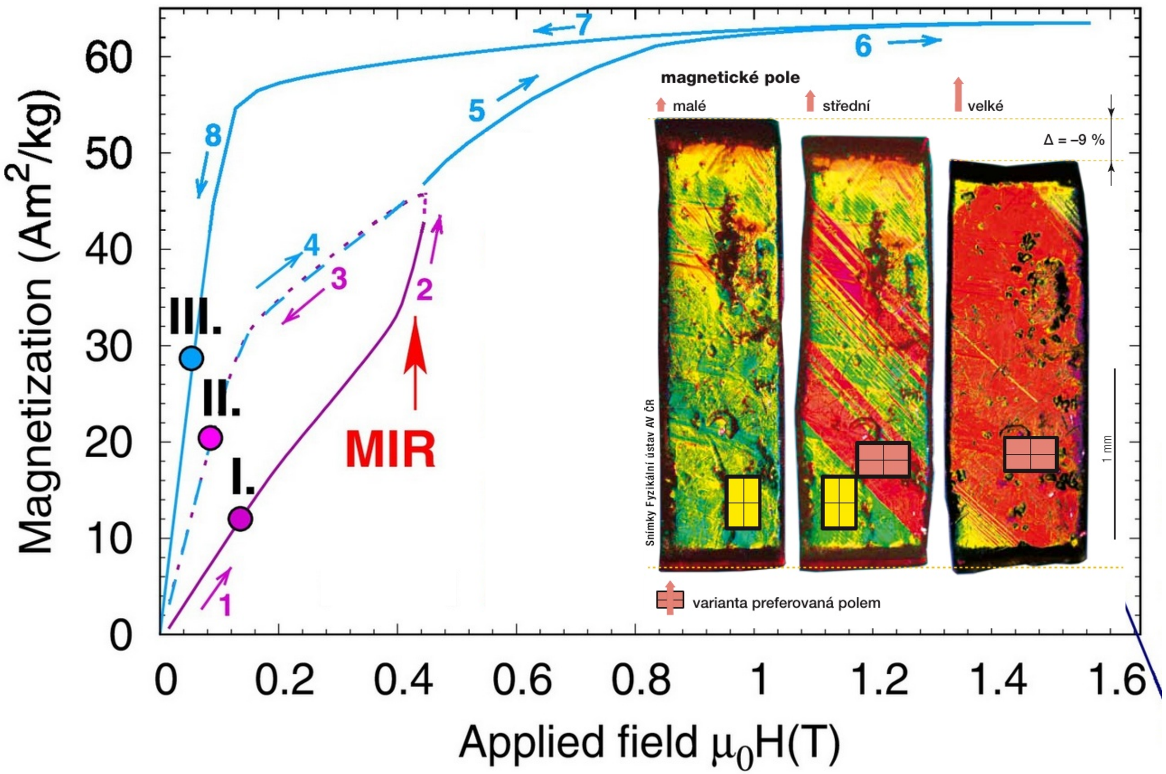

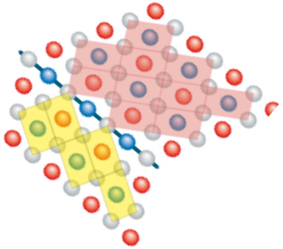

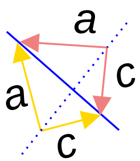

Martensite variant 1

Martensite variant 2

Twin boundary, (101) plane

Rameš, M., et al., Scripta Materialia 142 (2018): 61-65.

Summary I

- Prototype magnetic shape material = **single crystal of Ni-Mn-Ga**
- **Deformation up to 12% in mag. field observable macroscopically (naked eye)**
- Key enabler of the effect = **supermobility of twin boundaries** (1 MPa)
- Key principle = **switching between martensite variants** (reorientation) of tetragonal lattice
  - mechanically
  - **by magnetic field** (3 MPa)
- **No phase transformation directly involved**

The magic of magnetic shape memory…

- Intro & Macrotwins
- *Movie with examples*
- Microtwins
- Nanotwins
- Summary

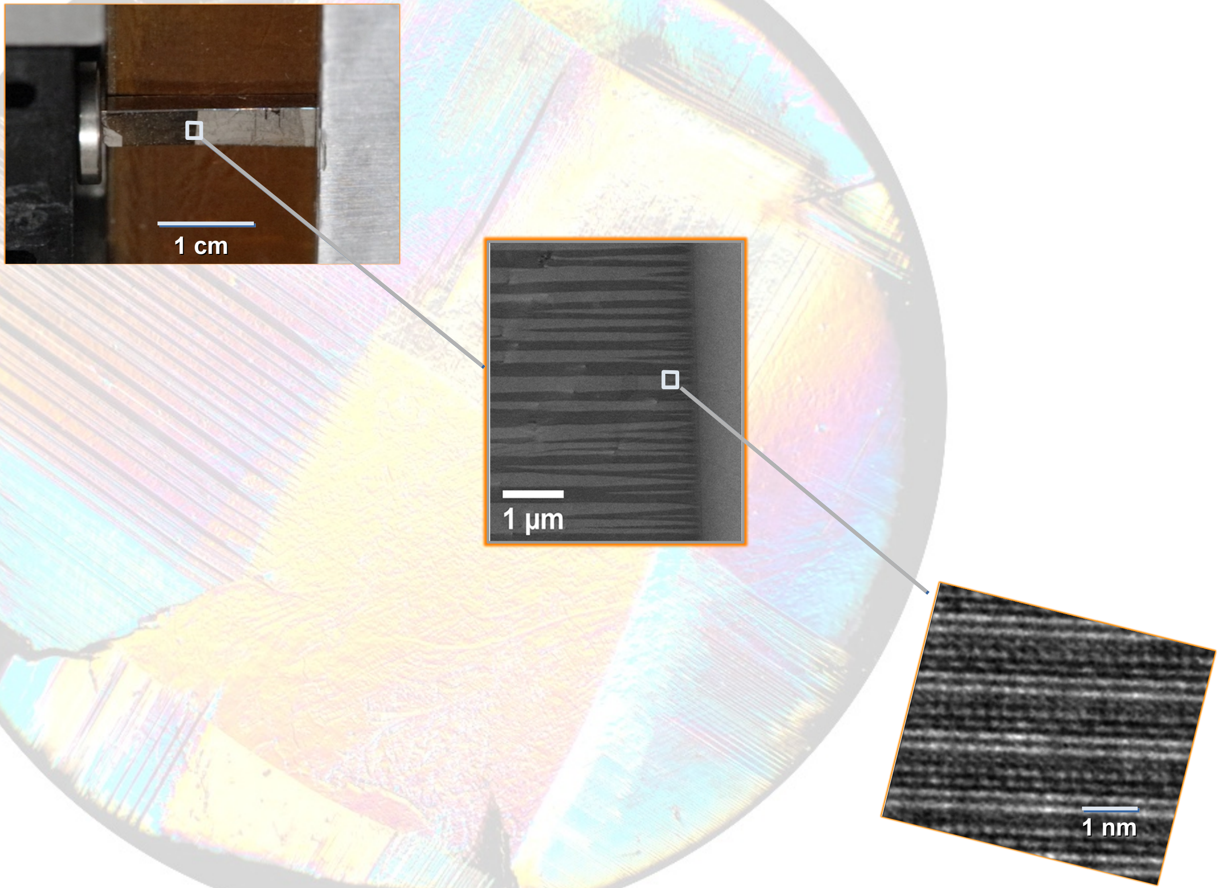

The magic of magnetic shape memory…

- Intro & Macrotwins
- *Movie with examples*
- Microtwins
- Nanotwins
- Summary

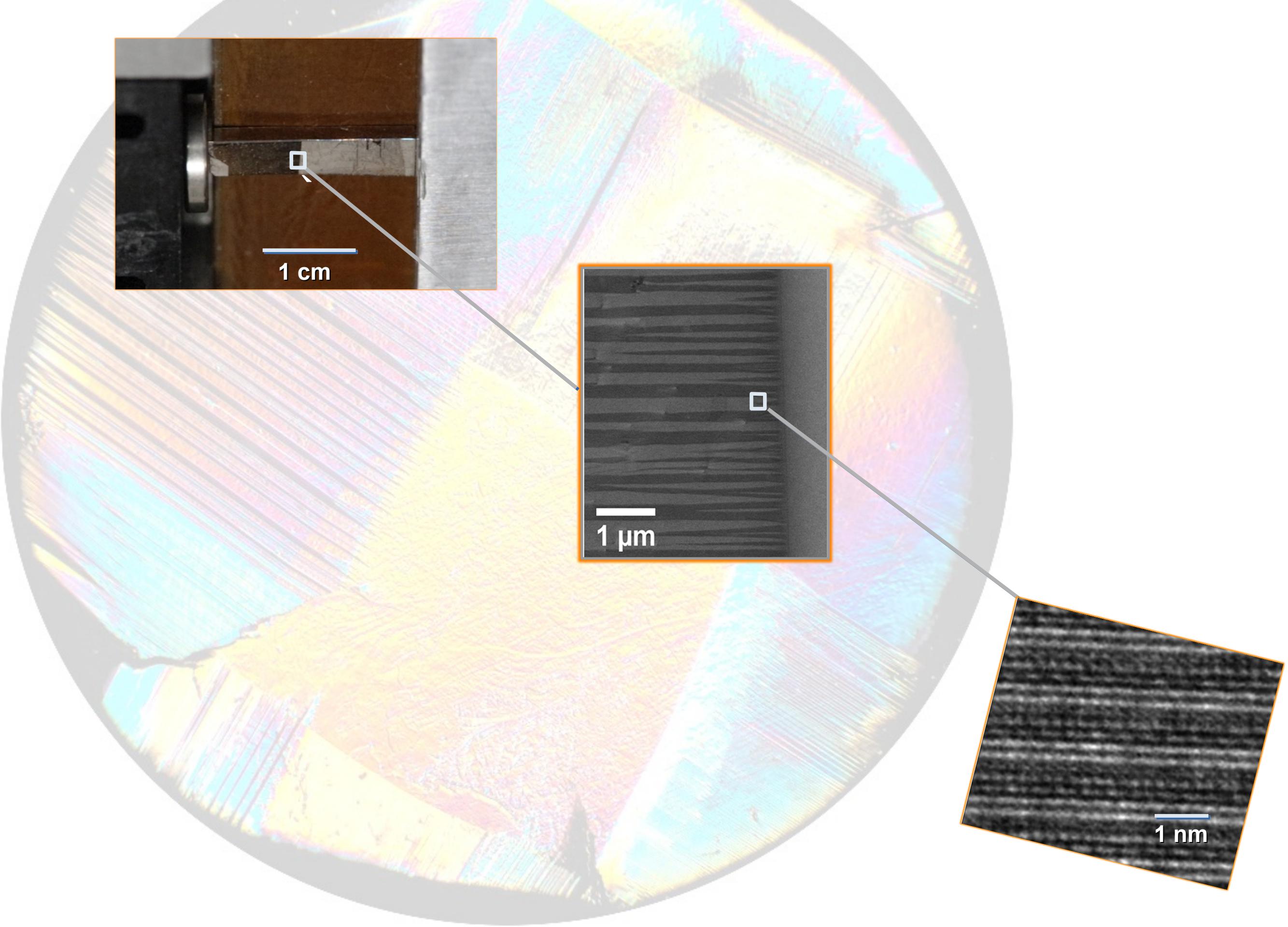

Twin microstructure

Tetragonal lattice : Enough to describe phenomenology

$a \approx b \approx 0.60$ nm
$c \approx 0.56$ nm
$\gamma \approx 90°$

$c/a \approx 0.94$

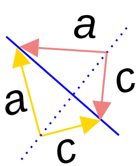

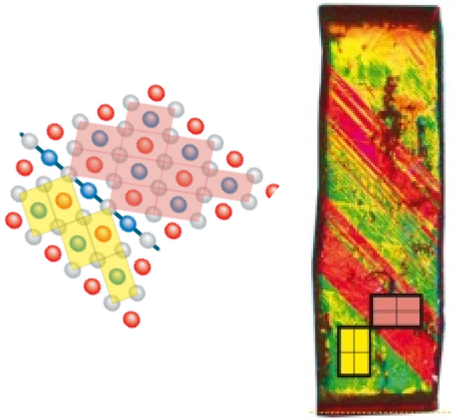

In reality slightly monoclinic: Needed to describe mechanisms & microstructure

$a = 0.5969$ nm
$b = 0.5953$ nm
$c = 0.5615$ nm
$\gamma = 90.3°$

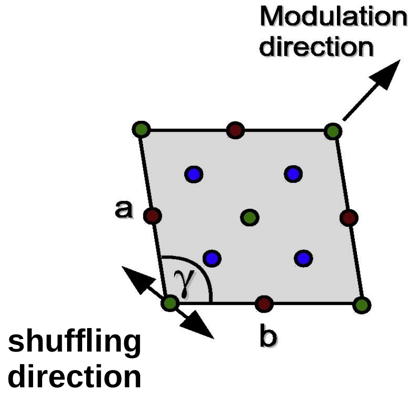

=> Other complex twinning in addition to *a/c* twins.

Straka, Ladislav, et al., Acta Materialia 59.20 (2011): 7450-7463.

Twin microstructure – 12 variants, 8 twinning systems, 5 different twin types

a = 0.5969 nm
b = 0.5953 nm
c = 0.5615 nm
γ = 90.3°

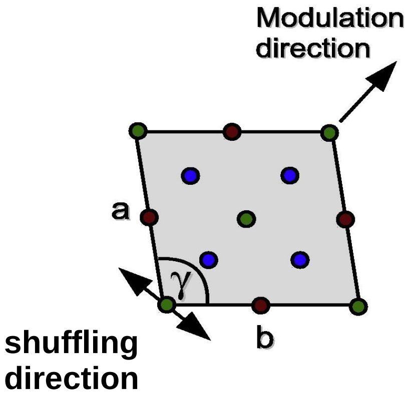

Variants	λ_2		n	$(F^{-1}b)/\lvert F^{-1}b\rvert$	Twinning type
1:2	1.0000	T_1	[0;1;0]	[1;0;0]	Modulation
		T_2	[1;0;0]	[0;1;0]	Modulation
1:3	1.0000	T_1	$1/\sqrt{2}[1;-1;0]$	$1/\sqrt{2}[1;1;0]$	Compound
		T_2	$1/\sqrt{2}[1;1;0]$	$1/\sqrt{2}[1;-1;0]$	Compound
1:4	1.0000	T_1	[−0.9509;0.3094;0]	[0.3094;0.9509;0]	Non-conventional[a]
		T_2	[0.3094;0.9509;0]	[0.9509;−0.3094;0]	Non-conventional[a]
1:5	1.0000	T_1	$1/\sqrt{2}[0;1;-1]$	[0.0682;0.7055;0.7055]	Type I
		T_2	[0.0779;0.7050;0.7050]	$1/\sqrt{2}[0;-1;1]$	Type II[b]
1:6	1.0000	T_1	[0.0779;0.7050;−0.7050]	$1/\sqrt{2}[0;1;1]$	Type II[b]
		T_2	$1/\sqrt{2}[0;1;1]$	[−0.0682;−0.7055;0.7055]	Type I
1:7	1.0094				
1:8	1.0094				
1:9	0.9907				
1:10	0.9907				
1:11	1.0000	T_1	$1/\sqrt{2}[1;0;-1]$	[0.7057;0.0637;0.7057]	Type I
		T_2	[0.7053;0.0721;0.7053]	$1/\sqrt{2}[-1;0;1]$	Type II[c]
1:12	1.0000	T_1	[0.7053;0.0721;−0.7053]	$1/\sqrt{2}[1;0;1]$	Type II[c]
		T_2	$1/\sqrt{2}[1;0;1]$	[−0.7057;−0.0637;0.7057]	Type I

landscape around *a/c* twins –
various interactions with a/c twins

***a/c* twins** – **propagating interface**,
resulting in large shape changes
(magnetic shape memory)

Straka, Ladislav, et al., Acta Materialia 59.20 (2011): 7450-7463.

Twin microstructure – 12 variants, 8 twinning systems, 5 different twin types

a = 0.5969 nm
b = 0.5953 nm
c = 0.5615 nm
γ = 90.3°

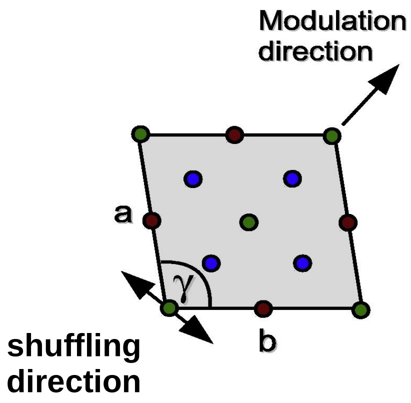

Type I twin - reflection

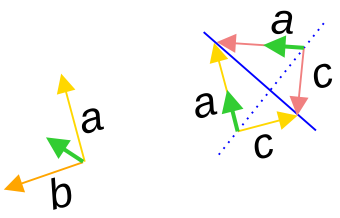

Type II twin – 180° rotation

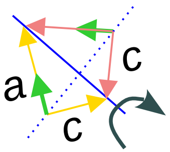

1:5	1.0000	T_1	$1/\sqrt{2}[0;1;-1]$	[0.0682;0.7055;0.7055]	Type I
		T_2	[0.0779;0.7050;0.7050]	$1/\sqrt{2}[0;-1;1]$	Type II[b]
1:6	1.0000	T_1	[0.0779;0.7050;−0.7050]	$1/\sqrt{2}[0;1;1]$	Type II[b]
		T_2	$1/\sqrt{2}[0;1;1]$	[−0.0682;−0.7055;0.7055]	Type I
1:7	1.0094				
1:8	1.0094				
1:9	0.9907				
1:10	0.9907				
1:11	1.0000	T_1	$1/\sqrt{2}[1;0;-1]$	[0.7057;0.0637;0.7057]	Type I
		T_2	[0.7053;0.0721;0.7053]	$1/\sqrt{2}[-1;0;1]$	Type II[c]
1:12	1.0000	T_1	[0.7053;0.0721;−0.7053]	$1/\sqrt{2}[1;0;1]$	Type II[c]
		T_2	$1/\sqrt{2}[1;0;1]$	[−0.7057;−0.0637;0.7057]	Type I

***a/c* twins – propagating interface**, resulting in large shape changes (magnetic shape memory)

Straka, Ladislav, et al., Acta Materialia 59.20 (2011): 7450-7463.

Twin microstructure – 12 variants, 8 twinning systems, 5 different twin types

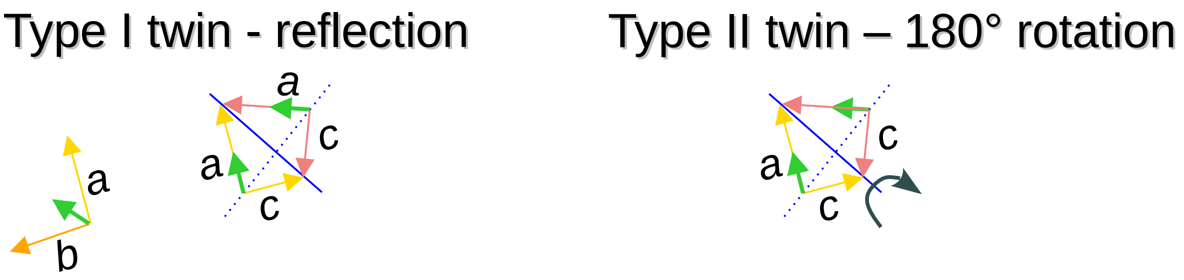

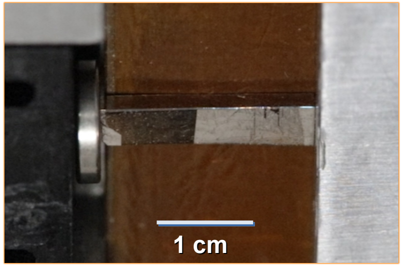

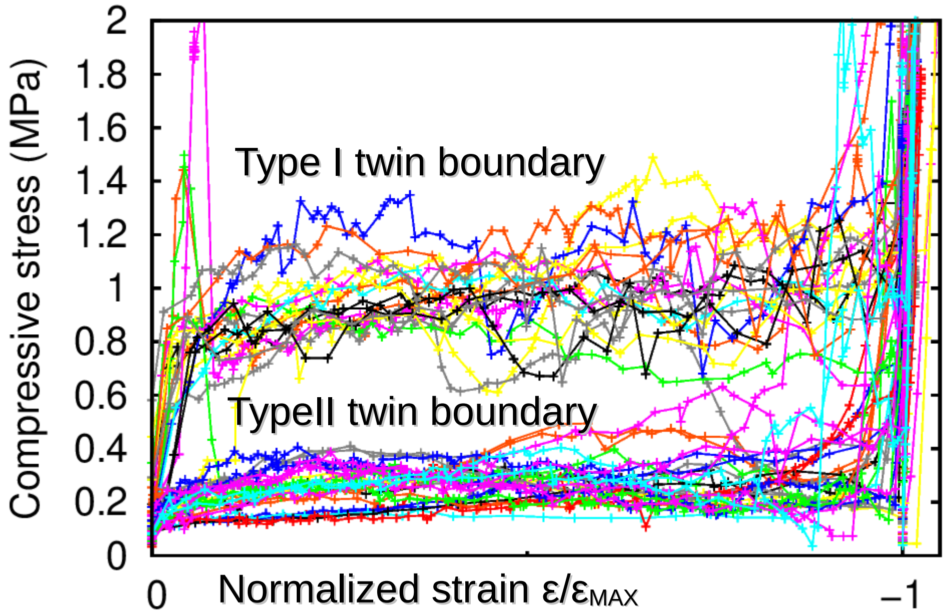

Straka, Ladislav, et al., Acta Materialia 59.20 (2011): 7450-7463.

Twin microstructure – 12 variants, 8 twinning systems, 5 different twin types

Type I twin - reflection

Type II twin – 180° rotation

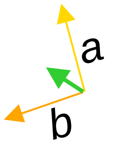

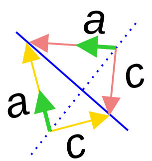

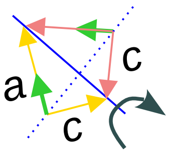

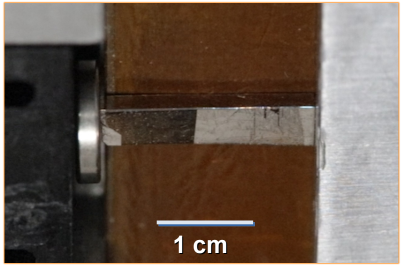

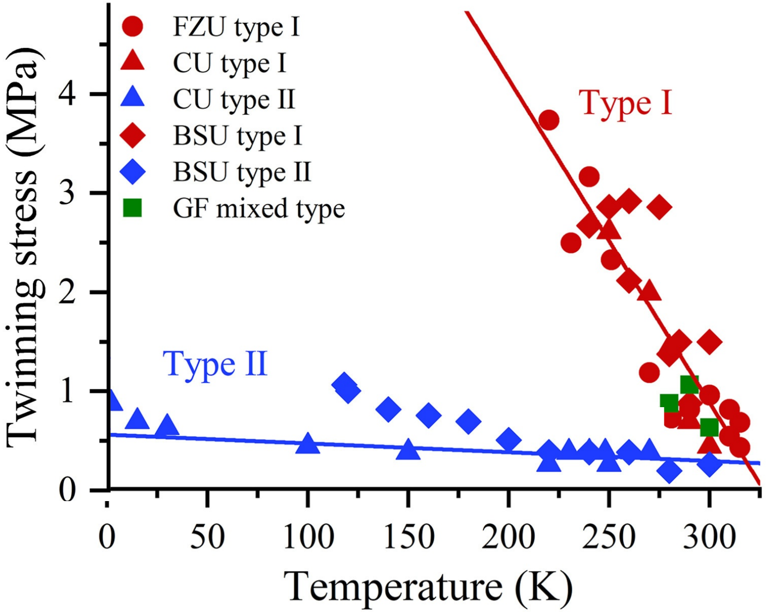

Musiienko, Denys, et al. J. Materials Research and Technology 14 (2021): 1934-1944.

Twin microstructure – 12 variants, 8 twinning systems, 5 different twin types

a = 0.5969 nm
b = 0.5953 nm
c = 0.5615 nm
γ = 90.3°

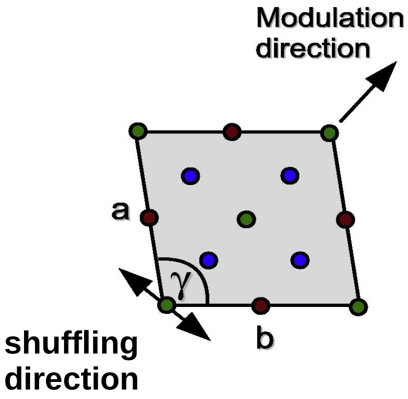

Variants	λ_2		n	$(F^{-1}b)/\|F^{-1}b\|$	Twinning type
1:2	1.0000	T_1	[0;1;0]	[1;0;0]	Modulation
		T_2	[1;0;0]	[0;1;0]	Modulation
1:3	1.0000	T_1	$1/\sqrt{2}[1;-1;0]$	$1/\sqrt{2}[1;1;0]$	Compound
		T_2	$1/\sqrt{2}[1;1;0]$	$1/\sqrt{2}[1;-1;0]$	Compound
1:4	1.0000	T_1	[−0.9509;0.3094;0]	[0.3094;0.9509;0]	Non-conventional[a]
		T_2	[0.3094;0.9509;0]	[0.9509;−0.3094;0]	Non-conventional[a]
1:5	1.0000	T_1	$1/\sqrt{2}[0;1;-1]$	[0.0682;0.7055;0.7055]	Type I
		T_2	[0.0779;0.7050;0.7050]	$1/\sqrt{2}[0;-1;1]$	Type II[b]
1:6	1.0000	T_1	[0.0779;0.7050;−0.7050]	$1/\sqrt{2}[0;1;1]$	Type II[b]
		T_2	$1/\sqrt{2}[0;1;1]$	[−0.0682;−0.7055;0.7055]	Type I
1:7	1.0094				
1:8	1.0094				
1:9	0.9907				
1:10	0.9907				
1:11	1.0000	T_1	$1/\sqrt{2}[1;0;-1]$	[0.7057;0.0637;0.7057]	Type I
		T_2	[0.7053;0.0721;0.7053]	$1/\sqrt{2}[-1;0;1]$	Type II[c]
1:12	1.0000	T_1	[0.7053;0.0721;−0.7053]	$1/\sqrt{2}[1;0;1]$	Type II[c]
		T_2	$1/\sqrt{2}[1;0;1]$	[−0.7057;−0.0637;0.7057]	Type I

landscape around *a/c* twins – various interactions with a/c twins

***a/c* twins** – **propagating interface**, resulting in large shape changes (magnetic shape memory)

Twin microstructure – 12 variants, 8 twinning systems, 5 different twin types

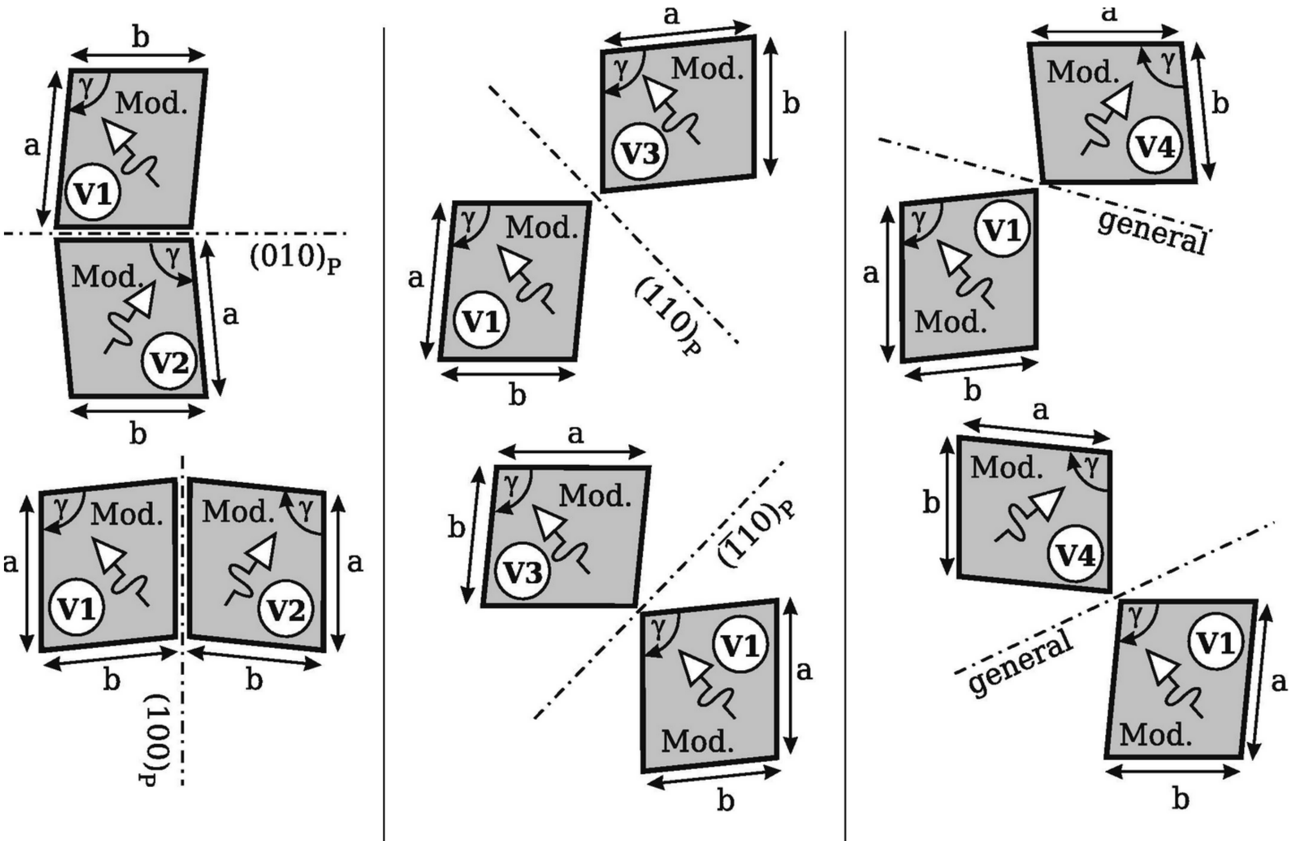

(a) Modulation twins (b) Compound twins (c) Non-conventional twins

Straka, Ladislav, et al., Acta Materialia 59.20 (2011): 7450-7463.

Martensite with deep twinning hierarchy

cm — mm — 100 µm — 10µm — SCALE — 1µm — 100 nm — 10 nm — 1 nm

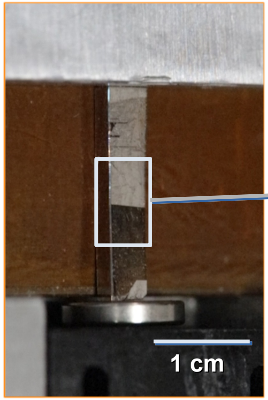

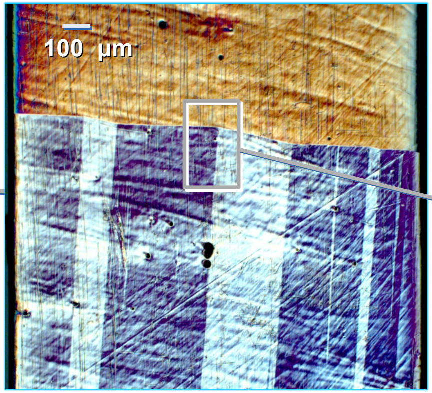

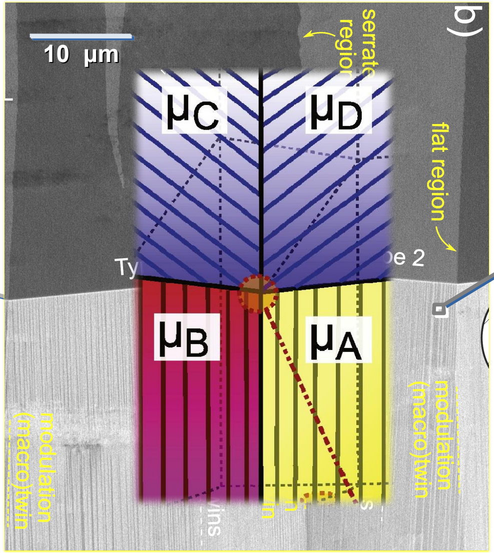

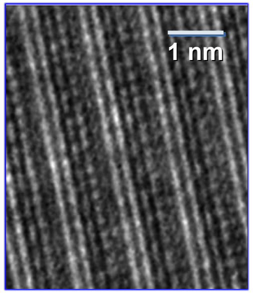

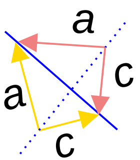

a/c twins
(101) Type I, Type II

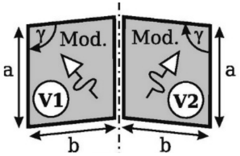

Monoclinic (modulation) twins
(100) compound

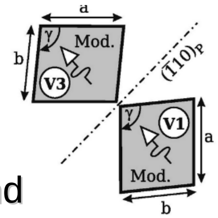

a/b twins
(110) compound

a/b nanotwins +
structural twins

Martensite with deep twinning hierarchy

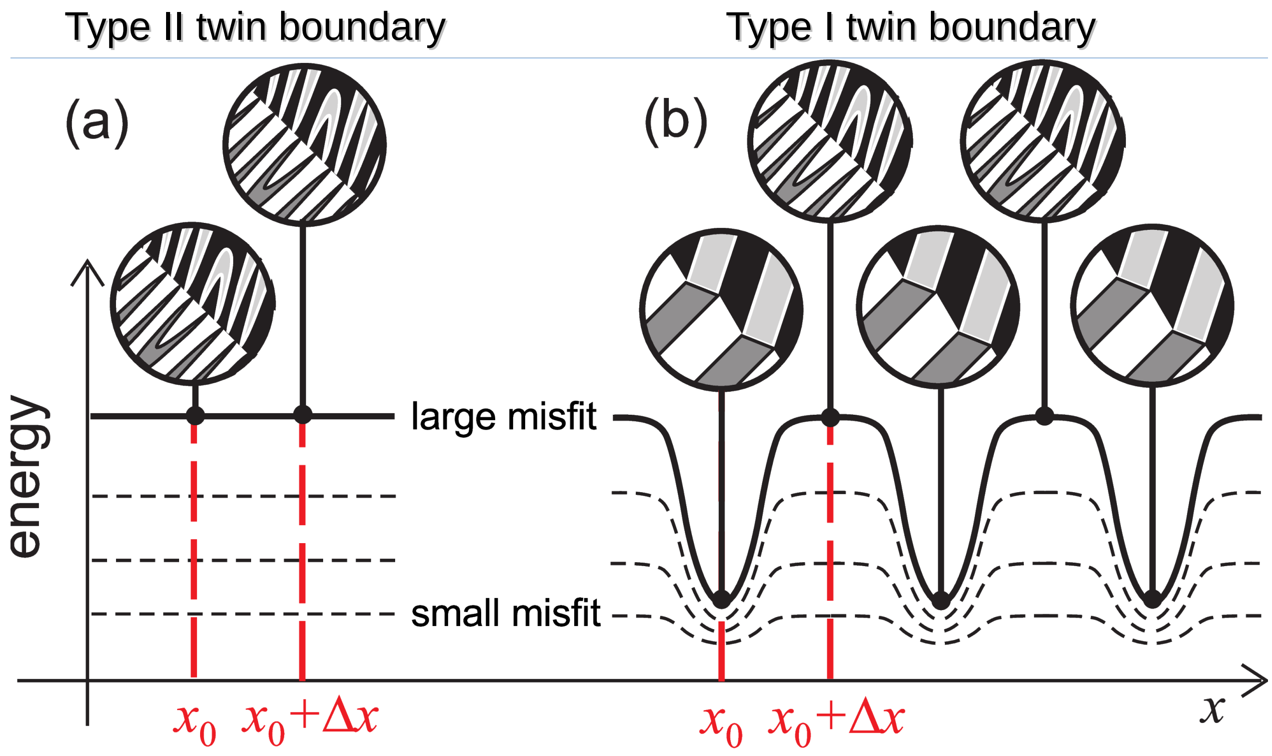

Seiner, Hanuš, Ladislav Straka, and Oleg Heczko, J. Mechanics and Physics of Solids 64 (2014): 198-211.

Microstructural model of Type I/Type II twin boundary propagation

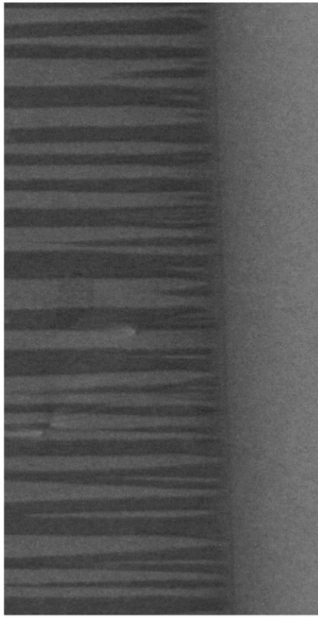

Type II

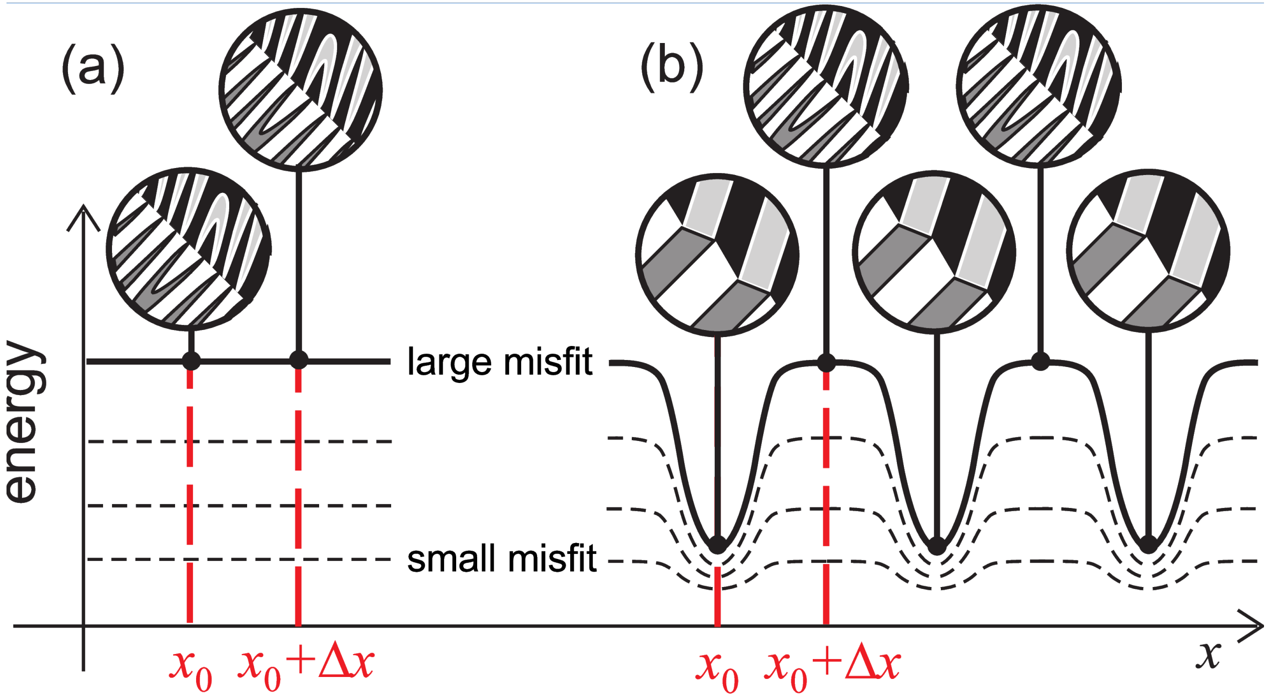

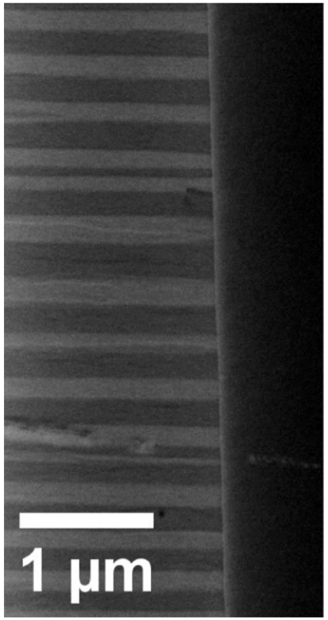

Type I

Seiner, Hanuš, Ladislav Straka, and Oleg Heczko, J. Mechanics and Physics of Solids 64 (2014): 198-211.
Heczko, Oleg, Ladislav Klimša, and Jaromír Kopeček, Scripta Materialia 131 (2017): 76-79.

Summary III

- Martensite with 5 different twin types & deep hierarchy
- a/c twins carry the deformation (Type I & Type II)
- Propagating a/c twin boundaries interact with other surrounding twins
- Microstructural model suggests a/b twins as the most important

The magic of magnetic shape memory…

- Intro & macrotwins
- *Movie with examples*
- Microtwins
- Nanotwins
- Summary

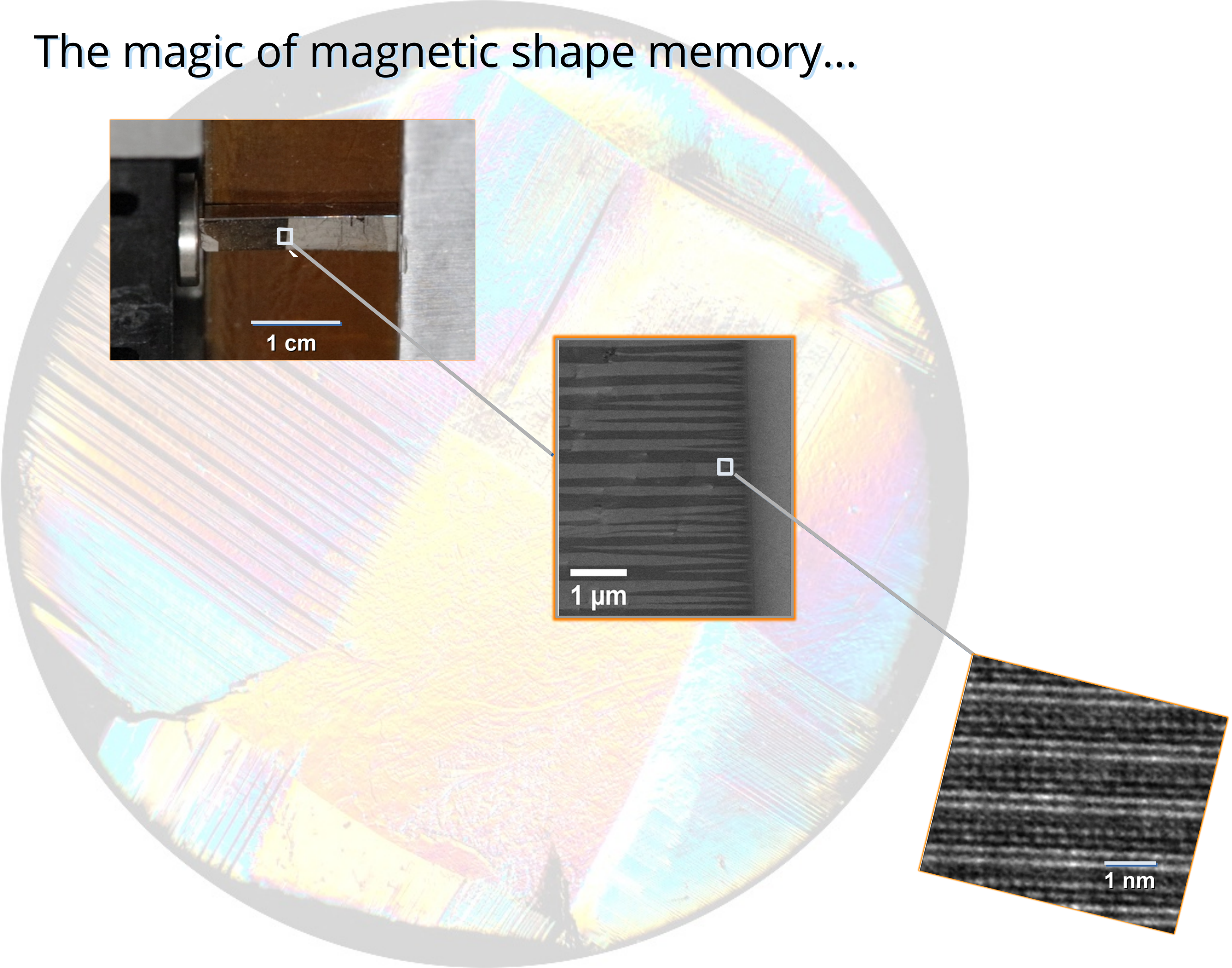

Structure as a $3\bar{2}$ stacking sequence

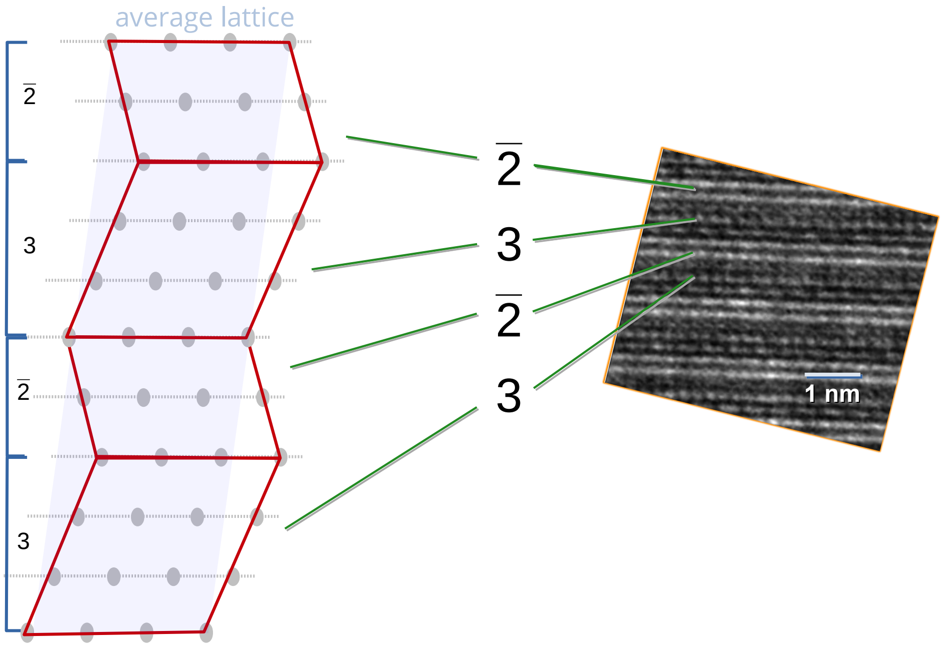

Straka, L., et al., Acta Materialia 132 (2017): 335-344.
Straka, L., et al., Scientific Reports 8.1 (2018): 11943.

Structure as a 3$\bar{2}$ stacking sequence

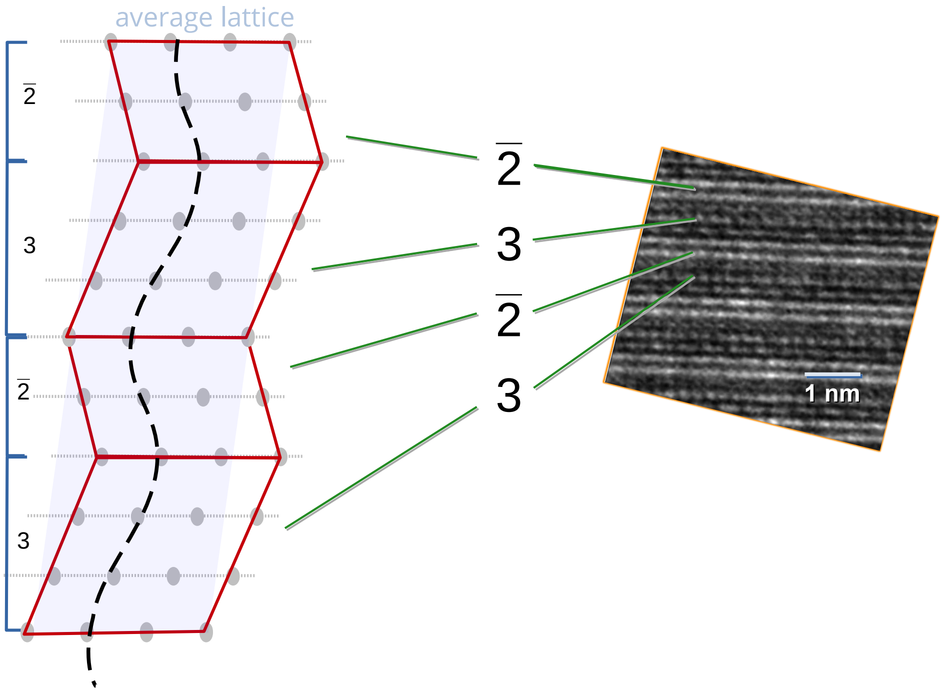

Straka, L., et al., Acta Materialia 132 (2017): 335-344.
Straka, L., et al., Scientific Reports 8.1 (2018): 11943.

Structure as a 3$\bar{2}$ stacking sequence

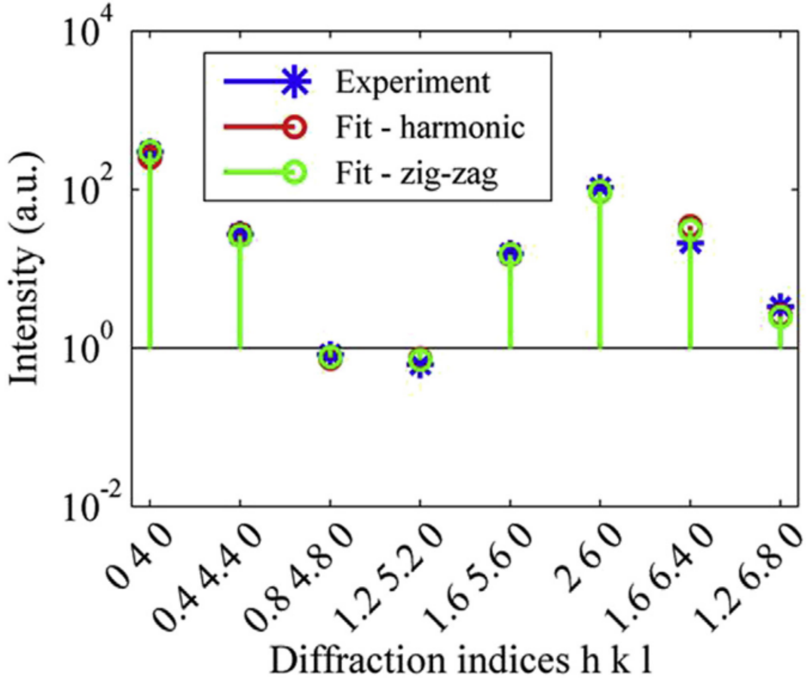

Heczko, Oleg, et al.Acta Materialia 115 (2016): 250-258.

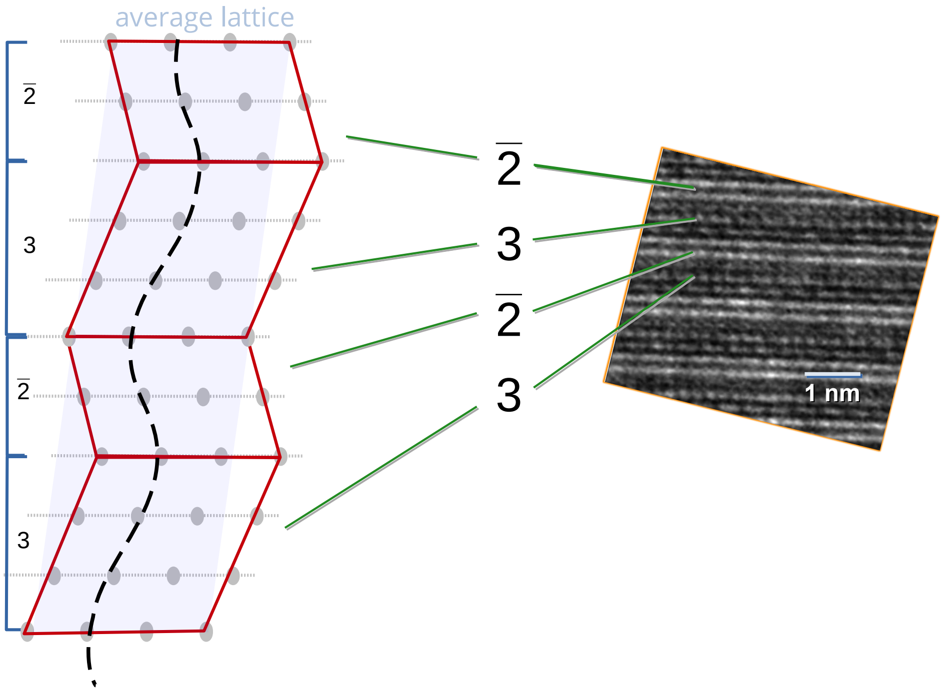

Straka, L., et al., Acta Materialia 132 (2017): 335-344.
Straka, L., et al., Scientific Reports 8.1 (2018): 11943.

Structure as a 3$\bar{2}$ stacking sequence

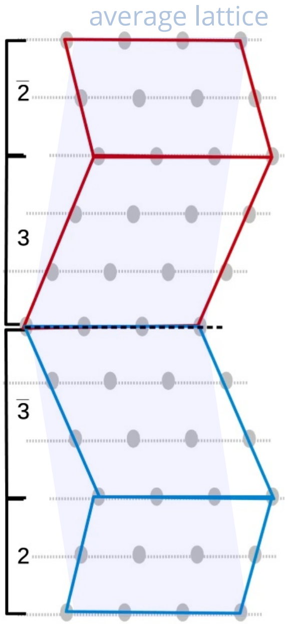

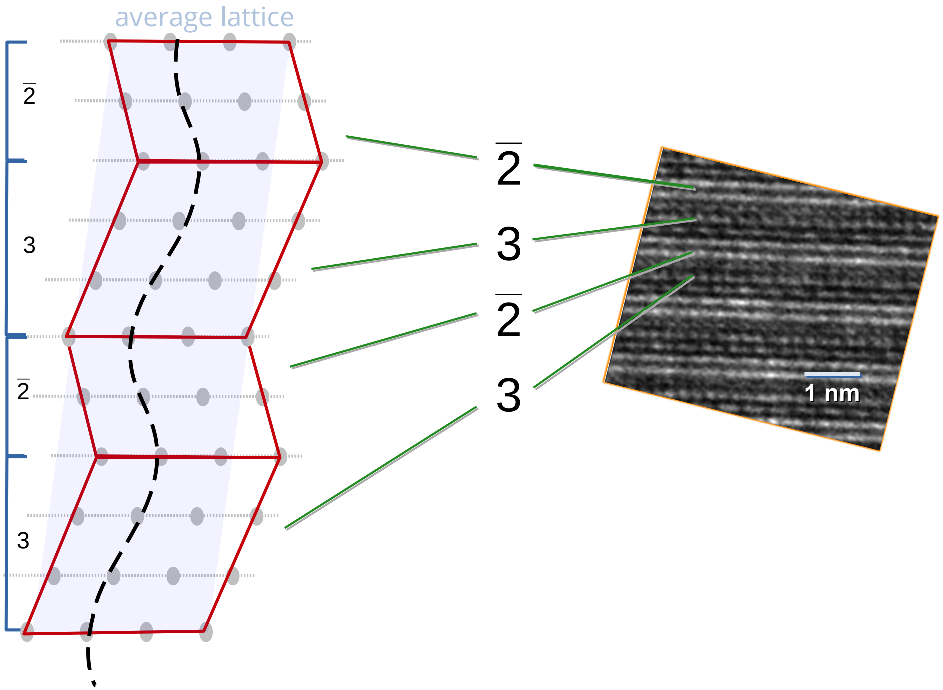

Straka, L., et al., Acta Materialia 132 (2017): 335-344.
Straka, L., et al., Scientific Reports 8.1 (2018): 11943.

Structure as a 3$\bar{2}$ stacking sequence

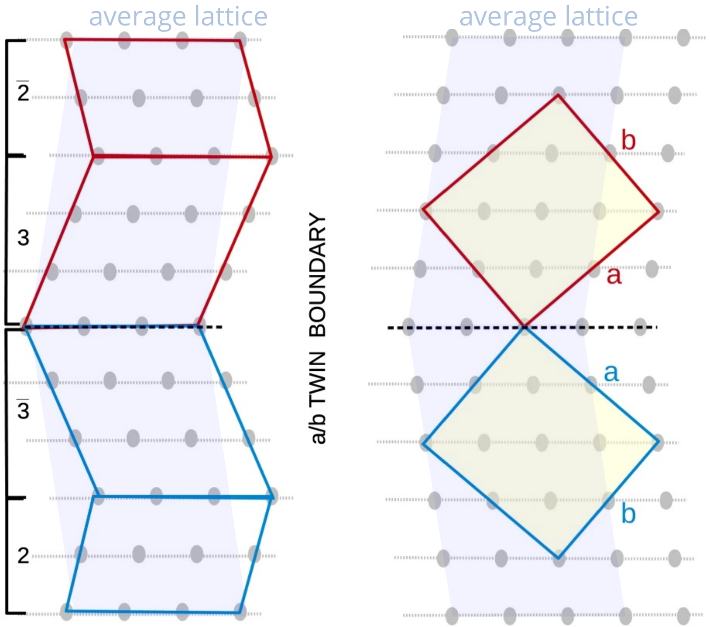

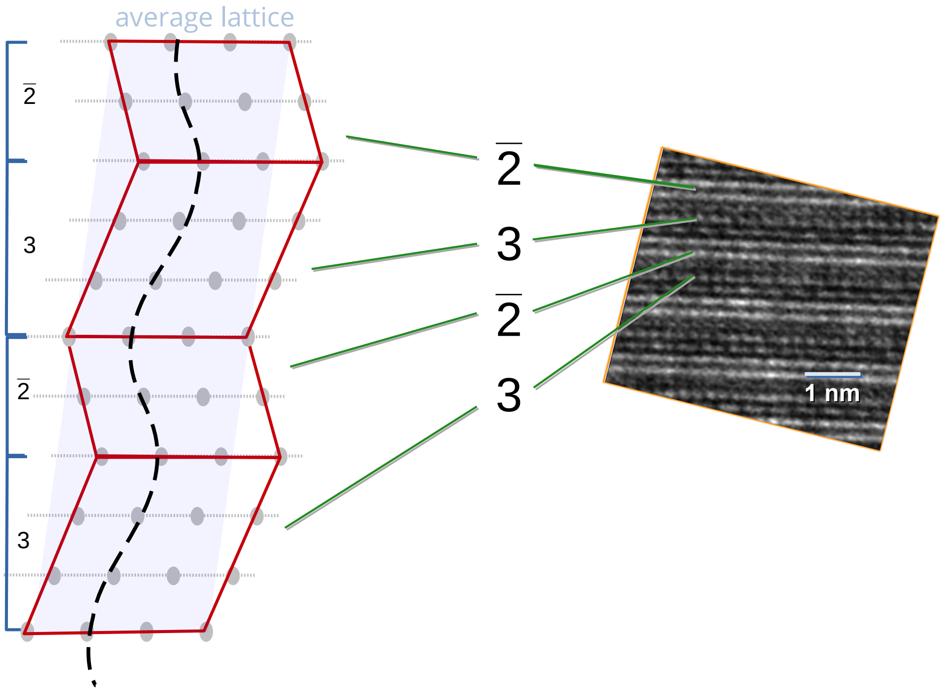

Straka, L., et al., Acta Materialia 132 (2017): 335-344.
Straka, L., et al., Scientific Reports 8.1 (2018): 11943.

a/b twins as a $3\bar{2}$ stacking sequence inversion

a/b twin boundary = stacking sequence inversion …$3\bar{2}3\bar{2}3\bar{2}|2\bar{3}2\bar{3}2\bar{3}$…

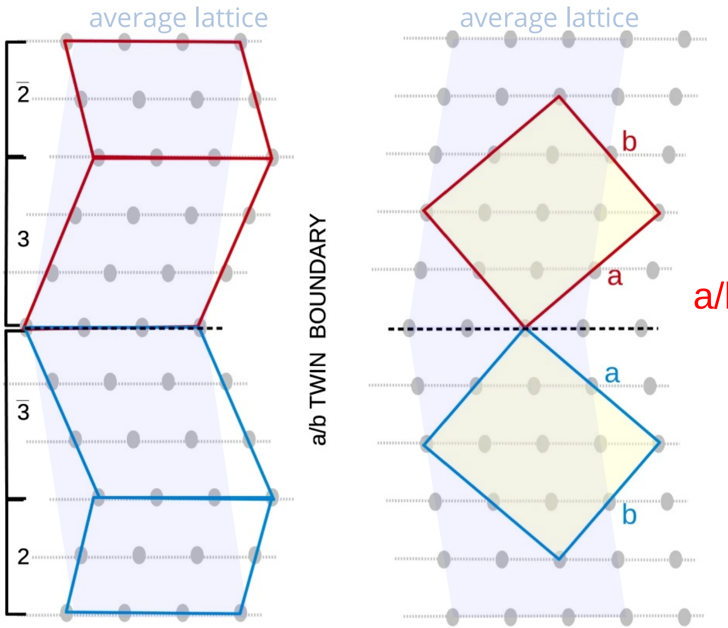

a/b twin bound.

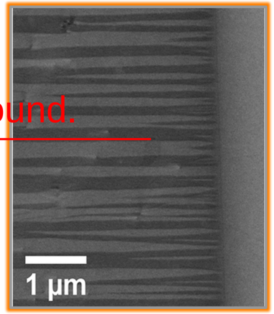

$\bar{2}$
3
$\bar{2}$
3

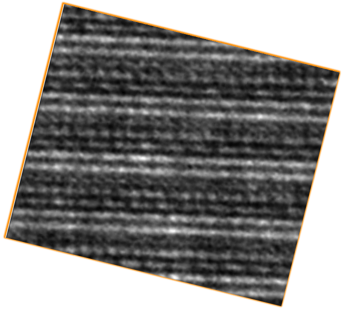

a/b twin bound.

$\bar{3}$
2
$\bar{3}$
2

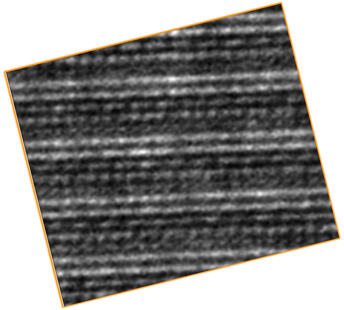

Straka, L., et al., Acta Materialia 132 (2017): 335-344.
Straka, L., et al., Scientific Reports 8.1 (2018): 11943.

a/b twins as a 3$\bar{2}$ stacking sequence inversion

a/b twin boundary = stacking sequence inversion …3$\bar{2}$3$\bar{2}$3$\bar{2}$|2$\bar{3}$2$\bar{3}$2$\bar{3}$…

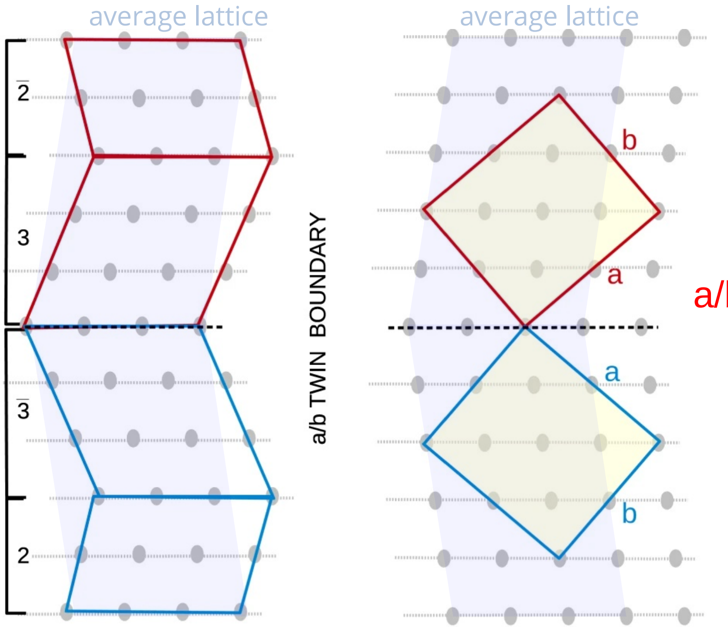

a/b twin bound.

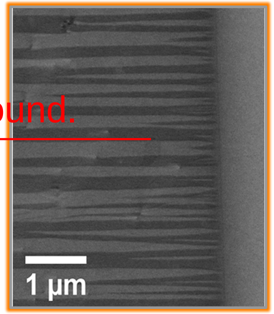

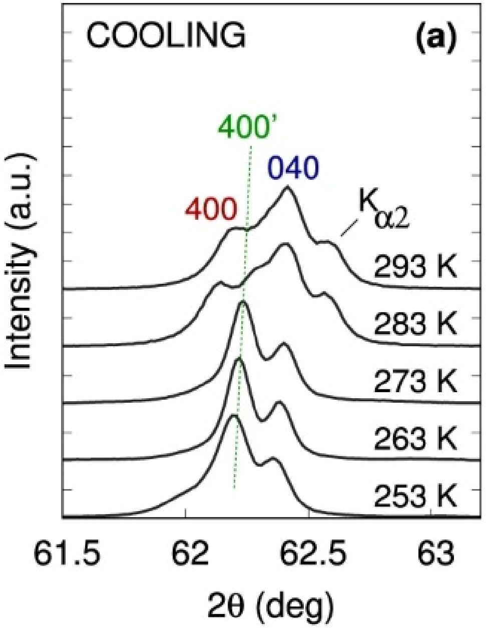

Straka, L., et al., Acta Materialia 132 (2017): 335-344.
Straka, L., et al., Scientific Reports 8.1 (2018): 11943.

a/b twins as a 3$\bar{2}$ stacking sequence inversion

a/b twin boundary = stacking sequence inversion …$3\bar{2}3\bar{2}3\bar{2}|2\bar{3}2\bar{3}2\bar{3}$…

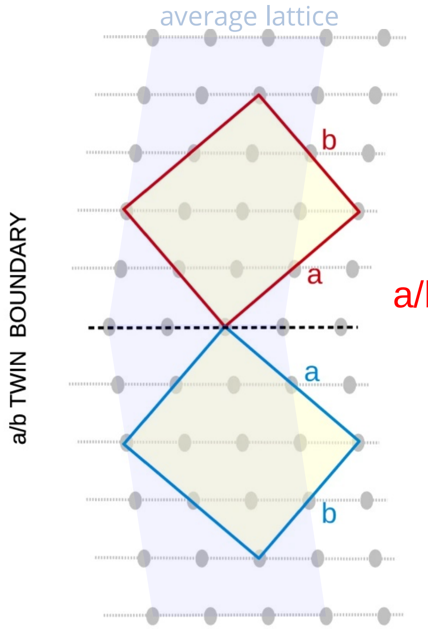

a/b twin bound.

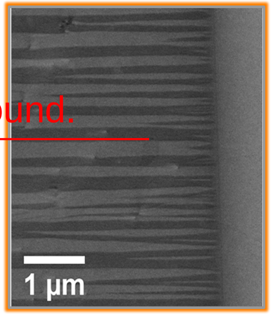

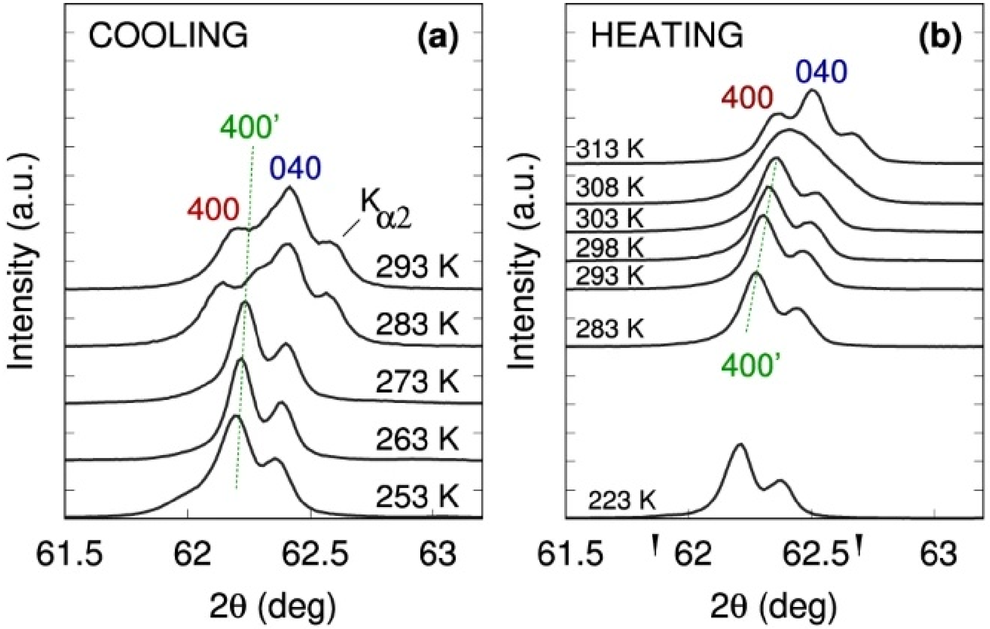

Straka, L., et al., Acta Materialia 132 (2017): 335-344.
Straka, L., et al., Scientific Reports 8.1 (2018): 11943.

a/b twins as a 3$\bar{2}$ stacking sequence inversion

a/b twin boundary = stacking sequence inversion ...3$\bar{2}$3$\bar{2}$3$\bar{2}$|2$\bar{3}$2$\bar{3}$2$\bar{3}$...

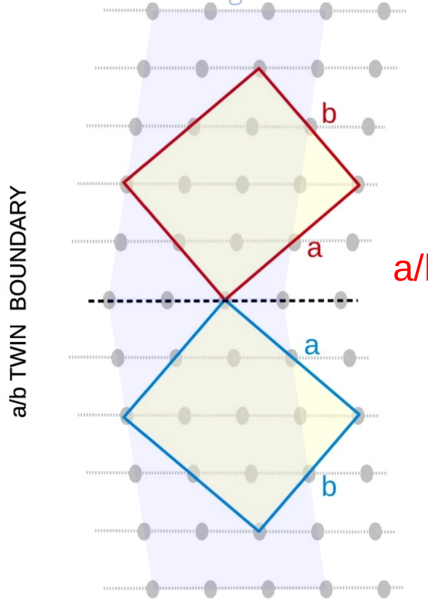

a/b twin bound.

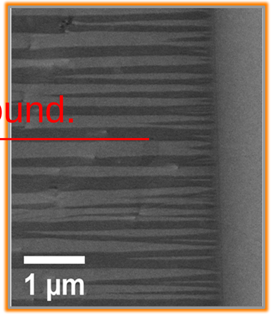

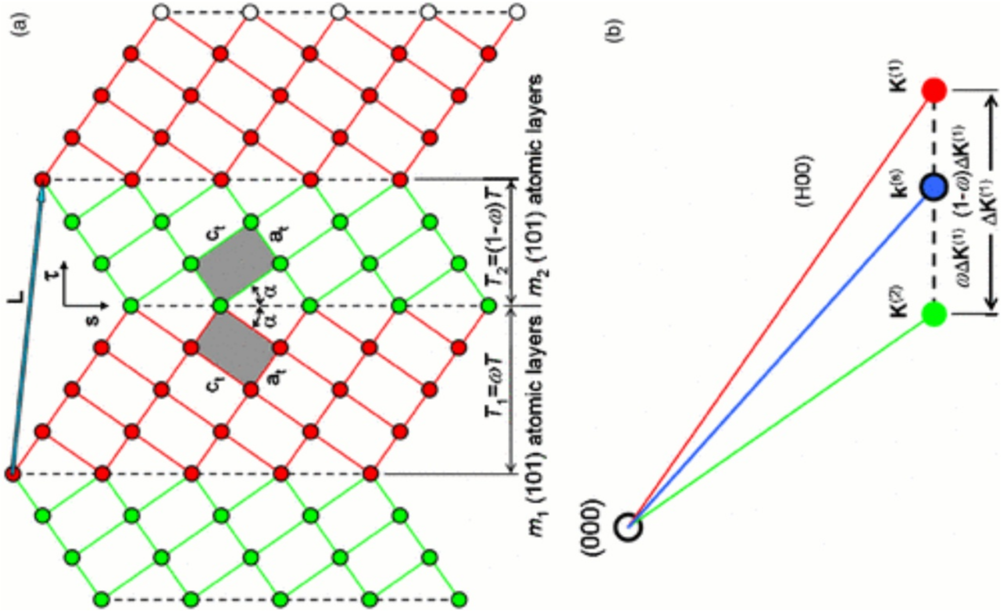

Yu U. Wang, Phys. Rev. B 74 (2006), 104109
Yu U. Wang,Phys. Rev. B, 76 (2007), Article 024108

a/b twins as a $3\bar{2}$ stacking sequence inversion

a/b twin boundary = stacking sequence inversion ...$3\bar{2}3\bar{2}3\bar{2}|2\bar{3}2\bar{3}2\bar{3}$...

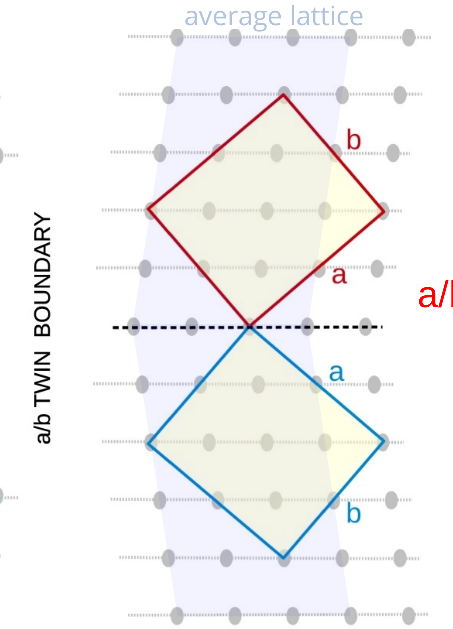

a/b twin bound.

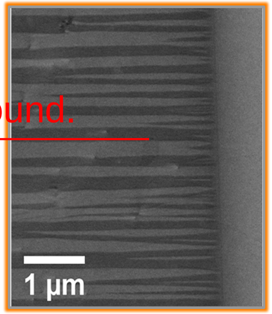

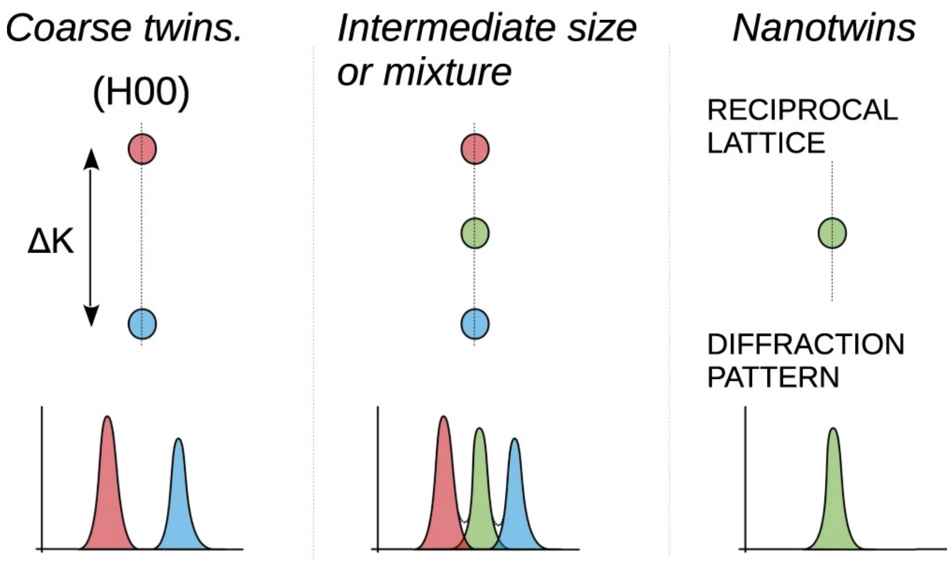

Straka, L., et al., Acta Materialia 132 (2017): 335-344.
Straka, L., et al., Scientific Reports 8.1 (2018): 11943.

a/b **nano**twins as a 3$\bar{2}$ stacking sequence inversion

a/b twin boundary = stacking sequence inversion ...3$\bar{2}$3$\bar{2}$3$\bar{2}$|2$\bar{3}$2$\bar{3}$2$\bar{3}$...

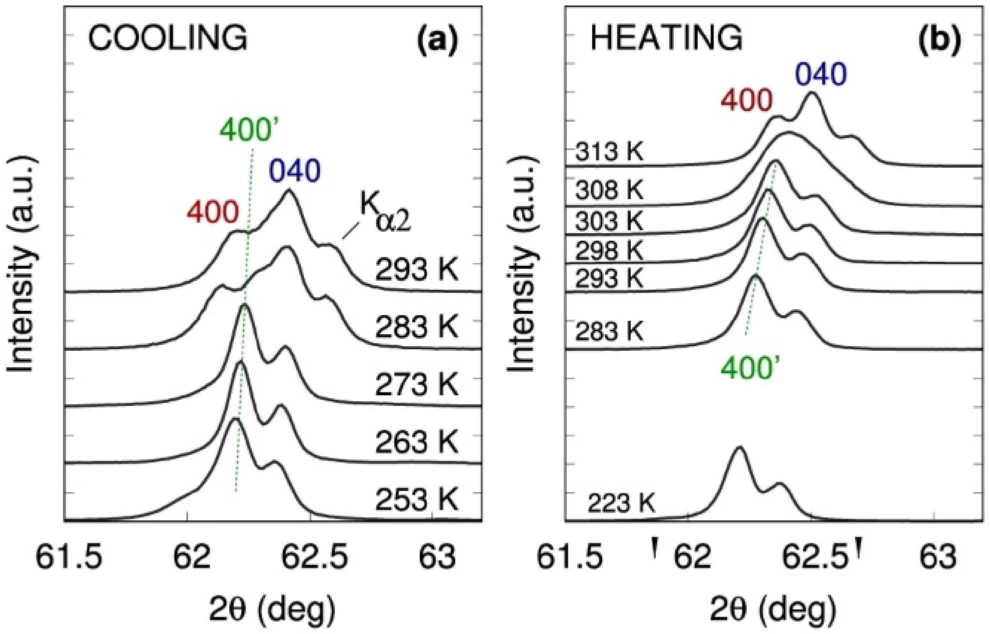

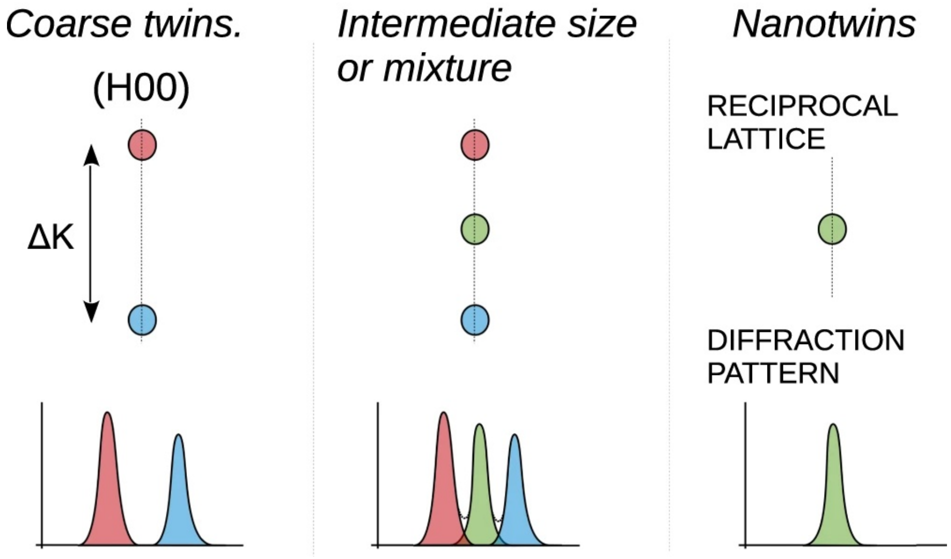

Straka, L., et al., Acta Materialia 132 (2017): 335-344.
Straka, L., et al., Scientific Reports 8.1 (2018): 11943.

a/b **nano**twins as a $3\bar{2}$ stacking sequence inversion

a/b twin boundary = stacking sequence inversion …$3\bar{2}3\bar{2}3\bar{2}|2\bar{3}2\bar{3}2\bar{3}$…

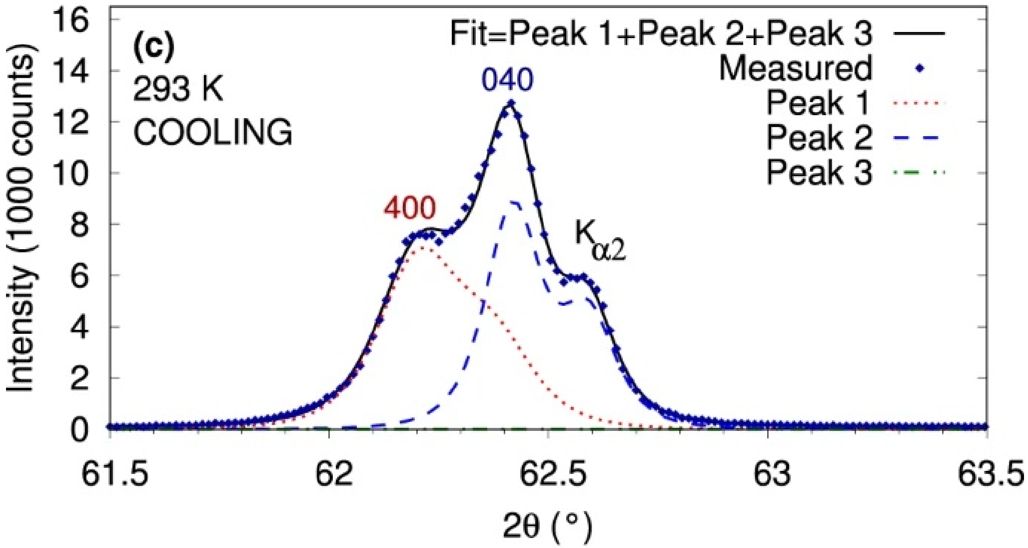

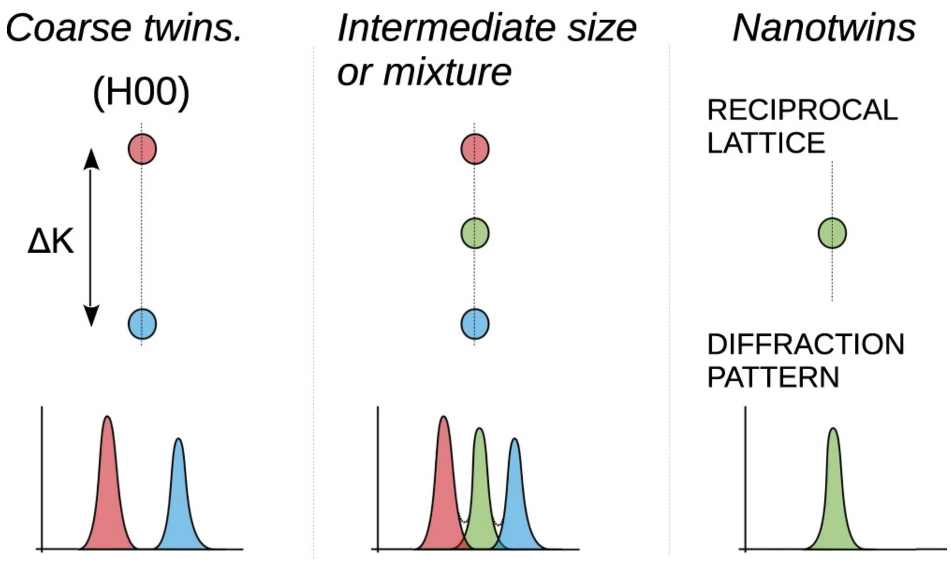

Straka, L., et al., Acta Materialia 132 (2017): 335-344.
Straka, L., et al., Scientific Reports 8.1 (2018): 11943.

a/b **nano**twins as a $3\bar{2}$ stacking sequence inversion

a/b twin boundary = stacking sequence inversion ...$3\bar{2}3\bar{2}3\bar{2}|2\bar{3}2\bar{3}2\bar{3}$...

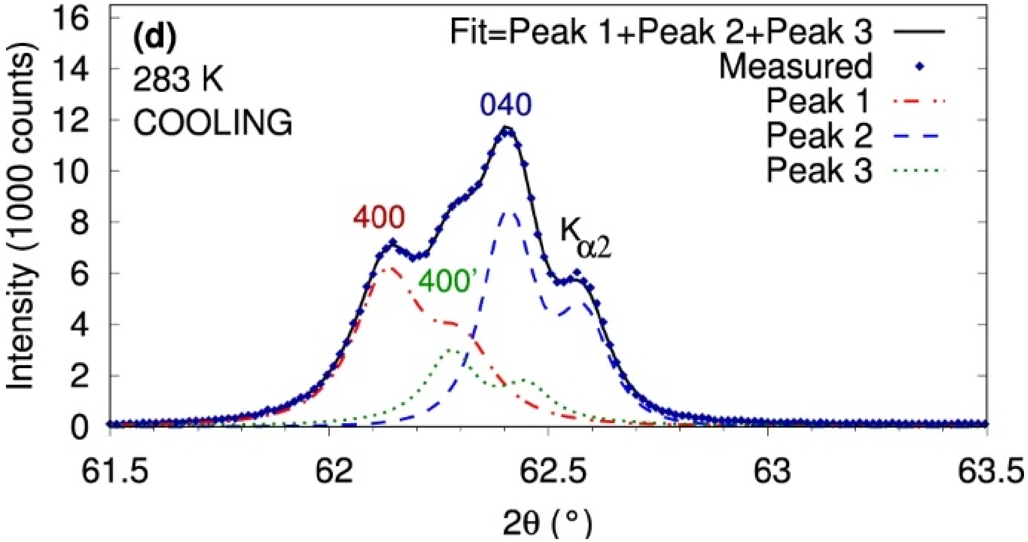

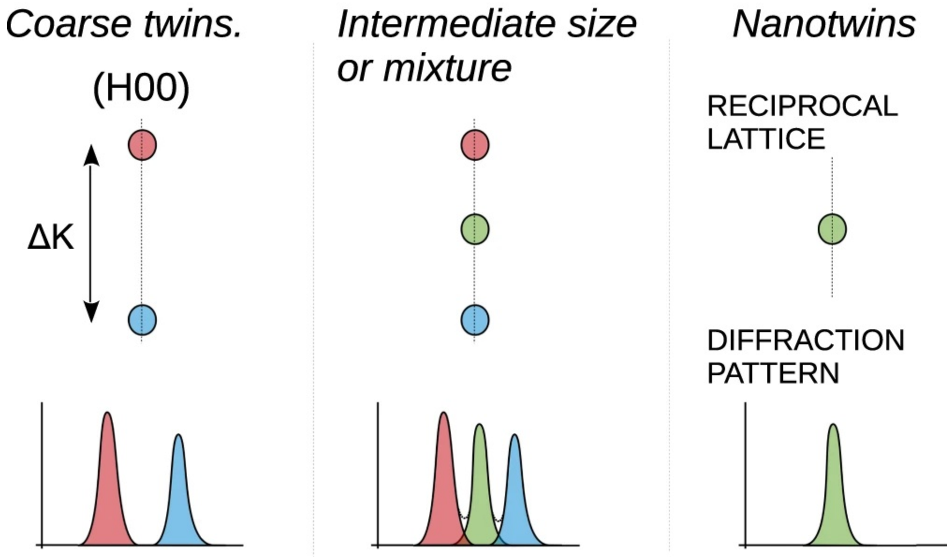

Straka, L., et al., Acta Materialia 132 (2017): 335-344.
Straka, L., et al., Scientific Reports 8.1 (2018): 11943.

a/b **nano**twins as a $3\bar{2}$ stacking sequence inversion

a/b twin boundary = stacking sequence inversion $...3\bar{2}3\bar{2}3\bar{2}|2\bar{3}2\bar{3}2\bar{3}...$

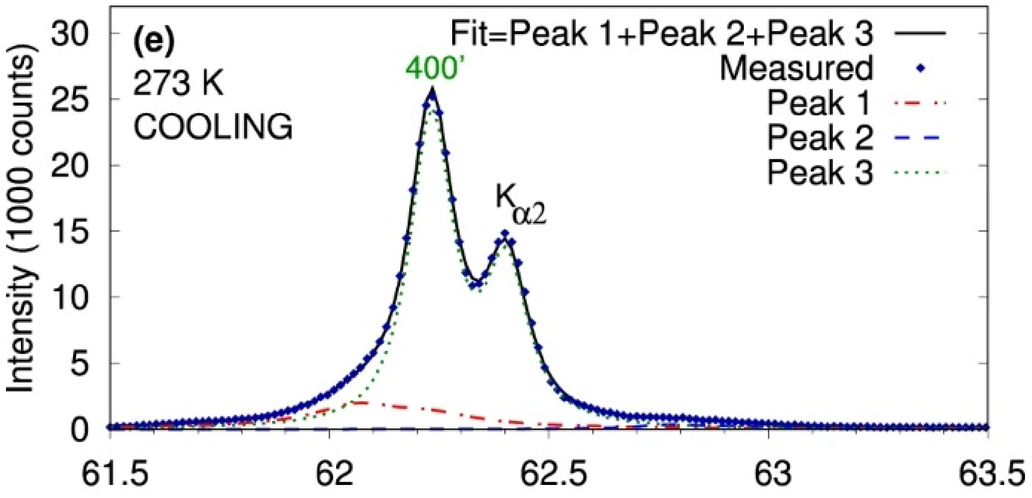

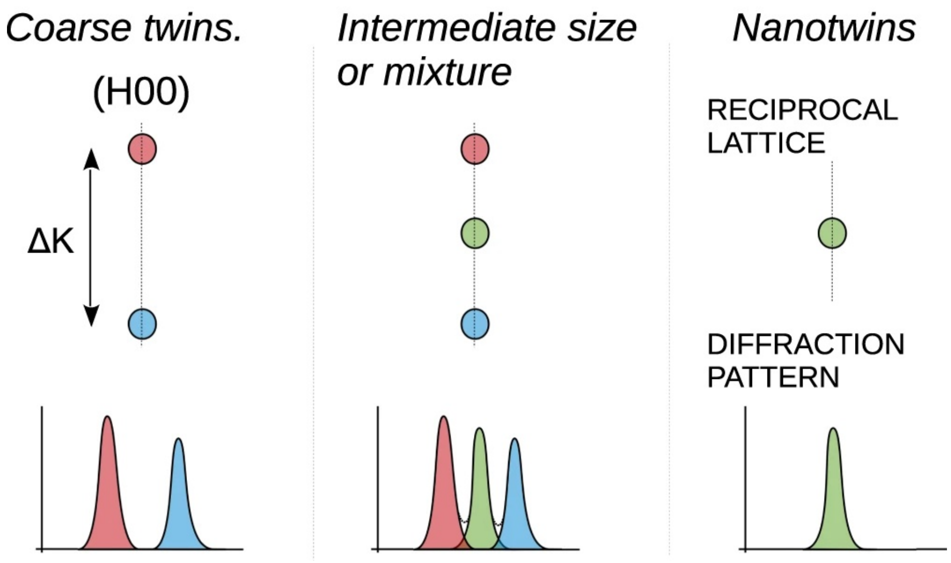

a/b **nano**twins as a 3$\bar{2}$ stacking sequence inversion

a/b twin boundary = stacking sequence inversion ...3$\bar{2}$3$\bar{2}$3$\bar{2}$|$\bar{2}$3$\bar{2}$3$\bar{2}$3...

Nanotwins - adaptive diffraction condition:

$$m < 2/sH$$

where s = 0.0045 is twinning shear and H = 4 is reciprocal space coordinate

=>

size of a/b twin

$$m < 20 \text{ nm (100 atomic planes)}$$

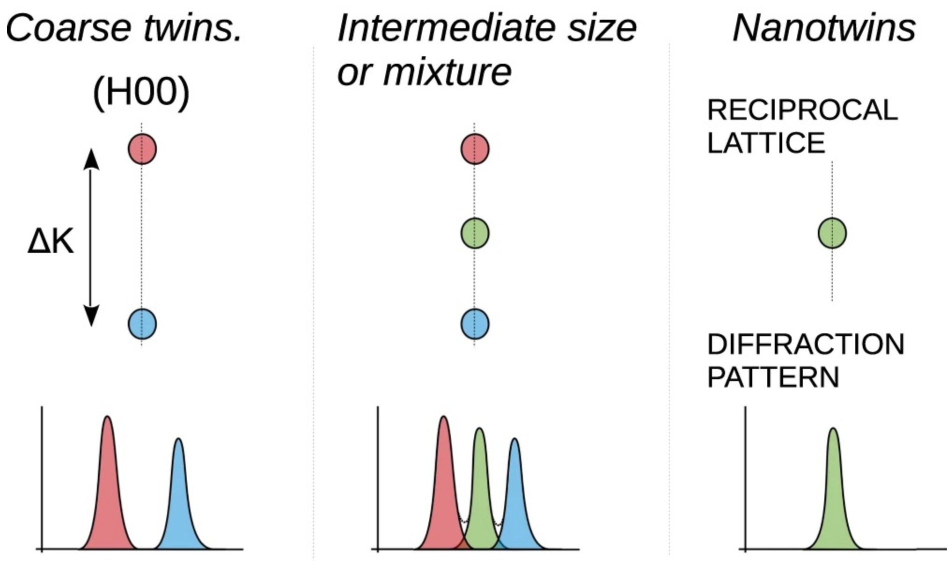

Straka, L., et al., Acta Materialia 132 (2017): 335-344.
Straka, L., et al., Scientific Reports 8.1 (2018): 11943.

a/b **nano**twins as a $3\bar{2}$ stacking sequence inversion

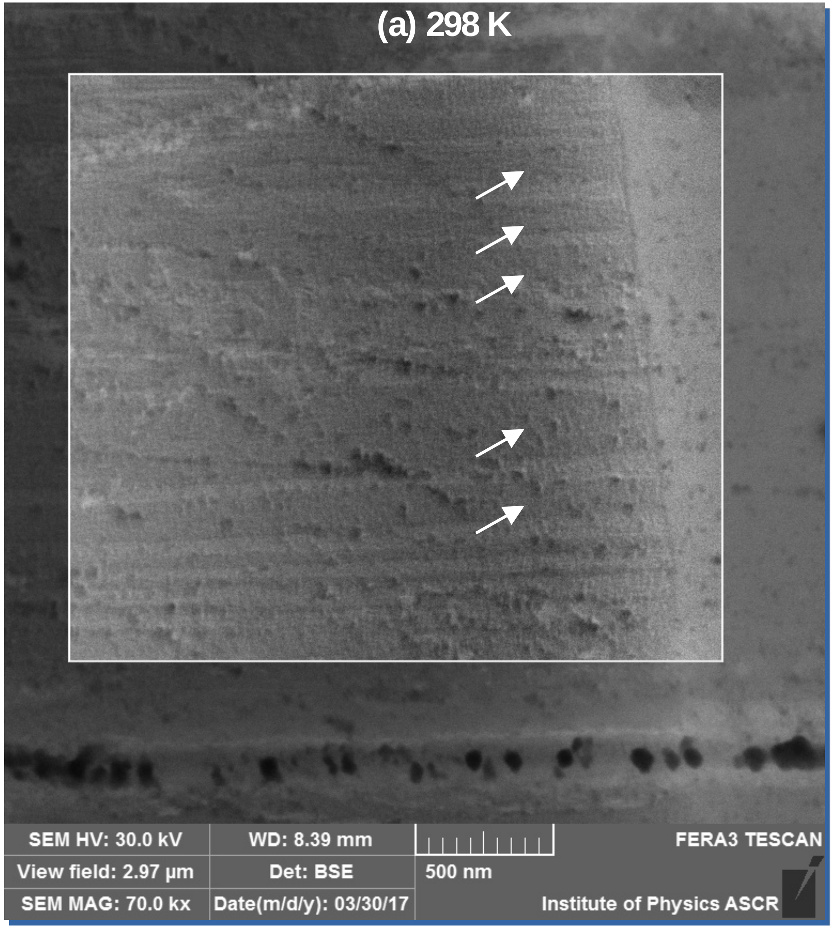

Nanotwins - adaptive diffraction condition:

$$m < 2/sH$$

where s = 0.0045 is twinning shear and H = 4 is reciprocal space coordinate

=>

size of a/b twin

$$m < 20 \text{ nm (100 atomic planes)}$$

Straka, L., et al., Acta Materialia 132 (2017): 335-344.
Straka, L., et al., Scientific Reports 8.1 (2018): 11943.

a/b **nano**twins as a $3\bar{2}$ stacking sequence inversion

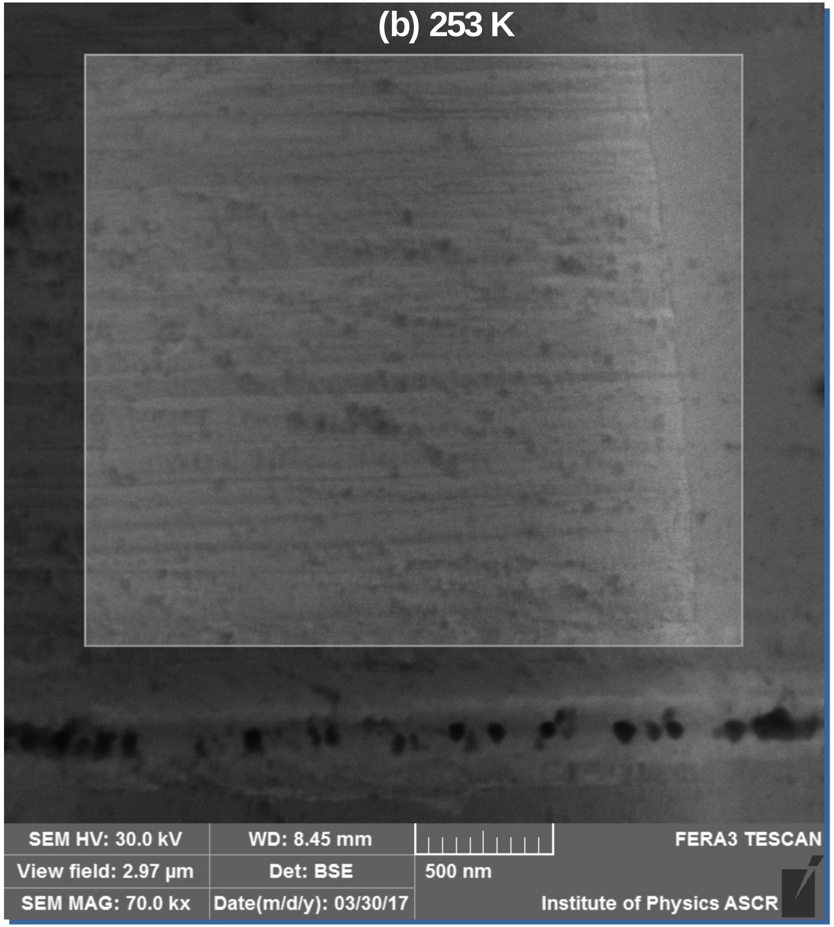

Nanotwins - adaptive diffraction condition:

$$m < 2/sH$$

where s = 0.0045 is twinning shear and H = 4 is reciprocal space coordinate

=>

size of a/b twin

$$m < 20 \text{ nm (100 atomic planes)}$$

Straka, L., et al., Acta Materialia 132 (2017): 335-344.
Straka, L., et al., Scientific Reports 8.1 (2018): 11943.

a/b **nano**twins as a 3$\bar{2}$ stacking sequence inversion

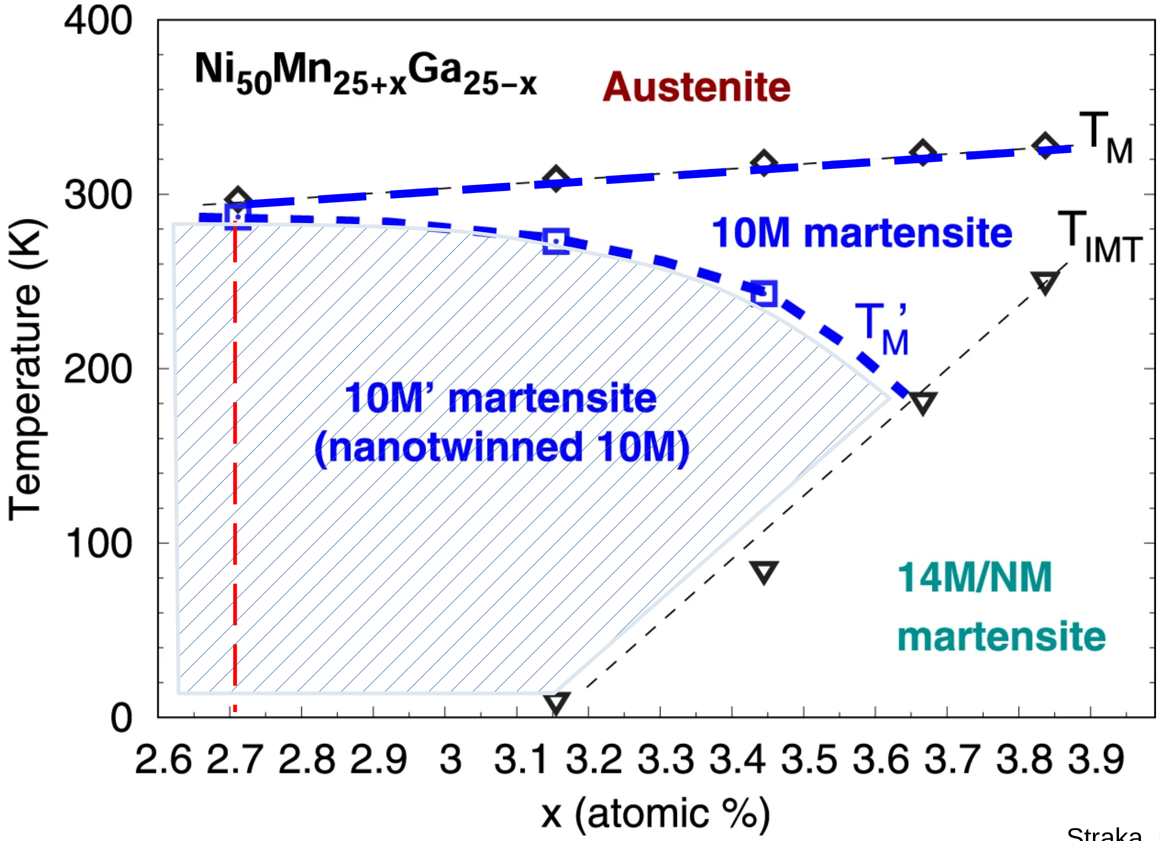

Straka, L., et al., Acta Materialia 132 (2017): 335-344.
Straka, L., et al., Scientific Reports 8.1 (2018): 11943.

Modulation

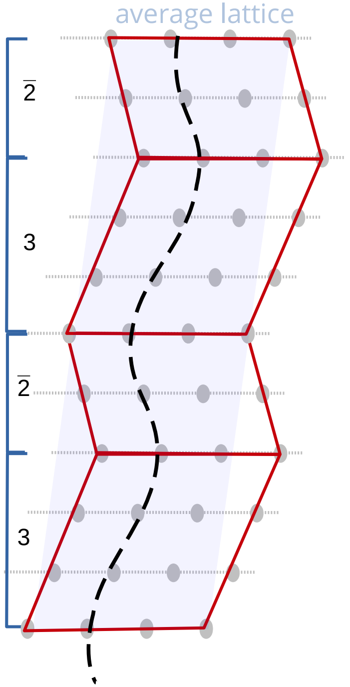

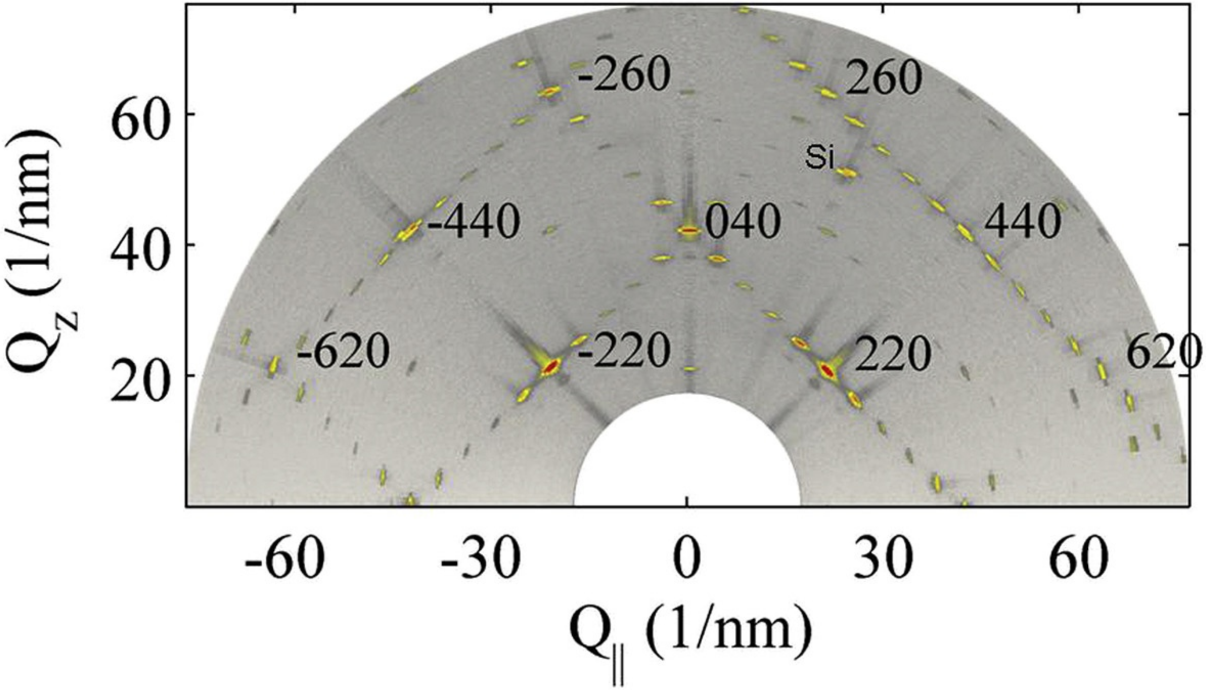

Heczko, Oleg, et al.Acta Materialia 115 (2016): 250-258.

Modulation

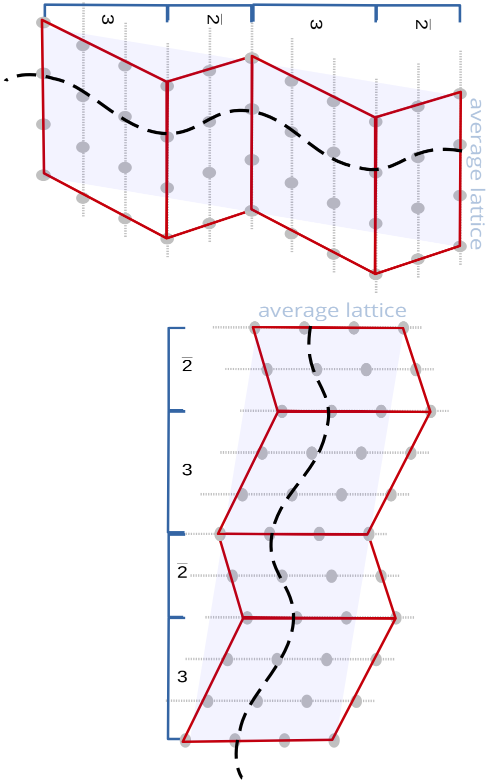

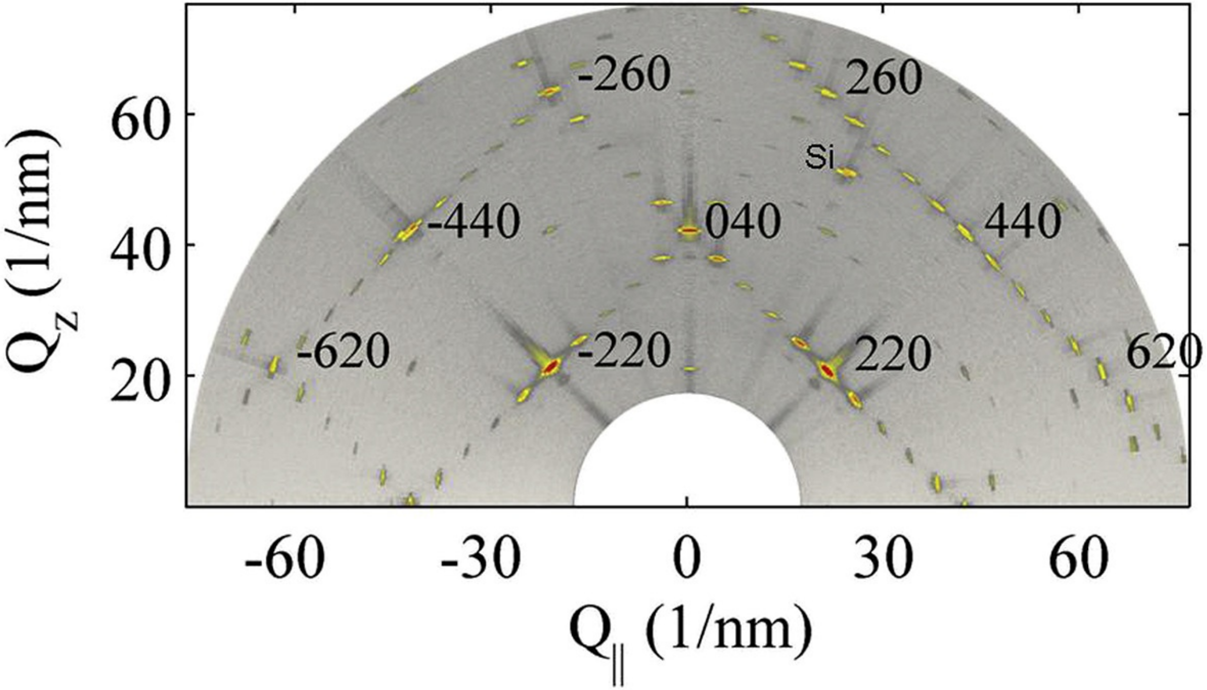

Heczko, Oleg, et al.Acta Materialia 115 (2016): 250-258.

Modulation – study by high-resolution q-scan

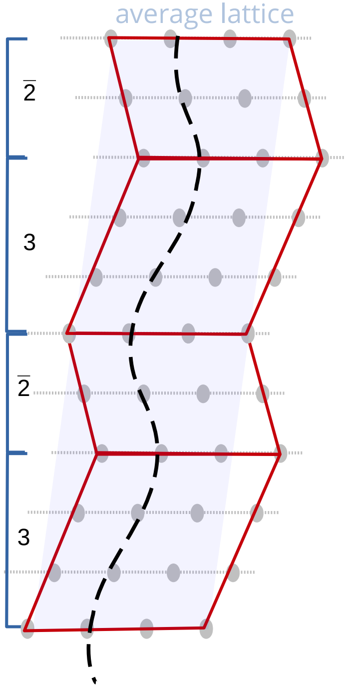

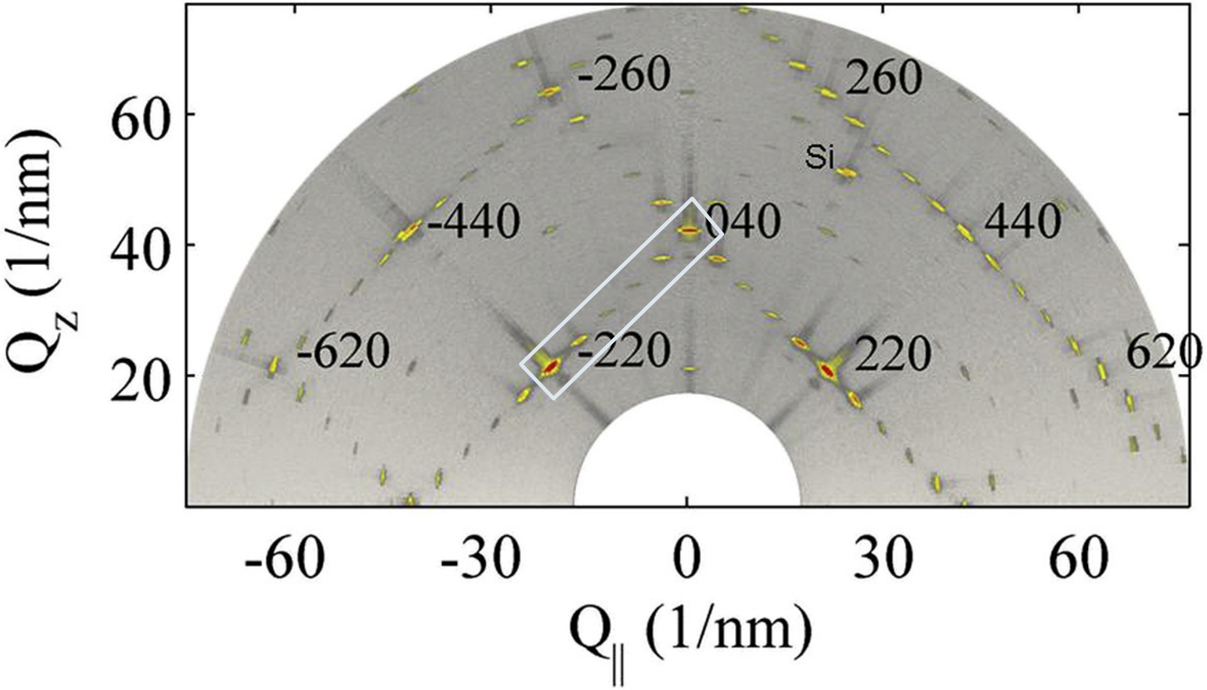

Heczko, Oleg, et al.Acta Materialia 115 (2016): 250-258.

Modulation – study by high-resolution q-scan

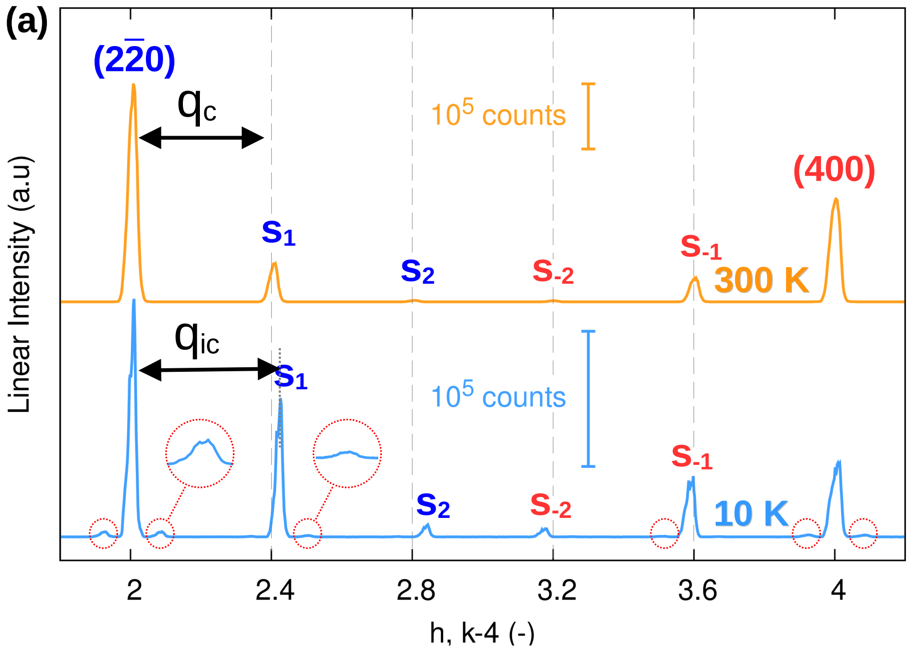

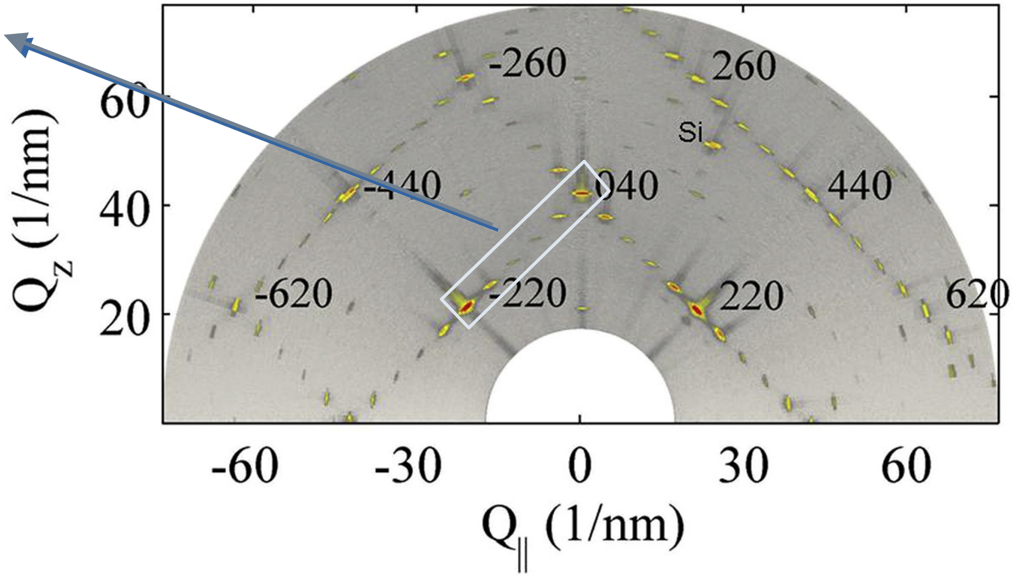

q=(q,q,0)
q'=2/q

Straka L. et al., submitted, http://dx.doi.org/10.2139/ssrn.4771525 Heczko, Oleg, et al.Acta Materialia 115 (2016): 250-258.

Modulation – study by high-resolution q-scan

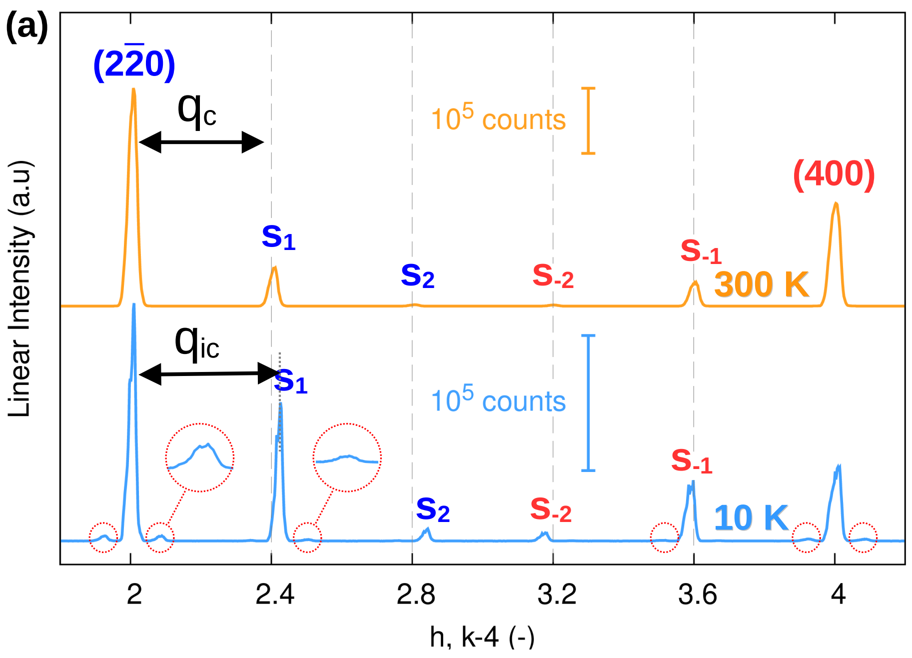

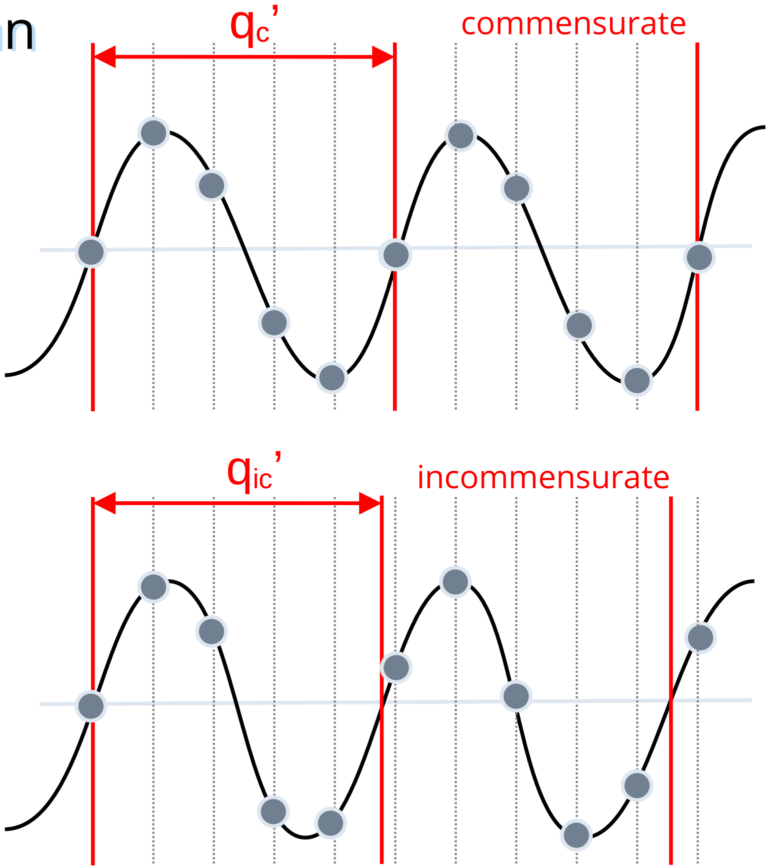

q=(q,q,0)
q'=2/q

Straka L. et al., submitted, http://dx.doi.org/10.2139/ssrn.4771525

Modulation – study by high-resolution q-scan

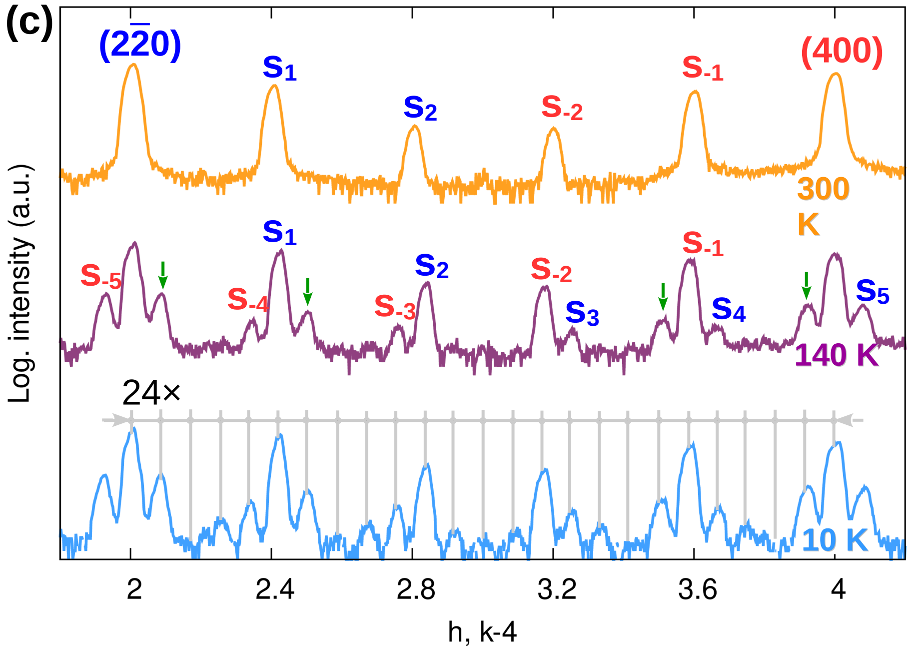

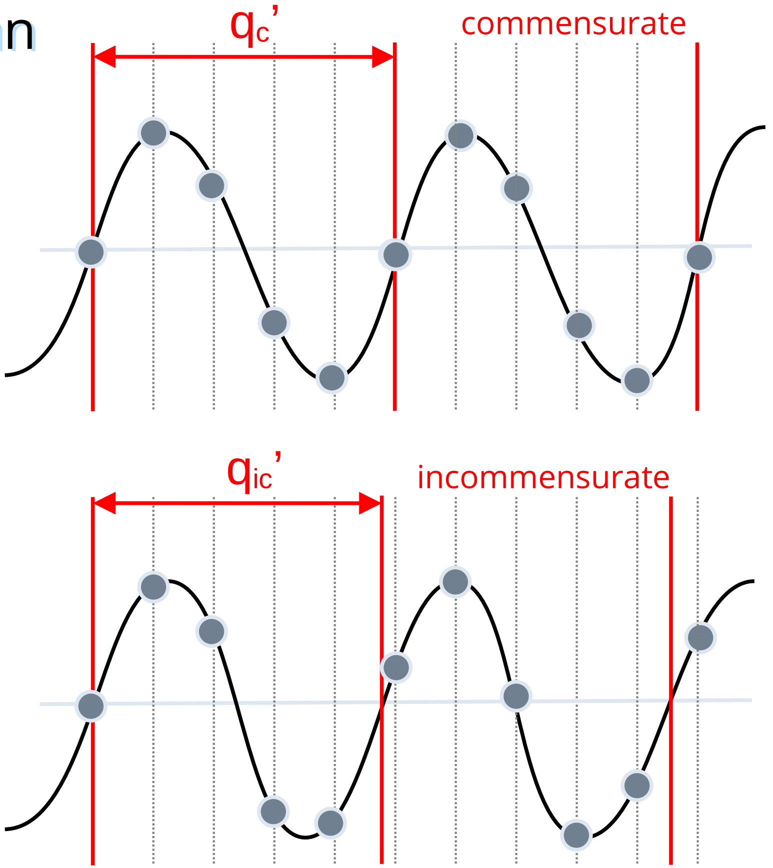

q=(q,q,0)
q'=2/q

Straka L. et al., submitted, http://dx.doi.org/10.2139/ssrn.4771525

	Commensurate (q=0.400)	**Incommensurate** (q=0.428)
Harmonic modulation (sine) 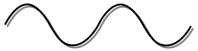	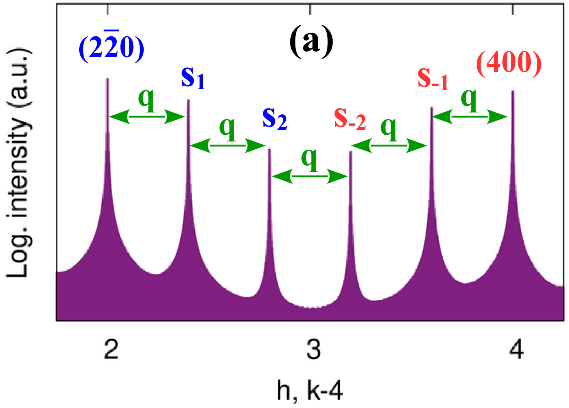	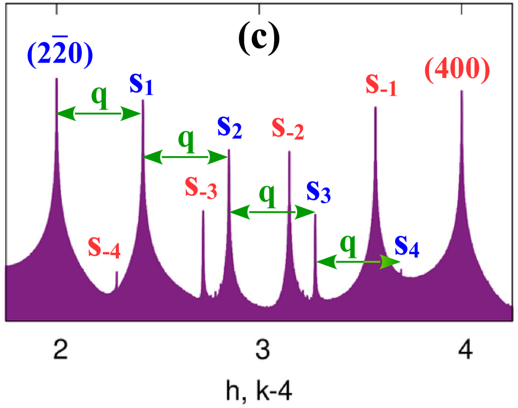

Straka L. et al., submitted, http://dx.doi.org/10.2139/ssrn.4771525

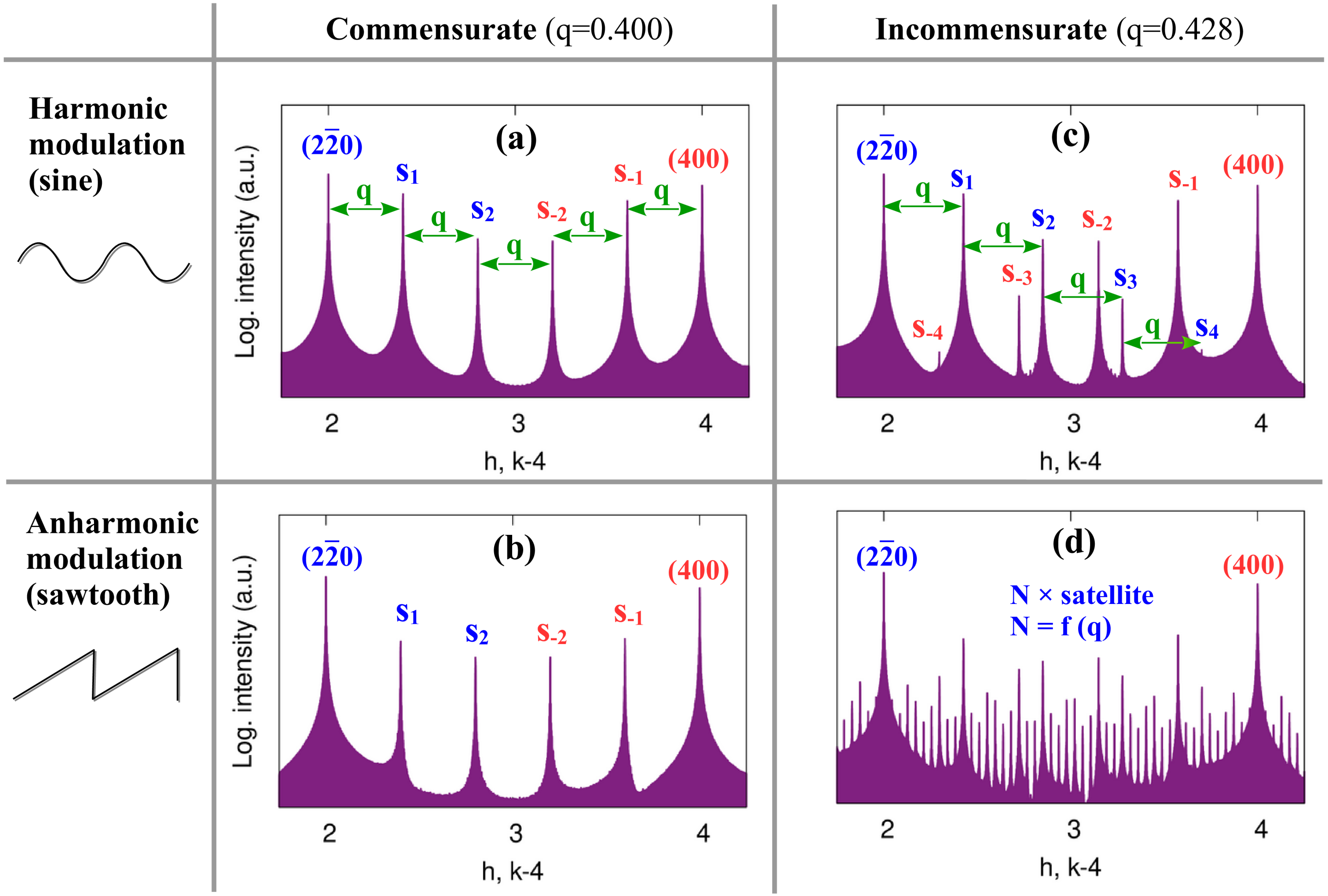

Straka L. et al., submitted, http://dx.doi.org/10.2139/ssrn.4771525

Modulation – study by high-resolution q-scan

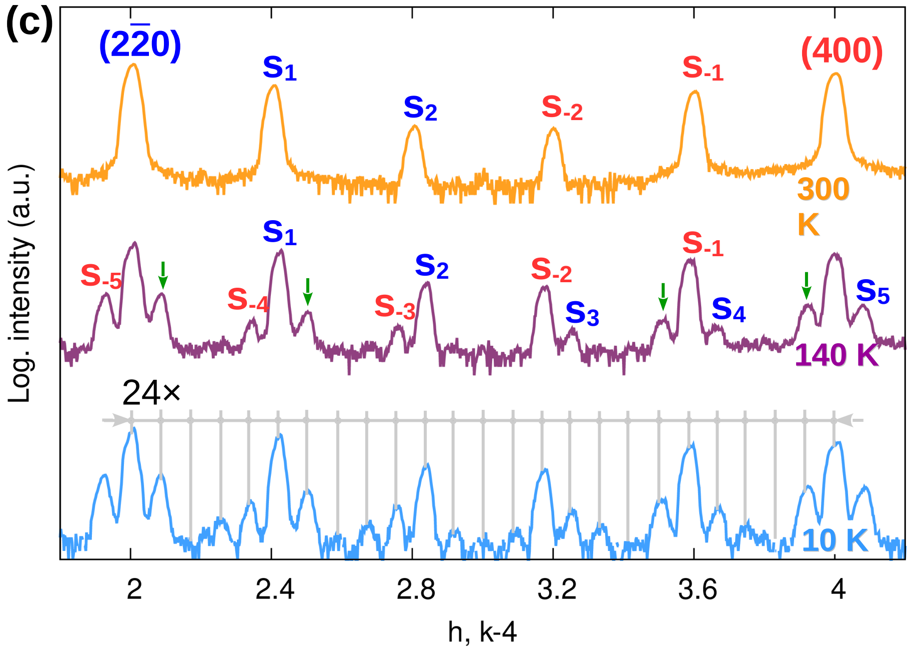

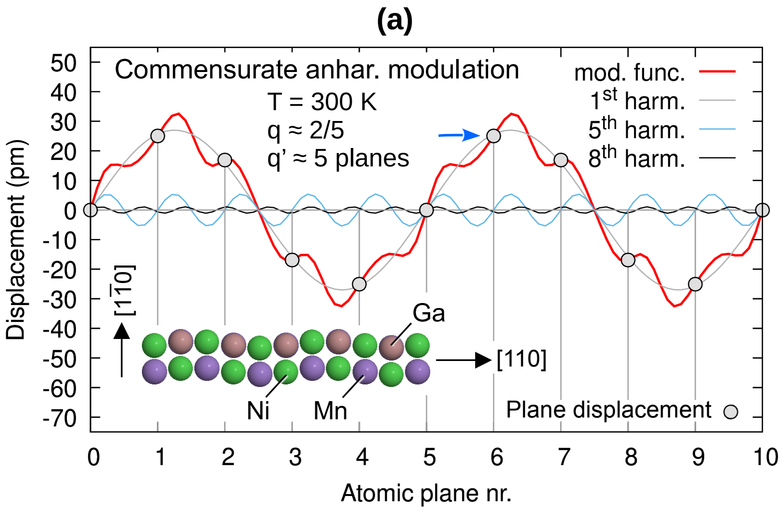

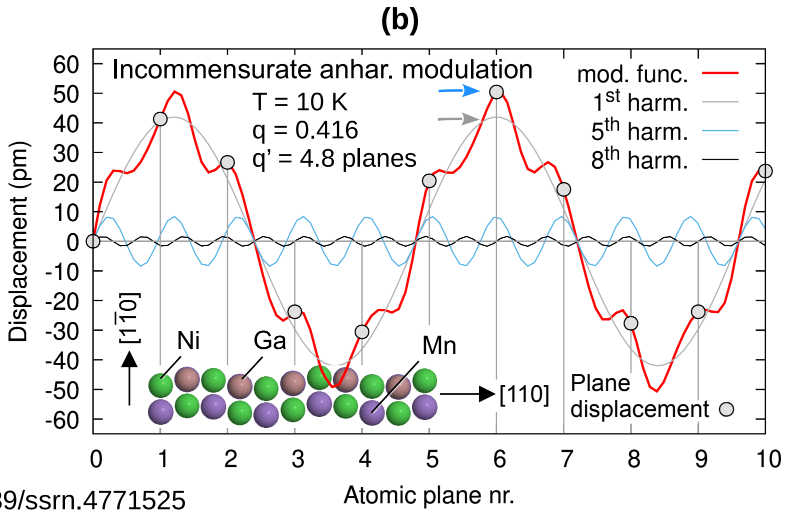

Straka L. et al., submitted, http://dx.doi.org/10.2139/ssrn.4771525

Modulation – study by high-resolution q-scan

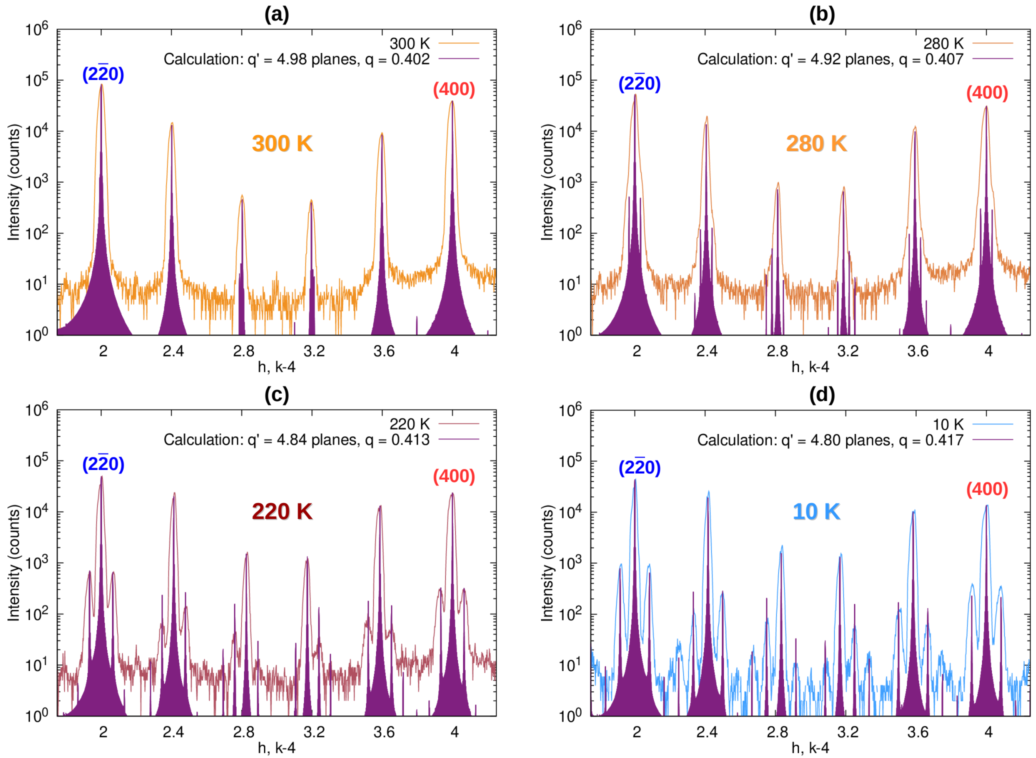

HKL(T) = f(q(T))

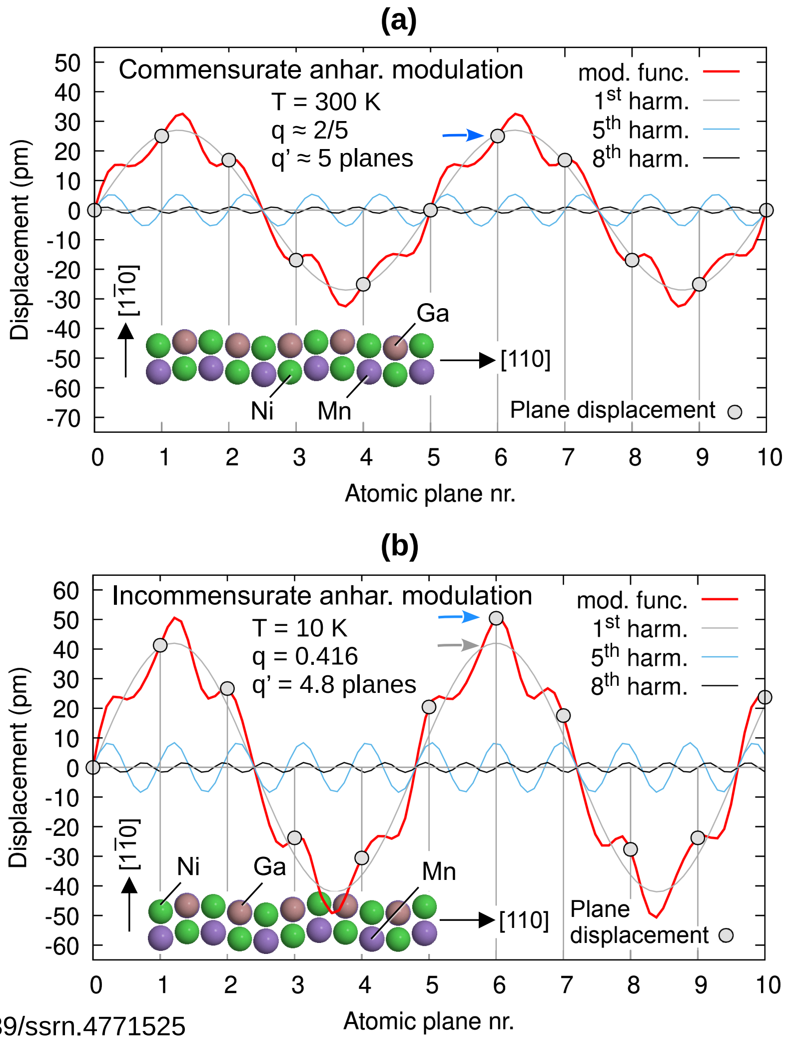

Straka L. et al., submitted, http://dx.doi.org/10.2139/ssrn.4771525

Aperiodicity – study by high-resolution q-scan

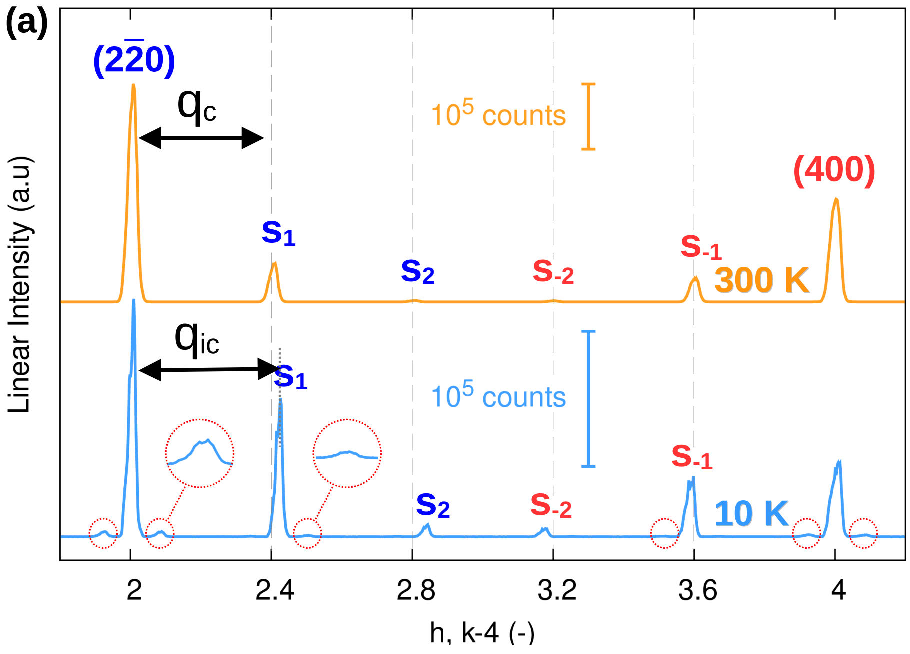

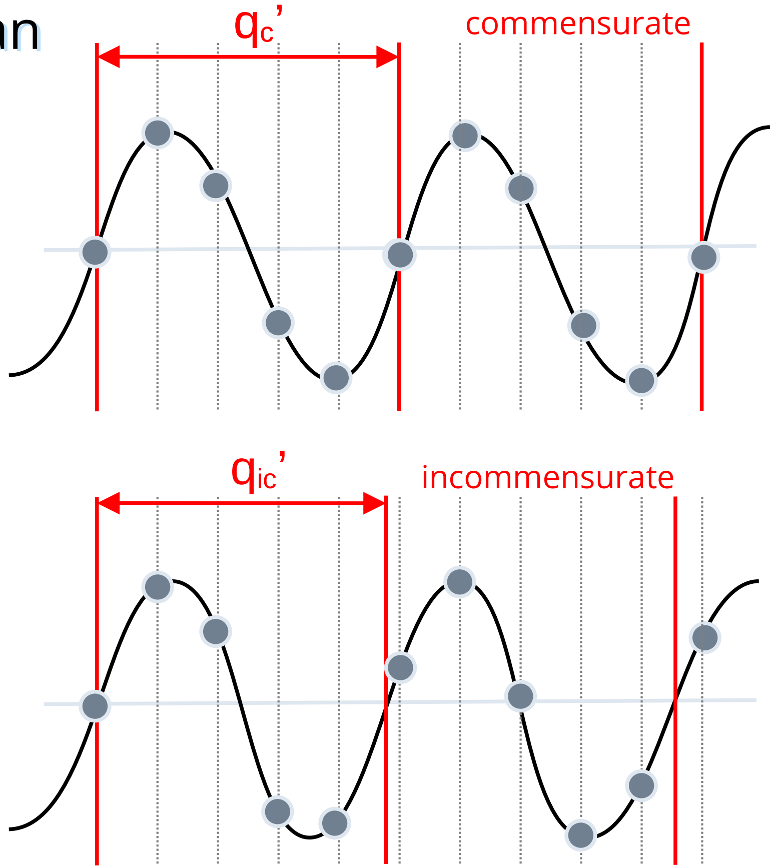

q=(q,q,0)

q'=2/q

Straka L. et al., submitted, http://dx.doi.org/10.2139/ssrn.4771525

Aperiodicity – study by high-resolution q-scan

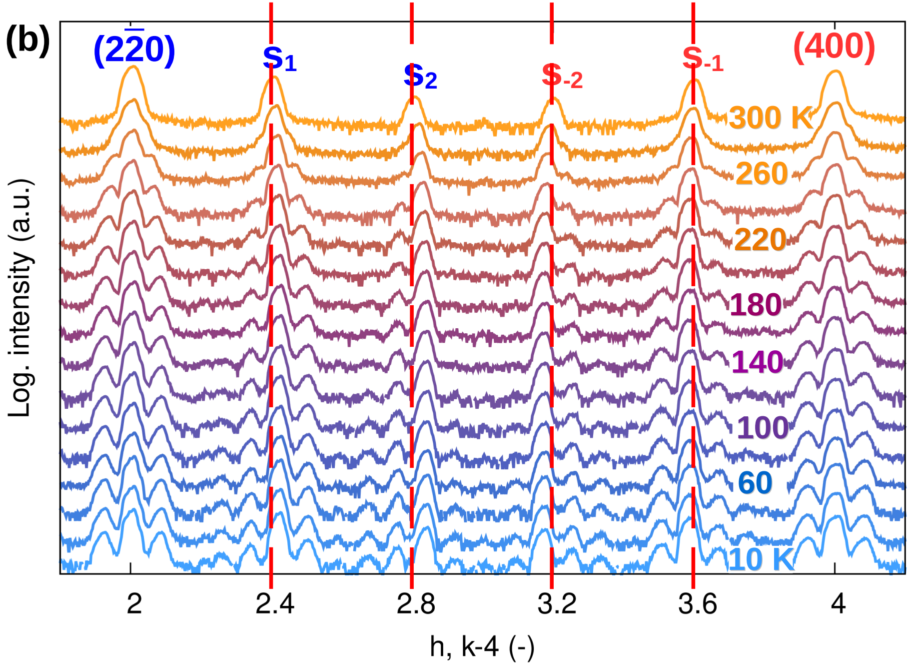

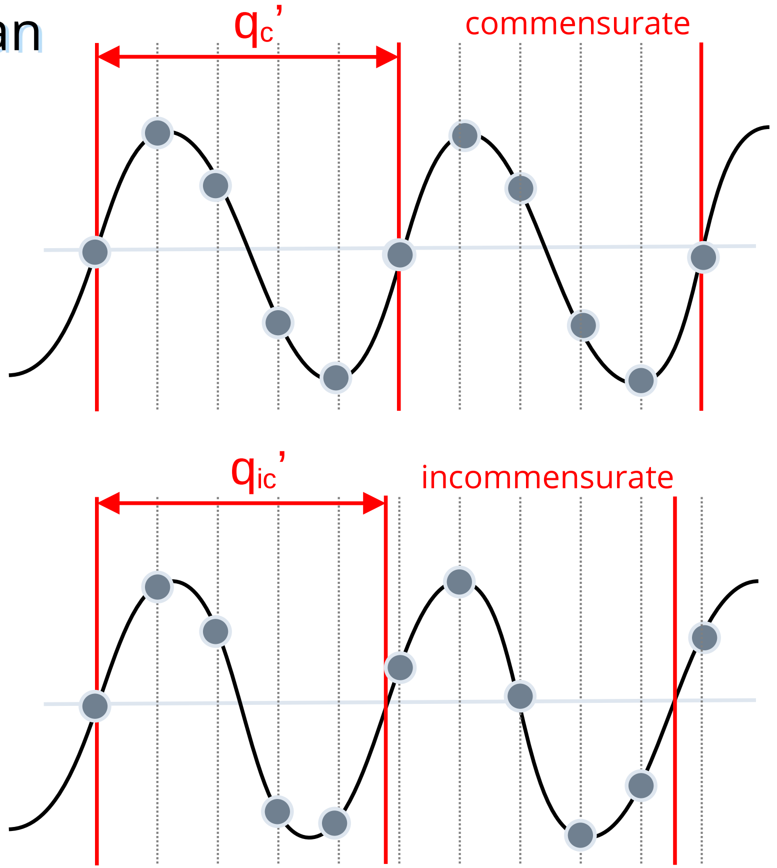

q=(q,q,0)
q'=2/q

Straka L. et al., submitted, http://dx.doi.org/10.2139/ssrn.4771525

Aperiodicity – study by high-resolution q-scan

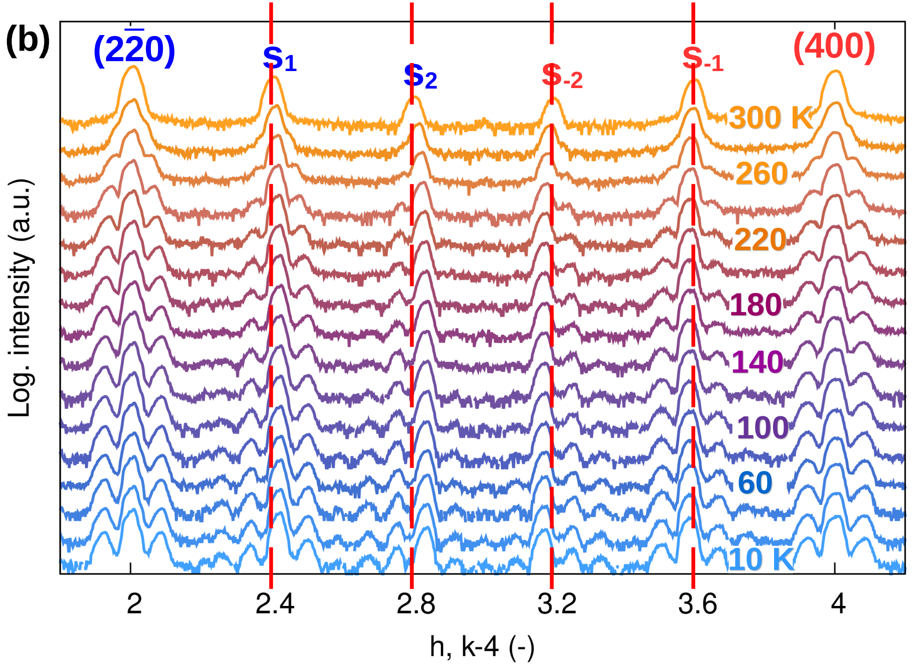

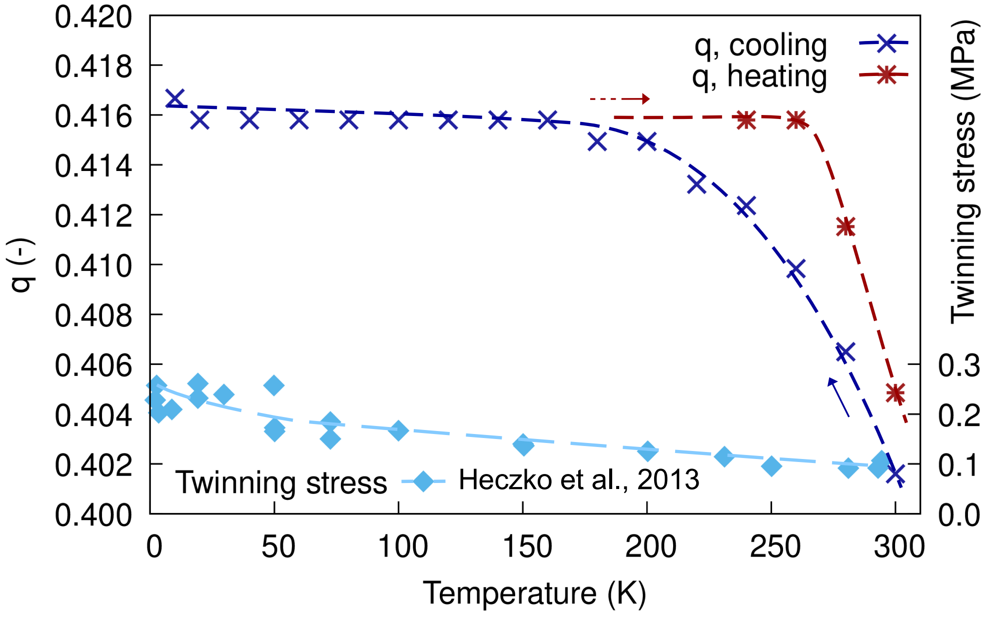

q=(q,q,0)
q'=2/q

Straka L. et al., submitted, http://dx.doi.org/10.2139/ssrn.4771525

Aperiodicity – study by high-resolution q-scan

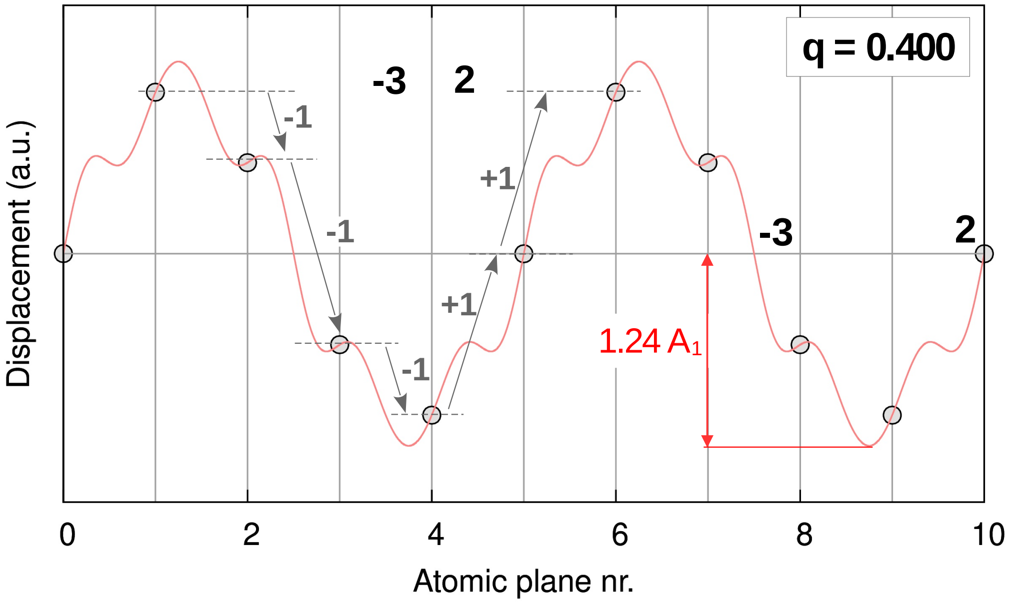

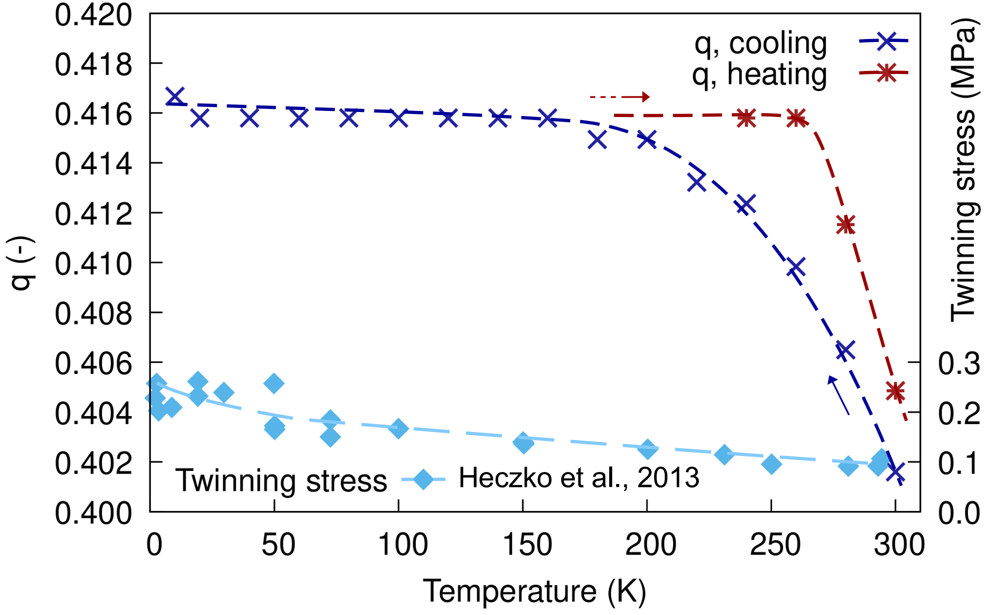

Straka L. et al., submitted, http://dx.doi.org/10.2139/ssrn.4771525

Aperiodicity – study by high-resolution q-scan

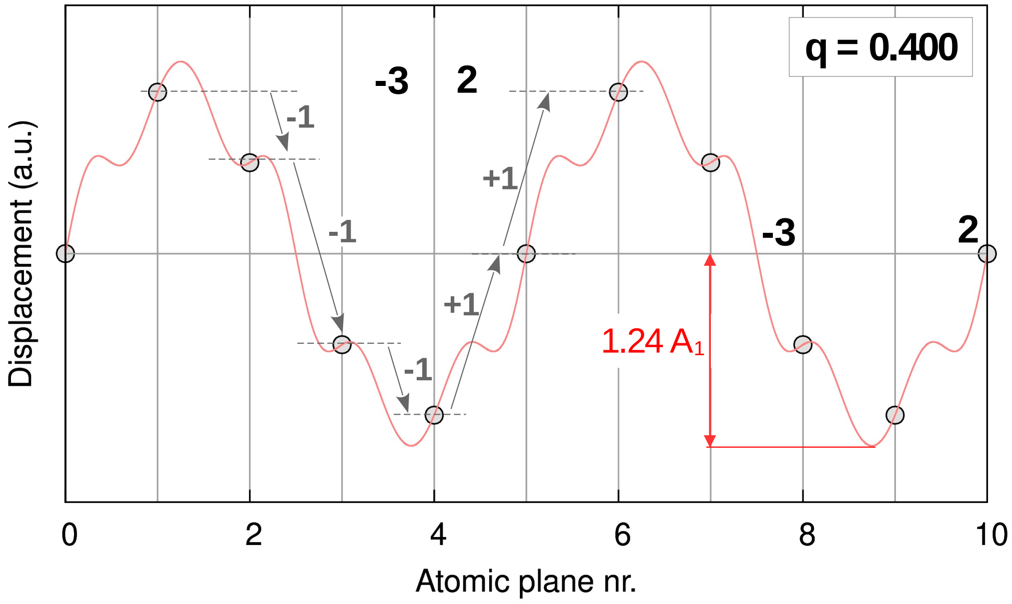

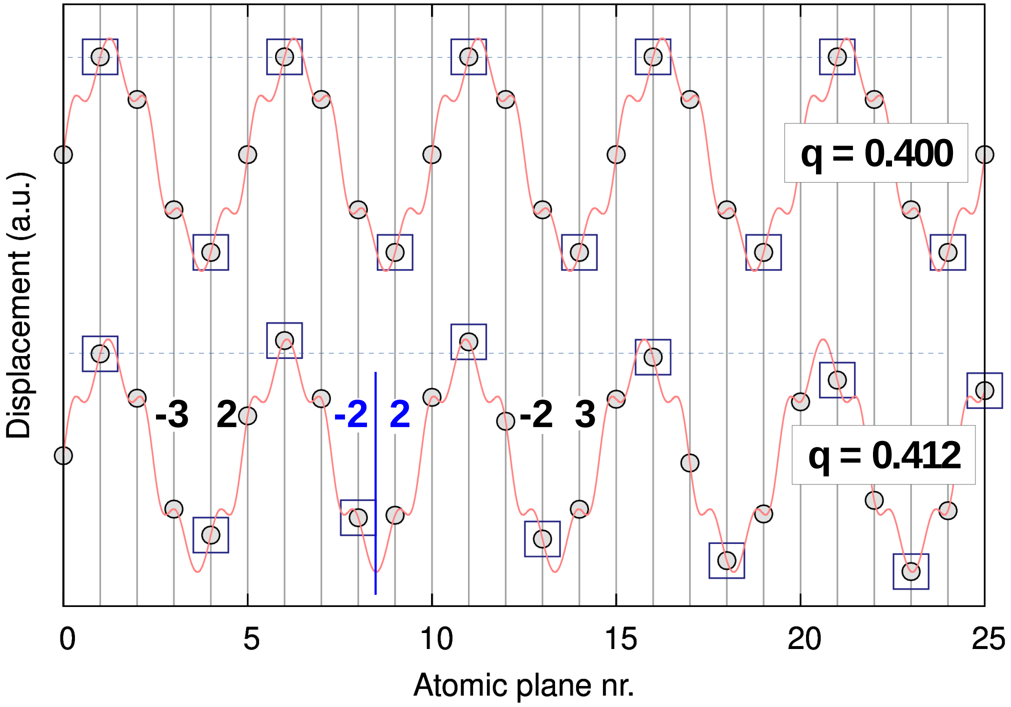

Straka L. et al., in preparation

Aperiodicity results in a/b nanotwinning (!!!)

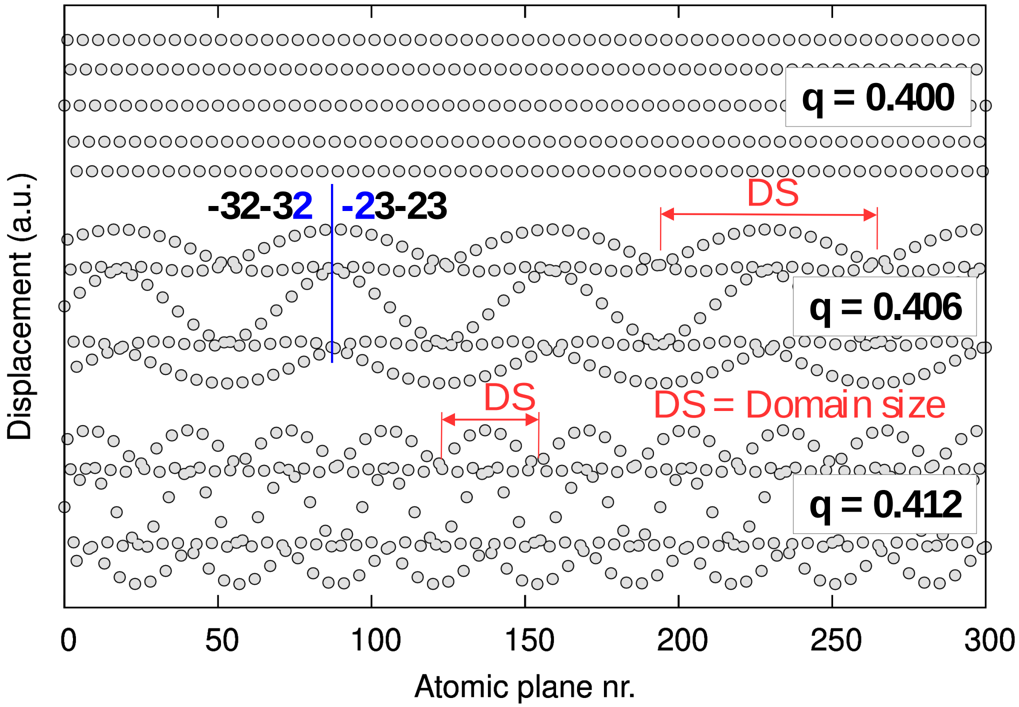

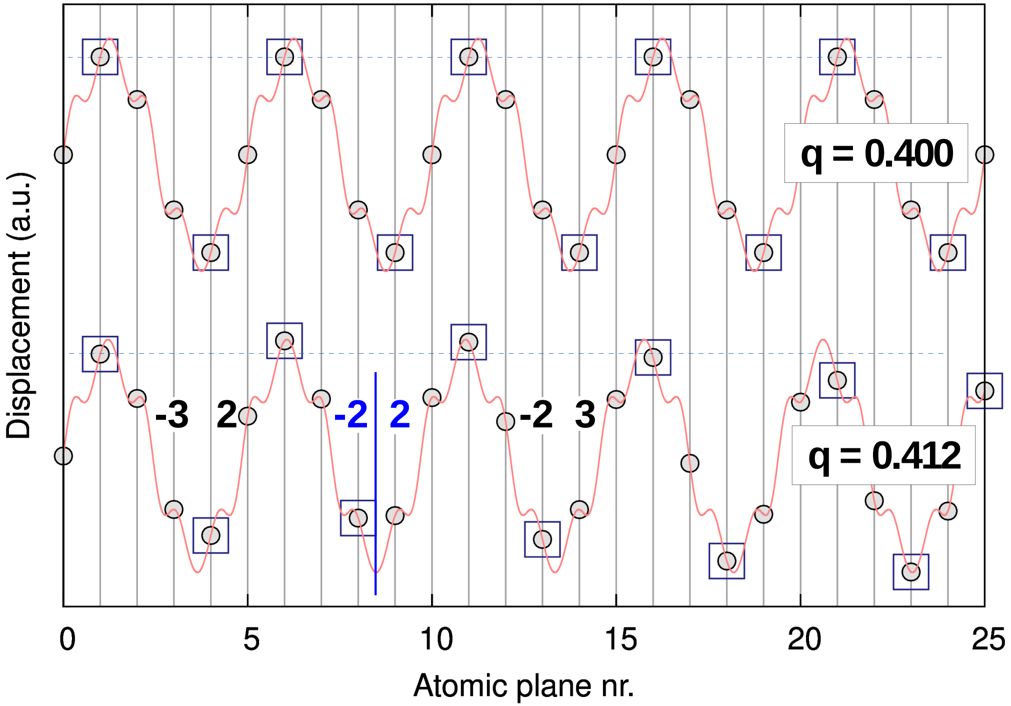

Straka L. et al., in preparation

Aperiodicity results in a/b nanotwinning (!!!)

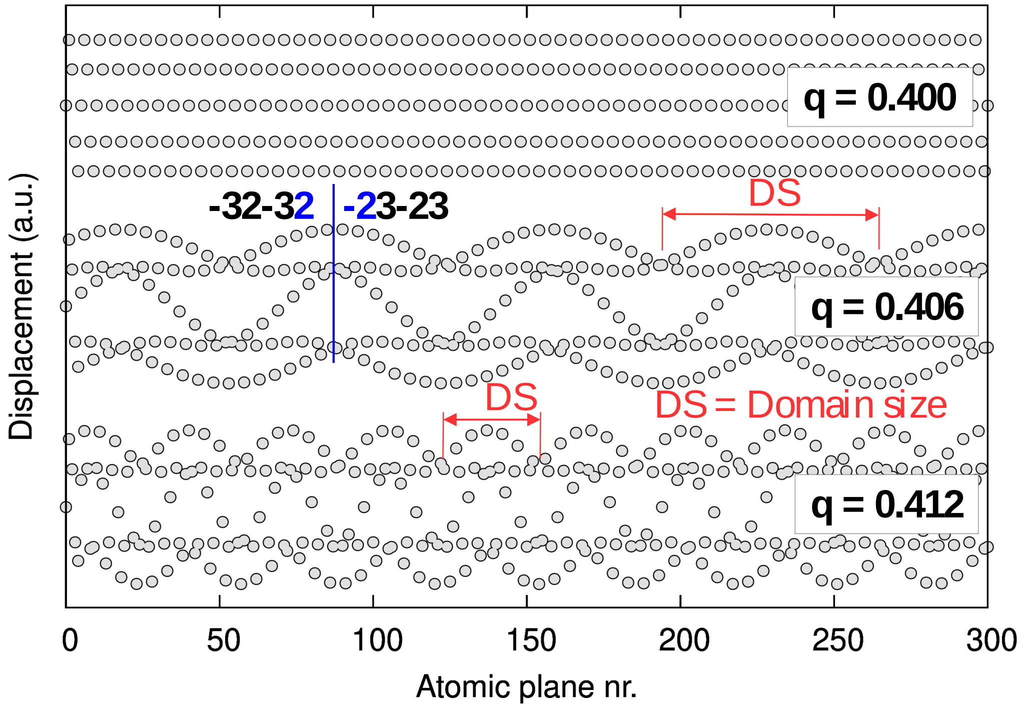

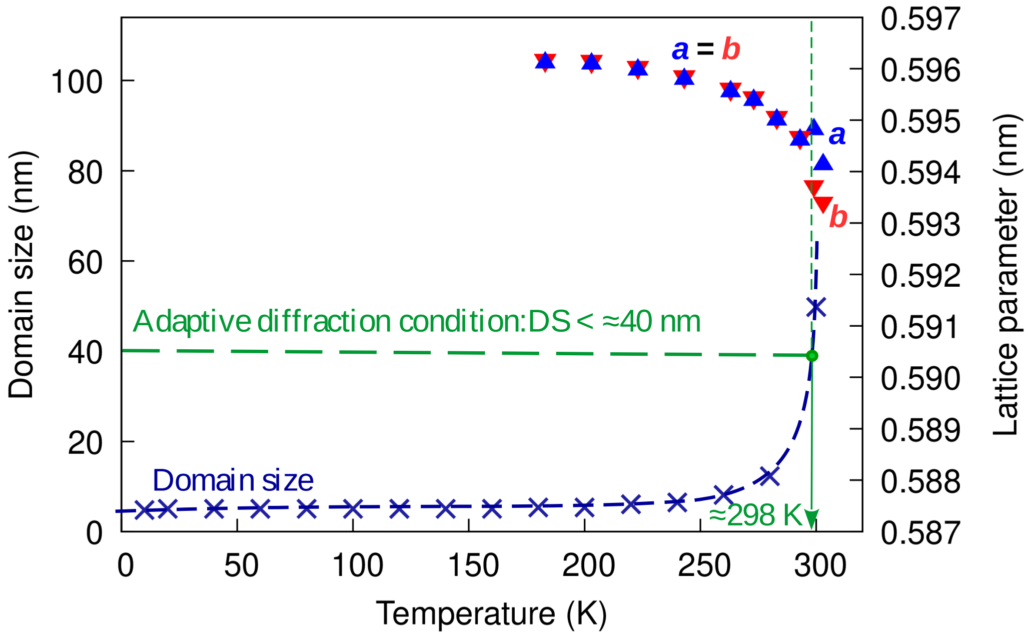

Straka L. et al., in preparation

Aperiodicity results in a/b nanotwinning (!!!)

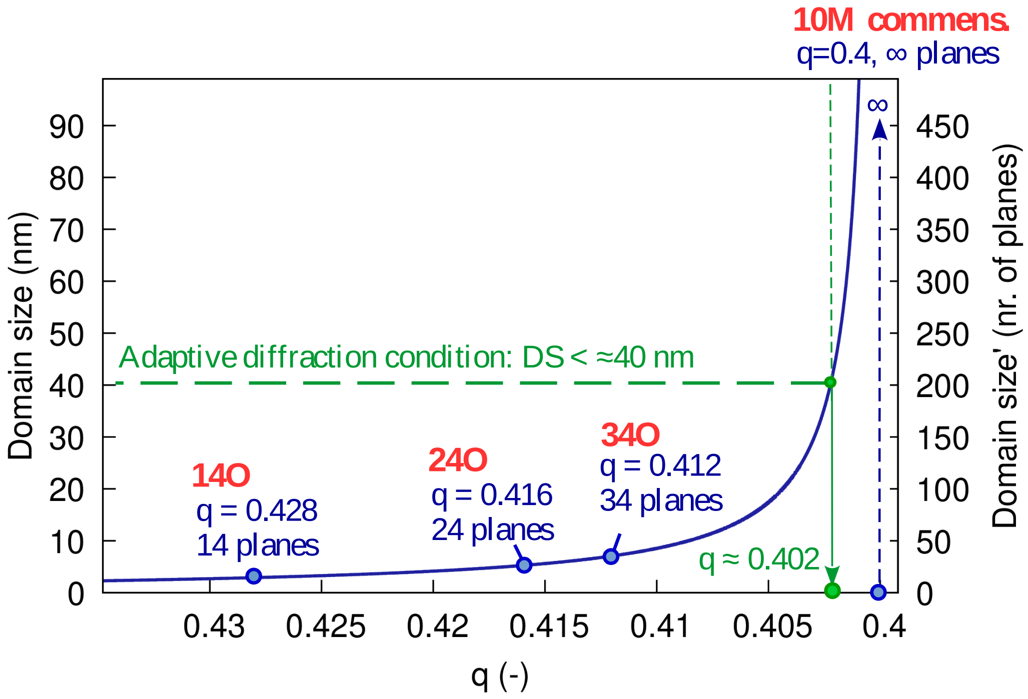

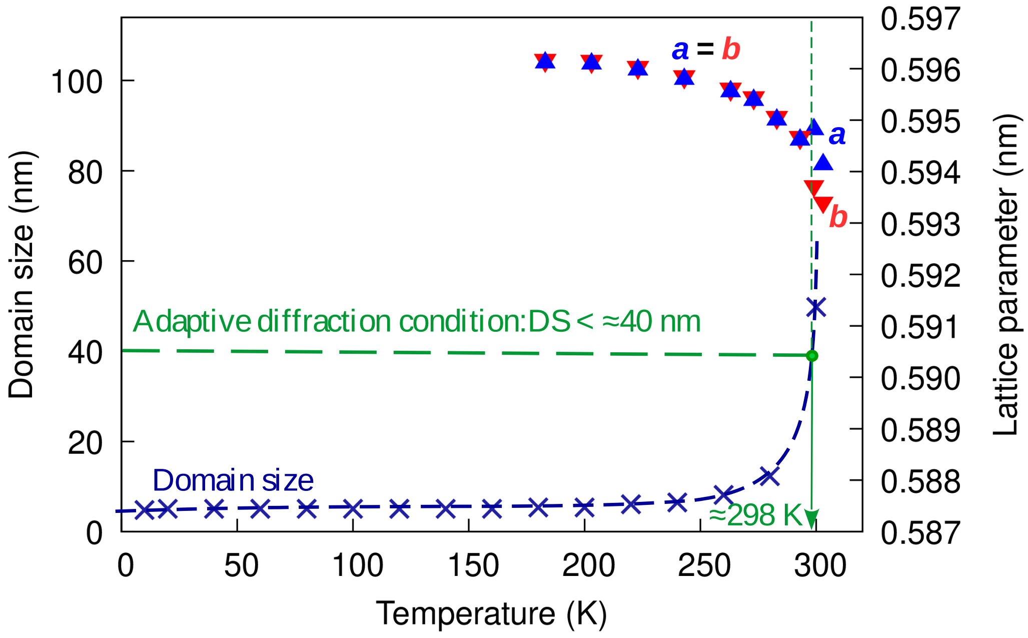

Straka L. et al., in preparation

Distinct identified nanotwins/structures

(a) q = 0.400, q’ = 5.00 (10M commensurate)

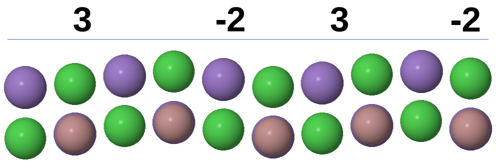

(b) q = 0.412, q’ = 4.86 (34 layers, 34O)

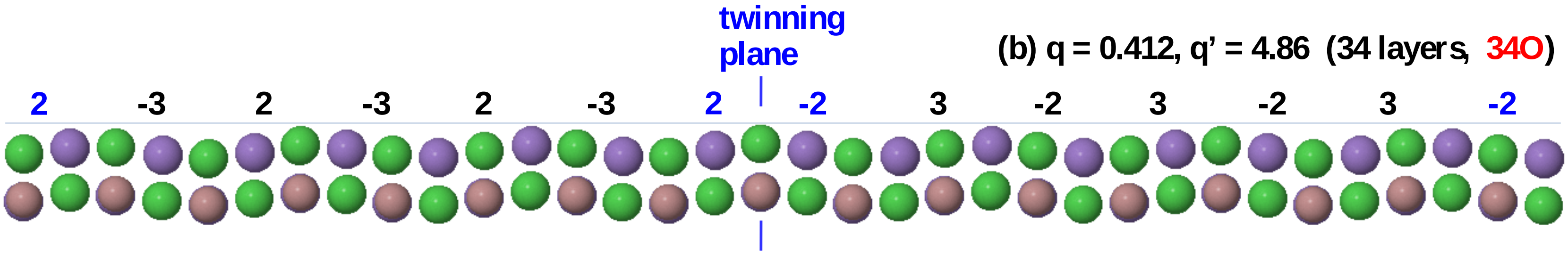

(c) q = 0.416, q’ = 4.80 (24 layers, 24O)

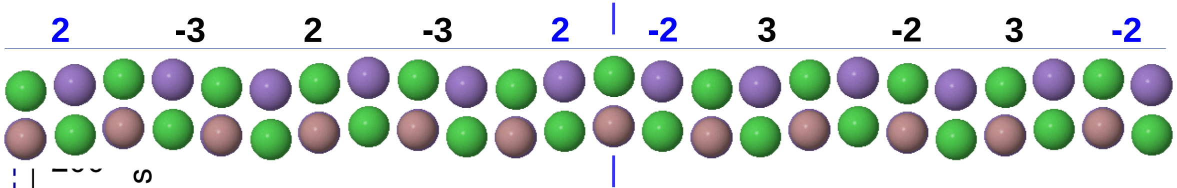

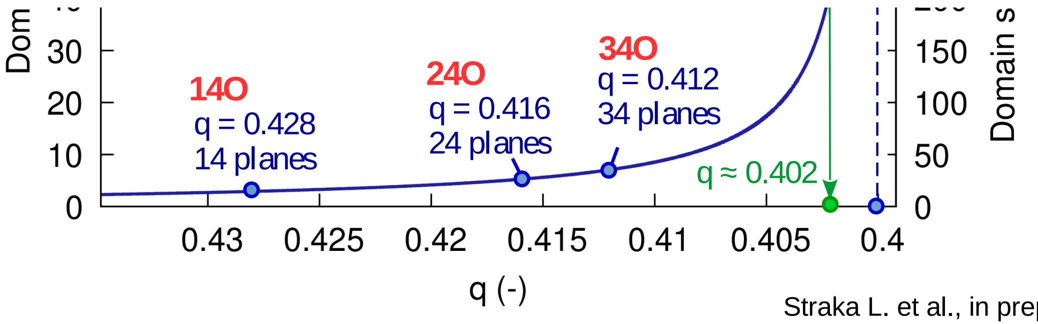

(d) q = 3/7 (0.428), q’ = 4.70 (14 layers, 14O)

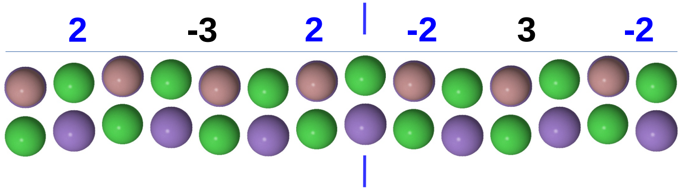

Straka L. et al., in preparation

Distinct identified nanotwins/structures

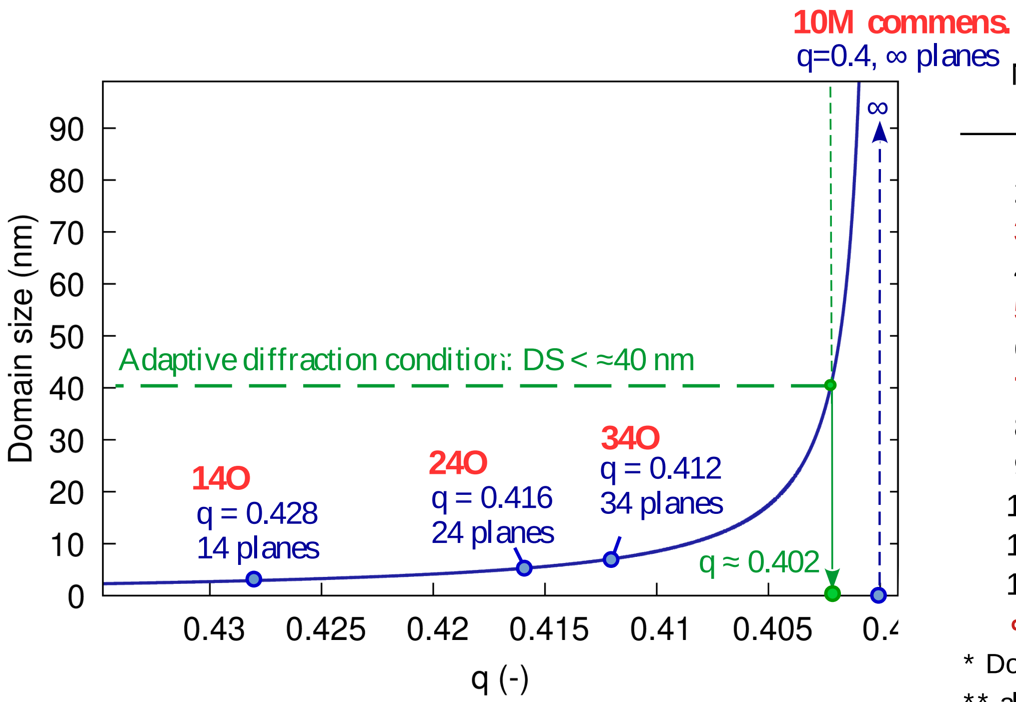

N -	q' (planes)	q (-)	Domain size (planes)	Domain size (nm)	Marking -
1	4.000	0.5000	4	0.8	4O
2	4.500	0.4444	9	1.9	18O*
3	**4.667**	**0.4286**	**14**	**2.9**	**14O**
4	4.750	0.4211	38	8.0	38O*
5	**4.800**	**0.4167**	**24**	**5.0**	**24O**
6	4.833	0.4138	58	12.2	58O*
7	**4.857**	**0.4118**	**34**	**7.1**	**34O**
8	4.875	0.4103	78	16.4	78O*
9	4.889	0.4091	44	9.2	44O
10	4.900	0.4082	98	20.6	98O*
11	4.909	0.4074	54	11.3	54O
12	4.917	0.4068	118	24.8	118O*
∞	**5.000**	**0.4000**	**∞**	**∞**	**10M comm.** **

* Double cell size to comply with the $L2_1$ order.

** also marked as 5M when neglecting ordering.

Straka L. et al., in preparation

Distinct identified nanotwins/structures as low energy/low temperature states

Hypothesis yet to be tested: q converges to one of the nanotwinned states

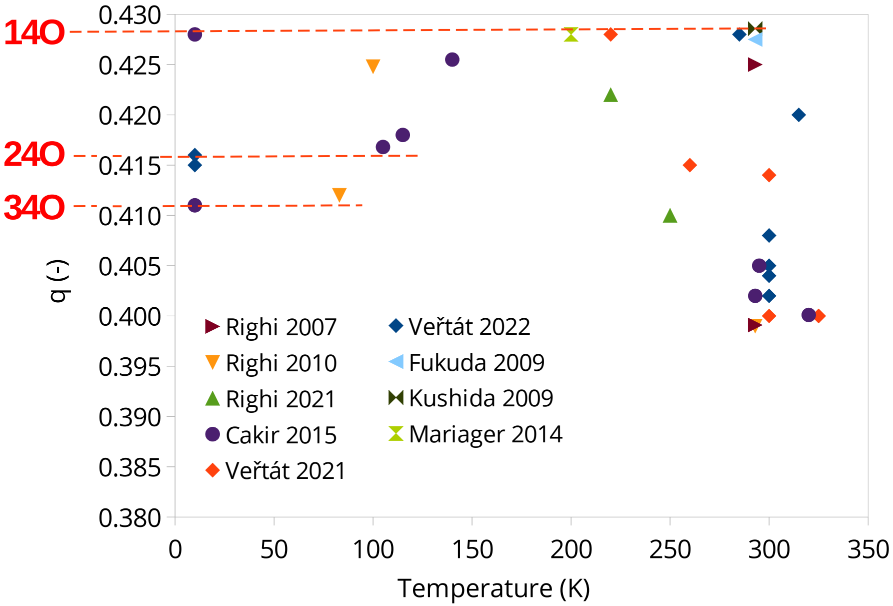

N -	q' (planes)	q (-)	Domain size (planes)	Domain size (nm)	Marking -
1	4.000	0.5000	4	0.8	4O
2	4.500	0.4444	9	1.9	18O*
3	**4.667**	**0.4286**	**14**	**2.9**	**14O**
4	4.750	0.4211	38	8.0	38O*
5	**4.800**	**0.4167**	**24**	**5.0**	**24O**
6	4.833	0.4138	58	12.2	58O*
7	**4.857**	**0.4118**	**34**	**7.1**	**34O**
8	4.875	0.4103	78	16.4	78O*
9	4.889	0.4091	44	9.2	44O
10	4.900	0.4082	98	20.6	98O*
11	4.909	0.4074	54	11.3	54O
12	4.917	0.4068	118	24.8	118O*
∞	**5.000**	**0.4000**	∞	∞	**10M comm.**

* Double cell size to comply with the $L2_1$ order.

** also marked as 5M when neglecting ordering.

Straka L. et al., in preparation

Summary IV

Aperiodic crystal
Anharmonic modulation

Wave modulation perspective **vs nanotwinning** perspective:

- **not exclusive concepts but complementary/intertwinned concepts in Ni-Mn-Ga**
- **nanotwinning is a result of crystal aperiodicity**
- Low temperature states are nanotwinned
- Nanotwinning ON/OFF (at r.t.)

Summary

Magnetic shape memory (Ni-Mn-Ga)

- very interesting at all scales

- magnetism important but (micro)structure critical for MSM functionality

- **a great platform for**

    - magnetoelastic and magnetomechanical effects (up to 12% deformation in mag. field)

    - martensite crystallography (deeply hierarchical martensite)

    - nanotwinning and aperiodic crystal concepts (**nanotwins on/of, aperiodicity on/offf**)

- major **future** tasks: alternatives & applications


Thank you!